GEOLOGICAL SURVEY OF FINLAND
Report of Investigation 209
2014

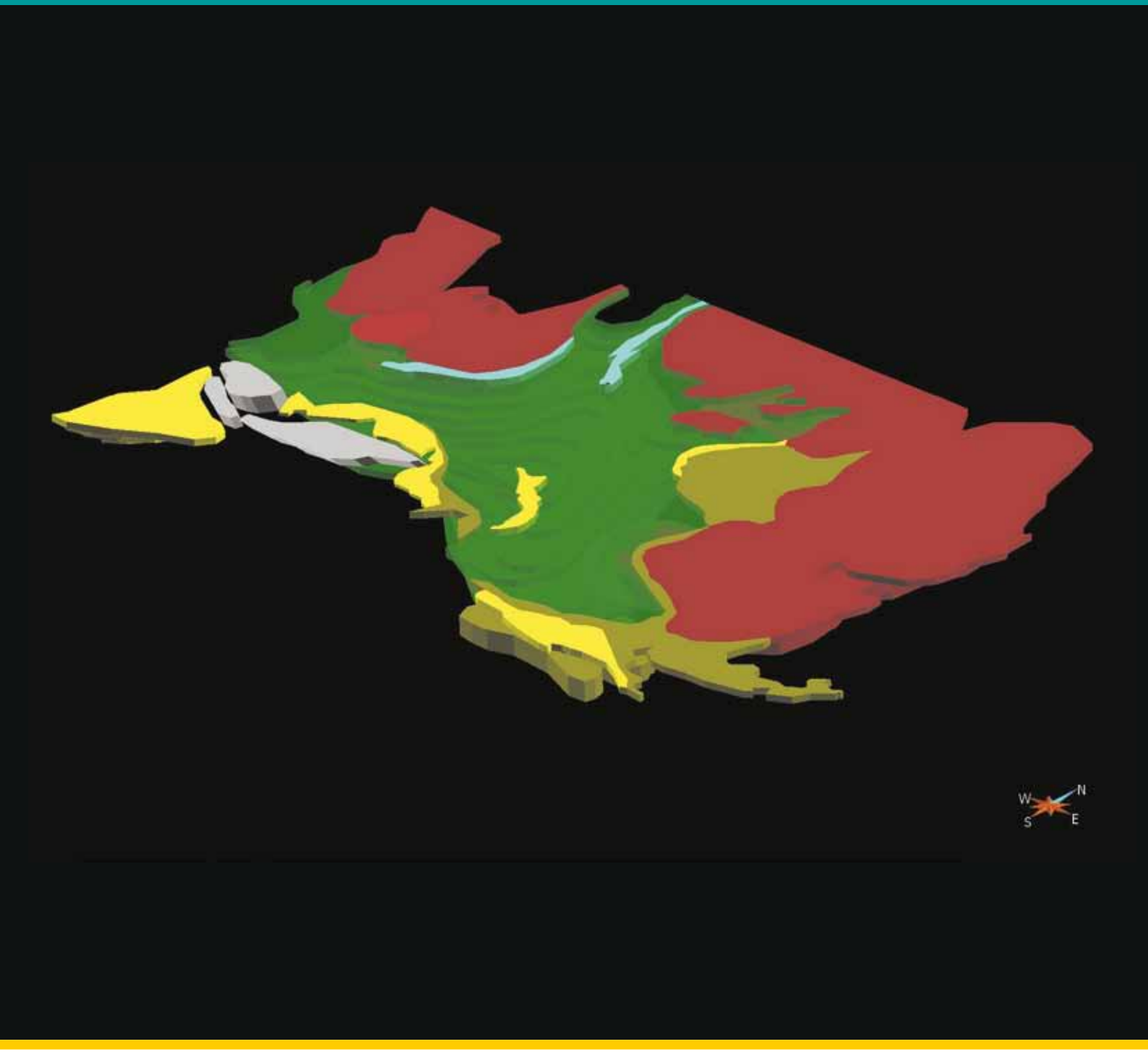

Central Lapland Greenstone Belt 3D modeling project
Final report

Tero Niiranen, Ilkka Lahti, Vesa Nykänen and Tuomo Karinen

GTK

GEOLOGIAN TUTKIMUSKESKUS **GEOLOGICAL SURVEY OF FINLAND**

Tutkimusraportti 209 Report of Investigation 209

Tero Niiranen, Ilkka Lahti, Vesa Nykänen and Tuomo Karinen

CENTRAL LAPLAND GREENSTONE BELT 3D MODELING PROJECT FINAL REPORT

Front cover: 3D gravity model of the Kittilä terrane and adjacent lithological units.

ISBN 978-952-217-302-7 (PDF)
ISSN 0781-4240

Layout: Elvi Turtiainen Oy
Espoo 2014

Niiranen, T., Lahti, I., Nykänen, V. & Karinen, T. 2014. Central Lapland Greenstone Belt 3D modeling project final report. *Geological Survey of Finland, Report of Investigation 209*, 78 pages, 55 figures and 3 tables.

This report presents results of the Central Lapland Greenstone Belt 3D modeling project carried out in 2007–2012. The report documents the utilization of the multiscale edge detection, or "worming", method for regional gravity data and in prospectivity modeling, presents a new Ni-Cu prospectivity model for the Central Lapland Greenstone Belt (CLGB) district, and documents five 3D geomodels from the Central Lapland area and their implications for the geological interpretation of the area.

The worming method was tested on gravity data from Central Lapland. The results indicate that worms, i.e. gravity gradient maxima, are highly useful in interpreting the major shear, thrust, and fault zones, as well as the contacts of lithological units, their depth extent and their dip orientations. Weights of evidence analysis indicates that in the Central Lapland area, the known orogenic gold and iron oxide-Cu-Au deposits display a spatial correlation with the gravity worms, and hence the gravity worms can be used as a tool for locating the most prospective areas for epigenetic mineral deposits.

A simple Ni-Cu prospectivity model of the CLGB was constructed using airborne magnetic and ground gravity data together with till geochemistry (Ni, Cu, Co) data. A high-pass filtering technique was used for till geochemistry to filter out regional anomalies and the data were integrated using fuzzy logic. The resulting prospectivity map identifies over 40 target areas for Ni-Cu deposits, including the Sakatti Ni-Cu and Kevitsa Ni-Cu-Au-PGE deposits.

A regional 3D model of the Kittilä terrane and the key adjacent structures was constructed using a multidisciplinary approach and a wide array of geophysical and geological data. The modeling results indicate that the Kittilä terrane forms a keel-shaped unit that is ca. 9 km thick at the thickest part, thinning out towards the margins. The shape and thickness suggest that the terrane was considerably thickened during thrusting from the S and NE. A rough estimate of the orogenic gold potential was carried out by applying a metamorphic source model for the gold deposits. Based on the modeling results, potentially up to 228 Moz of gold was mobilized from the Kittilä Group rocks alone during the metamorphic events related to the Svecofennian orogeny. This figure is about 30 times greater than the currently reported gold resources in the known deposits of the area, suggesting that significant undiscovered gold resources remain in the Kittilä terrane area.

A 3D model of the Kolari region was constructed using new seismic (HIRE) data from the Hannukainen-Rautuvaara area. The modeling results reveal that the Savukoski and Sodankylä group rocks form a gently SW-plunging open fold structure with an internal small-scale dome and basin structure. The SW–NE-striking Äkäsjoki shear zone has been formed in the axial plane of this fold. The modeling results indicate that the current stratigraphical interpretation is incorrect and needs revising. The results also indicate that the known Fe ± Cu-Au deposits in the area cannot be hosted by the same stratigraphical unit horizon, and are thus not strata-bound deposits, as they have previously been interpreted.

A 3D model of the Lapland Granulite Belt (LGB) was constructed using seismic FIRE and geophysical data. According to the model, the LGB consists of at least 4 tectonic blocks. The Vuotso complex immediately SW of the LGB consists of at least 2 tectonic blocks. These units comprise a listric thrust package limiting the Kittilä terrane at its NE contact.

Old Outokumpu Oyj drill core and ground geophysical data were used to constrain a deposit-scale model of the Saattopora Au-Cu deposit. The model shows the main shear zones and lithological units, as well as a block model of the two Au-Cu lodes. The modeling data together with the geological observations indicate that the northern 'A' lode appears to be controlled by the albitized phyllite unit between a komatiite unit in the south and a mafic tuff unit in the north. The southern 'B' lode is controlled by an ESE-striking subvertical shear zone. The modeling data imply that the deposit is open to depth at ca. 160 m below the surface. The data indicate that the ore-hosting veins cross-cut the regional F3 folding visible in outcrops and also in the modeled geological units, suggesting that the mineralization took place in the late stages of the regional deformation and metamorphism.

The Lauttaselkä 3D model is based on geophysics and the recent bedrock mapping and drilling campaign in the area. The modeling shows a west-vergent thrust system, with thrust folding explaining the repeating pattern of the Kautoselkä and Vesmajärvi formations in the western part of the area. In the eastern part of the study area, the Salla group rocks on top of the Sodankylä and Savukoski groups is explained by west-vergent thrusting of the Salla group on the latter two units.

Keywords (GeoRef Thesaurus, AGI): mineral exploration, gold ores, nickel ores, copper ores, iron ores, gravity methods, edge detection, seismic methods, three-dimensional models, Central Lapland Greenstone Belt, Lapland Granulite Belt, Kittilä, Kolari, Sodankylä, Lapland, Finland

Tero Niiranen, Ilkka Lahti, Vesa Nykänen and Tuomo Karinen
Geological Survey of Finland, P.O. Box 77, FI-96101 Rovaniemi, Finland
E-mail: tero.niiranen@gtk.fi

Niiranen, T., Lahti, I., Nykänen, V. & Karinen, T. 2014. Central Lapland Greenstone Belt 3D modeling project final report. *Geologian tutkimuskeskus, Tutkimusraportti 209*, 78 sivua, 55 kuvaa ja 3 taulukkoa.

Tässä raportissa esitetään vuosina 2007–2012 toimineen Keski-Lapin vihreäkivivyöhykkeen 3D-mallinnushankkeen tulokset. Raportissa esitetään monimittakaavaisten gradienttimaksimien käyttö potentiaalikenttäaineistolle ja niiden käyttöä prospektiivisuusmallinnuksessa, uusi Ni-Cu-prospektiivisuusmalli Keski-Lapin alueelle sekä dokumentoidaan viisi geologista 3D-mallia ja esitellään niiden pohjalta tehdyt johtopäätökset.

Monimittakaavaisten gradienttimaksimien käyttöä testattiin Keski-Lapin painovoima-aineistolla. Painovoimagradienttimaksimit ovat erittäin käyttökelpoisia suurten hierto- ja ylityöntörakenteiden sekä litologisten kontaktien tulkinnassa. Gradienttimaksimien perusteella pystytään linjaamaan näiden rakenteiden paikkaa, kaateen suuntaa ja syvyysulottuvuutta. Weight-of-Evidence-analyysin tulokset osoittavat, että Keski-Lapin alueen painovoimagradienttimaksimit korreloivat tunnettujen orogeenisten kulta- ja rautaoksidi-kulta-kupariesiintymien kanssa. Näin ollen gradienttimaksimeja voidaan käyttää apuna epigeneettisten malmiesiintymien paikantamisessa.

Keski-Lapin alueelta tehtiin uusi Ni-Cu-esiintymien prospektiivisuusennuste käyttäen hyväksi magneettista lentomittausaineistoa, painovoima-aineistoa sekä moreenigeokemiaa (Ni, Cu, Co). Moreenigeokemian aineisto käsiteltiin käyttämällä ylipäästösuodatusmenetelmää suodattamaan alueelliset anomaliat pois ja aineistot yhdistettiin käyttäen hyväksi sumean logiikan menetelmää. Tuloksena saatu prospektiivisuuskartta osoittaa yli 40 Ni-Cu-potentiaalista kohdetta mukaan lukien tunnetut Sakatin Ni-Cu- ja Kevitsan Ni-Cu-Au-PGE-esiintymät.

Kittilän terraanin geologinen 3D-malli ja sen välittömässä läheisyydessä olevat tärkeimmät rakenteet mallinnettiin käyttäen hyväksi laajaa geofysiikan ja geologian aineistoa. Mallinnustulokset osoittavat Kittilän terraanin olevan kölin muotoinen, maksimissaan noin yhdeksän kilometriä paksu yksikkö, joka ohenee reunojaan kohti. Yksikön muoto ja paksuus viittaavat siihen, että terraani paksuuntui merkittävästi etelästä ja koillisesta suuntautuneiden ylityöntöjen vaikutuksesta. Kittilän alueen orogeenisten kultaesiintymien esiintymispotentiaalia tarkasteltiin siten, että tehtiin mallinnustulosten pohjalta kvantitatiivinen arvio kullan mobilisuudesta käyttäen oletuksena metamorfista metallinlähdemallia orogeenisille kultaesiintymille. Tulokset viittaavat siihen, että jopa 7 000 tonnia kultaa mobiloitui metamorfoosin vaikutuksesta pelkästään Kittilän ryhmän kivistä. Luku on noin 30 kertaa suurempi kuin tällä hetkellä on raportoitu alueen tunnetuista esiintymistä. Tämä viittaa siihen, että alueen vielä löytymättömät kultavarannot ovat merkittävät.

Kolarin alueen 3D-malli tehtiin pääasiassa käyttäen hyväksi uutta seismistä (HIRE) aineistoa Hannukaisen-Rautuvaaran alueelta. Mallinnustulosten perusteella Savukosken ja Sodankylän ryhmien kivet muodostavat loivasti lounaaseen kaatuvan poimurakenteen, jossa on pienimittakaavainen sisäinen doomiallasrakenne. Koillis-luodesuuntainen Äkäsjoki-hiertovyöhyke on muodostunut kyseisen poimurakenteen akselitasoon. Mallinnustulokset osoittavat, että nykyinen stratigrafinen tulkinta alueelta on virheellinen ja vaatii korjauksen. Tulokset myös osoittavat, että Kolarin alueen rauta ± kupari-kultaesiintymät eivät voi liittyä yhteen stratigrafiseen yksikköön eivätkä siten ole kerrossidonnaista tyyppiä, kuten aiemmin on joissain lähteissä esitetty.

Lapin granuliittivyöhyke mallinnettiin käyttäen hyväksi geofysiikan aineistoja sekä seismistä FIRE-profiilia. Mallinnuksen perusteella granuliittivyöhyke koostuu vähintään neljästä tektonisesta yksiköstä. Granuliitin välittömässä luoteiskontaktissa olevasta Vuojärvikompleksista voidaan erottaa vastaavasti kaksi tektonista yksikköä. Nämä yksiköt muodostavat listrisen ylityöntöpinkan, joka rajaa Kittilän terraanin koillisosan.

Saattoporan Au-Cu-esiintymä mallinnettiin käyttäen hyväksi vanhaa Outokumpu Oyj:n kairaus- ja maanpintageofysikaalista aineistoa. Esiintymästä mallinnettiin merkittävimmät hiertovyöhykkeet, pääkivilajiyksiköt sekä kaksi Au-Cu-malmiota. Mallinnuksen perusteella pohjoista A-malmiota kontrolloi voimakkaasti albiittiutunut fylliittiyksikkö, joka rajaantuu etelässä komatiitti- ja pohjoisessa mafiseen tuffiyksikköön. Eteläistä B-malmiota kontrolloi itäkaakko-länsiluode suuntainen, lähes pysty hiertovyöhyke. Mallinnuksen perusteella esiintymä on avoin noin 160 metrin syvyydellä maanpinnasta. Malmipitoiset juonet leikkaavat alueen F_3-poimutusta, joka on havaittavissa niin mallinnetuissa geologisissa yksiköissä kuin paljastumillakin. Tämä viittaa siihen, että malmi on syntynyt myöhäisessä vaiheessa suhteessa alueelliseen deformaatioon ja metamorfoosiin.

Lauttaselän 3D-malli tehtiin käyttäen hyväksi alueella tehtyjä uusia kairaus- ja kartoitustöitä sekä olemassa olevaa geofysiikkaa. Malli kuvaa länteen suuntautuneen ylityöntösysteemin, johon liittyvä ylityöntöpoimutus selittää Vesmajärven ja Kautoselän muodostumien vuorottelun alueen länsiosassa. Sallan ryhmän kivien esiintyminen Sodankylän ja Savukosken ryhmien päällä alueen itäosassa selittyy Sallan ryhmän ylityöntymisellä näiden päälle.

Asiasanat (Geosanasto, GTK): malminetsintä, kultamalmit, nikkelimalmit, kuparimalmit, rautamalmit, painovoimamenetelmät, reunantunnistus, seismiset menetelmät, kolmiulotteiset mallit, Keski-Lapin vihreäkivivyöhyke, Lapin granuliittivyöhyke, Kittilä, Kolari, Sodankylä, Lappi, Suomi

Tero Niiranen, Ilkka Lahti, Vesa Nykänen ja Tuomo Karinen
Geologian tutkimuskeskus, PL 77, 96101 Rovaniemi
Sähköposti: tero.niiranen@gtk.fi

CONTENTS

PREFACE AND SUMMARY

The Paleoproterozoic Central Lapland Greenstone Belt (CLGB) extends ca. 450 km from Norway through Finnish Lapland to the western part of Russian Karelia, covering an area of roughly 35 000 km^2. It records a prolonged history of rifting stages, sedimentation, and magmatism between 2.44 Ga and 2.0 Ga, culminating in deformation and metamorphism during the Svecofennian orogeny in 1.91–1.79 Ga. A considerable amount of geological research has been carried out relating to the stratigraphy, metamorphism, deformation, and age determinations, providing insights into the geological evolution of the CLGB. Active exploration has been ongoing in parallel with the academic research, and as a result of this, several significant mineral deposits as well as numerous interesting prospects have been discovered. The most significant deposits relate to gold and base metals, but there is also a potential for other metals in the district. The discoveries clearly indicate that the CLGB is one of the most prospective Paleoproterozoic greenstone belts in Europe. Despite the several-decades-long exploration history, most parts of the CLGB remain underexplored, and the region is very likely to host a number of undiscovered mineral deposits.

Geological research and exploration in the CLGB have resulted in extensive geological and geophysical datasets on the area. Most of the interpretations of this data have been carried out in 2D, focusing on the surface geology, with limited interpretations of the geology at depth. The few studies focusing on the geology below the first few hundreds of meters of the current bedrock surface were also carried out in 2D as cross sections. A few deposit-scale 3D models have been constructed for the district. Almost all of them have focused on resource modeling and resolving the form, shape, size, and/or continuation of individual ore bodies. Geological 3D modeling or geomodeling became a standard tool for the gas and oil industry during the early 1990s, when geomodeling software, the development of which started in the 1980s, became mature. During the past 15 years, the use of geomodeling in visualizing and solving geological problems in mineral deposits and crystalline bedrock areas has become increasingly popular. In 2007, the Geological Survey of Finland initiated a 3D modeling project on the Central Lapland Greenstone Belt. The aims of the project were to: update the geological maps in selected areas, test the suitability of 3D modeling methods for geological modeling in targets at local and regional scales, develop methods for processing geophysical data sets to support the modeling, and develop GIS-based prospectivity maps. The modeling was carried out by combining available extensive geological and geophysical data sets, using a multidisciplinary approach in the interpretation. This report presents the results of the Central Lapland Greenstone Belt 3D modeling project in the following chapters. The locations of the study areas are presented in Figure 1.

Chapter I describes the use of the multiscale edge detection method or "worming" for the regional gravity data set on the CLGB. The work demonstrated that using worms enables us to better outline the major thrust and shear zones and that the worming data may be utilized in prospectivity analysis for epigenetic mineral deposits. The worming data presented in Chapter I were also used in 3D modeling presented in following chapters.

Chapter II presents a new Ni-Cu prospectivity model of the CLGB area, which was constructed using combined till geochemistry, airborne magnetics and regional gravity data. The results have identified more than 40 target areas favorable for Ni-Cu deposits. These include the Kevitsa Ni-Cu-Au-PGE deposit and the Sakatti Ni-Cu discovery, the former of which is currently under mining and the latter u nder active exploration and development. The high-pass filtering technique was used in filtering out the regional anomalies and enhancing the local anomalies in the data. Model validation indicates a clear spatial association with the current Ni exploration areas defined by exploration licenses.

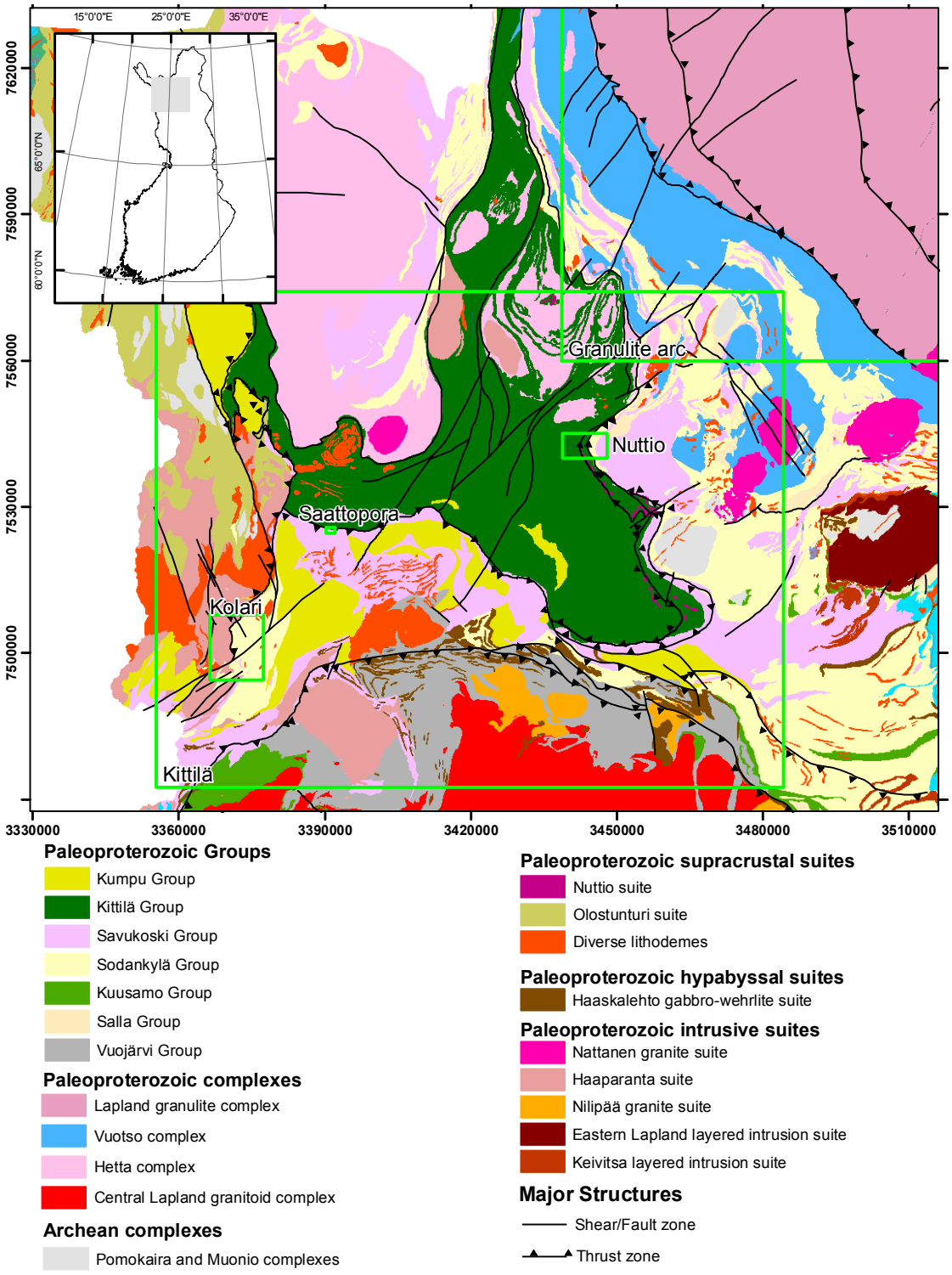

Fig. 1. Location of the study areas. Geology modified after the Bedrock of Finland – DigiKP. Contains data from the National Land Survey of Finland Topographic Database 03/2013 © NLS and HALTIK.

Chapter III describes a regional-scale 3D model of the Kittilä terrane and adjacent structures, including the northward-directed Sirkka and Venejoki thrust systems, the gold-critical NE–SW-striking Muusa and Kiistala shear zones, and the crustal-scale Enontekiö shear zone. The results demonstrate that the Kiistala terrane is up to 9 km thick in its thickest part and shows considerable thickness variation, which is most likely a result of thickening via stacking and folding during the compressional tectonic events. Based on the model, the gold potential of the Kittilä terrane has been estimated. This suggests that the undiscovered gold resources within the terrane may total up to several tens of millions of ounces.

Chapter IV presents a visual 3D model of the Kolari region based on new seismic data. The modeling results reveal issues in current 2D geological maps of the area. The results indicate that the current division of the Savukoski Group into the Rautuvaara and Kolari formations is not justified, but the two units should be merged into one. This also has direct implications for the exploration model of the Fe ± Cu-Au deposits in the area, which have been considered by some researchers to be strata-bound deposits. The results imply that the structural control rather than certain strata should be emphasized in exploration.

Chapter V presents a visual 3D model of the Lapland Granulite Belt (LGB) and adjacent Vuotso complex units. The model supports the work of several authors, suggesting that the Lapland Granulite Belt represents a listric, SE-vergent thrust system. Combining the modeling results and published metamorphic data on the LGB and adjacent Vuotso complex rocks, it appears that there was considerable variation in the transport distances of the different tectonic blocks during the thrusting event at 1.91–1.89 Ga.

A visual 3D model of the Saattopora Au-Cu deposit, an Au-Cu resource model, and new field observations are presented in Chapter VI. The modeling results reveal a folding pattern of the lithological units, the orientation of which corresponds to the F_3 folding from the outcrops. The southern 'B' ore body is controlled by a sub-vertical ESE-striking shear zone and the northern 'A' ore body is for the most part hosted by an intensely albitized phyllite unit located between komatiite and a mafic tuff unit. The mineralization appears to have taken place during the late phase of the regional D_3, or post-dates it. Based on the available drill core data, the mineralization is open to depth at ca. 120 below the surface.

Chapter VI presents a visual 3D model of the Lauttaselkä area located in the eastern margin of the Kittilä terrane. The model shows a thrust zone with west-vergent thrust folding, and reveals that the older Salla Group rocks have been thrusted on top of the younger Kittilä Group rocks, and the Nuttio suite ophiolite fragments have been obducted into the rock package.

CHAPTER I.
GRAVITY WORMS IN THE EXPLORATION OF EPIGENETIC GOLD DEPOSITS: NEW INSIGHTS INTO THE PROSPECTIVITY OF THE CENTRAL LAPLAND GREENSTONE BELT, NORTHERN FINLAND

Ilkka Lahti, Vesa Nykänen and Tero Niiranen

BACKGROUND

The spatial relationship between hydrothermal mineral deposits and faults and crustal discontinuities has been recognized and discussed by several authors (e.g., Groves et al. 1998, Goldfarb et al. 2001, Bierlein et al. 2006). Large deposits appear to have formed from large hydrothermal systems that are commonly located around major crustal structures (Jaques et al. 2002). However, secondary structures adjacent to larger primary structures also have an important role in ore-forming processes, as they act as pathways for mineralized fluids to the uppermost crust, and orogenic gold deposits, for example, are typically hosted by these second or lower order structures in relation to the larger structures (e.g., Sibson et al. 1988, Groves et al. 1998, McCuaig & Kerrich 1998, Chernicoff et al. 2002).

Various fault types and other geological discontinuities are commonly associated with petrophysical variations, causing potential field gradients. These gradients can be detected by geophysical measurements and subsequent interpretation of geophysical maps. The conventional interpretation of a geophysical map image essentially involves tracing contacts or edges between bodies of contrasting density or magnetic susceptibility by separating local extremes. Sun angles, vertical derivatives and upward continuations are commonly applied to enhance and simplify the image. Specifically, the horizontal derivatives of potential field data are often used to map the edges of bodies that generate gravity or magnetic anomalies. In both cases, the maxima of the horizontal derivative will be above a vertical contact. Multiscale edges, or in other words, worms, a term introduced by Hornby et al. (1999), are representations of potential field gradient maxima at various upward continuation levels. The technique has also been discussed and developed by Archibald et al. (1999) and Holden et al. (2000). Figure 2 shows the concept and processing stages of multiscale edge detection for gravity data.

The technique automatically detects the positions of gradient maxima at various upward continuation levels. The upward continuation level models the response of measurements collected at different heights above ground level. Worms obtained from low upward continuation levels are short wavelength gradient maxima that usually relate to shallow sources. High upward continuation worms, in turn, are long wavelength gradient maxima, which typically result from deeper crustal sources.

Worms are commonly associated with geological discontinuities such as faults, thrusts, and alteration zones that might be prospective for ore deposits (e.g. Bierlein et al. 2006, Austin and Blenkinsop 2008). For example, Archibald et al. (2001) noted a strong correlation between gravity worms of the Australian continental gravity dataset and the locations of large Zn–Pb and Cu deposits. A spatial relationship between worms and orogenic gold deposits has also recently been recognized (e.g. Bierlein et al. 2006).

In general, a worm image that contains results from several upward continuation levels can provide information on the apparent dip direction of geological contacts and boundaries. It is notewor-

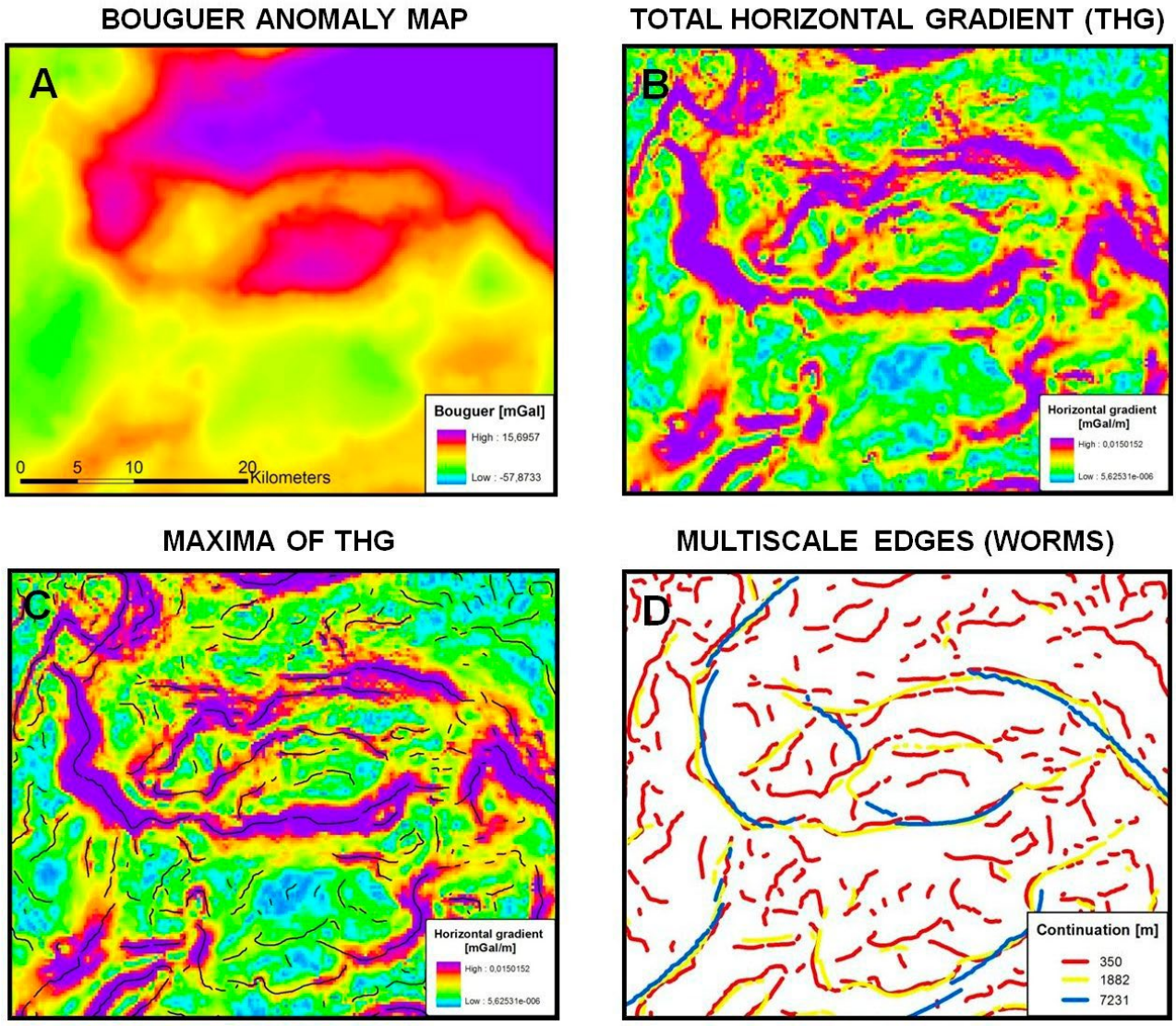

Fig, 2. The concept and processing stages of gravity worms.

thy that worms can identify geological features provided there is significant petrophysical variation to generate a contrast in the magnetic or gravity data set. Although worms are usually blind to geological structures that lack petrophysical contrast, some such boundaries (e.g. cross faults) may be inferred through linear truncations and offsets of gravity worms.

Recent advances in the processing and integration of large and diverse data sets have enabled geoscientists to increasingly apply computer-based GIS and conceptual strategies that can make the exploration process more effective. In this chapter, we describe the use of the worming technique on the gravity dataset from the Central Lapland Greenstone Belt. By including more than 19 000 ground gravity observations with an average site distance of ca. 0.5–2 km, the gravity Bouguer dataset can be considered relatively extensive and dense. The aim of the present study was to evaluate the spatial correlation of gravity worms and known gold deposits using the weights of evidence calculation procedure. We also aimed to reveal new prospective structures and thereby improve the confidence in area selection during gold exploration in the area.

REGIONAL GEOLOGICAL SETTING

Figure 3 presents a geological map of the study area. The Central Lapland Greenstone Belt (CLGB) is one of the largest Proterozoic greenstone terrains in the world. The CLGB consists of Paleoproterozoic volcanic and sedimentary cover (2.5–1.97 Ga) on the Archean granite gneiss basement (3.1–2.6 Ga) (Lehtonen et al. 1998, Hanski & Huhma 2005). The Paleoproterozoic bedrock of the CLGB consist of a 2.44–1.98 Ga supracrustal sequence of mafic to ultramafic metavolcanic rocks, quartzites, phyllites, and graphitic schists that are intruded by 2.2–2.05 Ga mafic dykes and sills, 1.91–1.86 Ga mafic to felsic intrusions, and 1.80–1.77 Ga felsic intrusions (e.g. Hanski et al. 2001, Hanski &

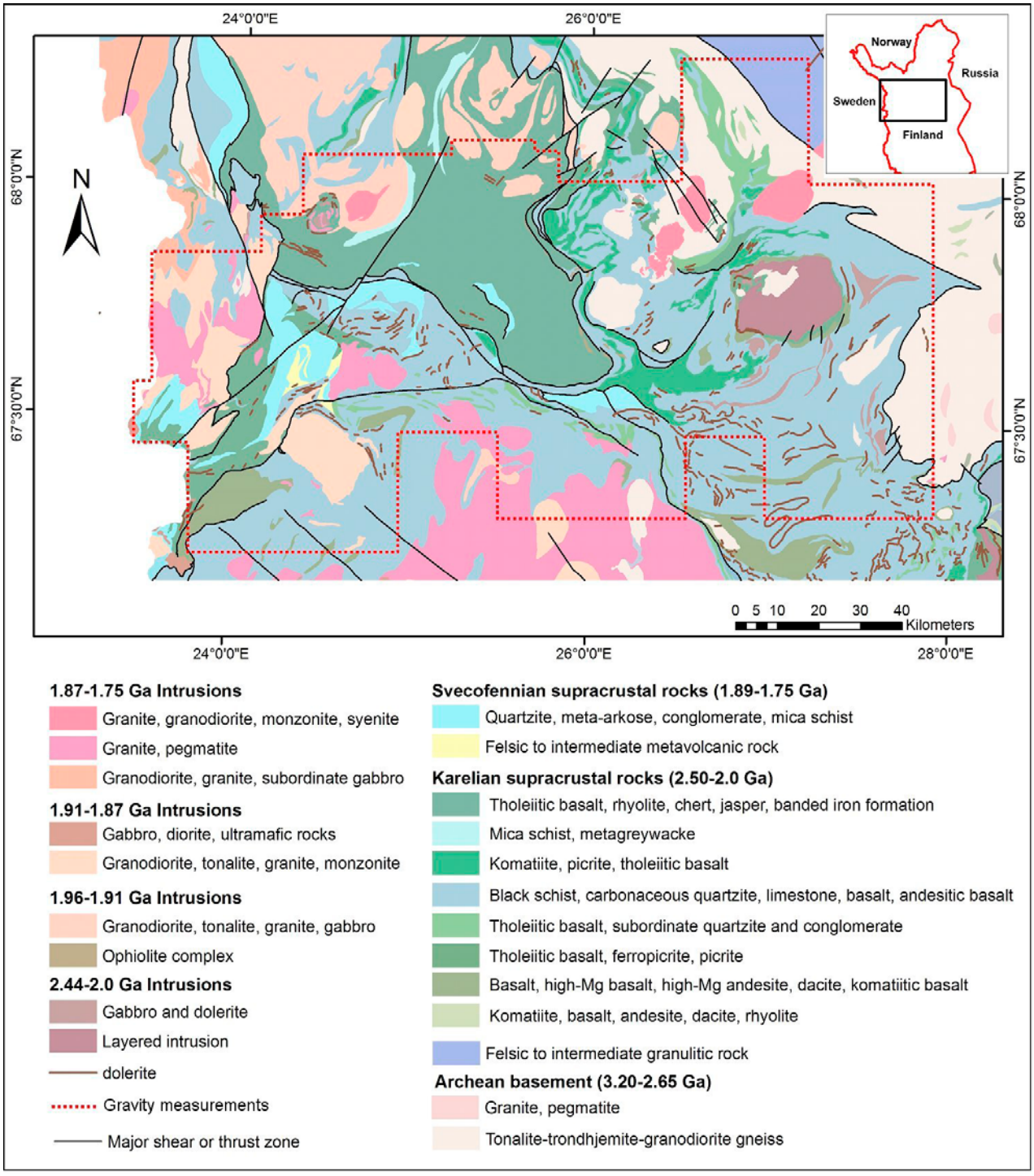

Fig. 3. Geological map of the study area. The red dashed line indicates the area of gravity measurements. Contains data from the National Land Survey of Finland Topographic Database 03/2013 © NLS and HALTIK.

Huhma 2005). Lehtonen et al. (1992) and Hanski (1997) have linked the volcanites of the CLGB to an allochthon that is overthrusted. The core of the CLGB consists of a thick sequence of mafic volcanic rocks of the ca. 2.0 Ga Kittilä group, which has been interpreted to represent an allochthonous to para-autochthonous unit bound by tectonic contacts with the surrounding units (Lehtonen et al. 1992, Hanski 1997, Hanski & Huhma 2005) Interpretations from reflection seismic studies (Patison et al. 2006, Niiranen et al. 2009) and potential field modeling (Elo et al. 1989, Lehtonen et al. 1998) suggest that the volcanic rock-dominated greenstone belt has a maximum thickness of roughly 6–10 km.

Two operating gold mines (Pahtavaara and Suurikuusikko) together with more than 30 drilling-indicated gold occurrences are located within the CLGB (Eilu 1999, 2007). The majority of the gold occurrences fall into the orogenic gold category. These greenstone-hosted gold mineralizations are similar in many ways to those in more established mineral districts such as the Yilgarn region of Western Australia and Superior Province of Canada (Patison 2007). Currently, the largest known orogenic gold deposit in the area is the Suurikuusikko deposit, with current resources exceeding 6 million ounces of Au. Iron oxide-copper-gold (IOCG) deposits with extensive albite alteration haloes around them are also known within the region (e.g. Eilu et al. 2007). The gold-bearing occurrences in the western part of the study area are mainly of the IOCG-type. The largest known gold resources in an IOCG-type deposit are in the Hannukainen deposit, with ca. 200 000 ounces of gold. There are also a few Paleoplacer gold deposits in the study area, but these are not considered in this work.

DESCRIPTION OF THE DATA AND PROCESSING

Gravity data

Finland is exceptionally well covered by gravity measurements. The Finnish Geodetic Institute has established a national gravity net with an average station separation of 5 km (e.g. Kääriäinen & Mäkinen 1997). In addition, the Geological Survey of Finland (GTK) has performed both target and regional scale gravity surveys for decades. In 1972, GTK initiated regional gravity surveys in order to obtain more dense regional gravity data than that of the Finnish Geodetic Institute. The measurements have primarily focused on regions with high mineral potential and areas having key roles in crustal studies (Elo 1998). The average station interval is about 1–6 sites per km^2. In 2008, the regional gravity register of GTK contained 264 500 gravity observations covering an area of 75 150 km^2, which is more than 20% of the Finnish territory. Data acquisition has primarily been carried out using Worden, Scintrex CG-3, and CG-5 gravity meters.

The gravity measurements of the CLGB area started in 1972, while the latest measurements used in this analysis were carried out in the summer of 2009. The total number of gravity observations used in this study was 19 273. The density of gravity observations is mainly 1–4 sites per square kilometer. The most dense observations have been made in the northern and northwestern parts of the study area, representing the latest measurements using novel data acquisition procedures.

Figure 4 displays the Bouguer gravity grid that was obtained using the minimum curvature gridding algorithm and the cell size of 250 x 250 m. The gold mines are indicated by yellow stars. Bouguer gravity values range from -58 to 16 mGal, with a mean value of -24.7 mGal in the study area. The extensive Bouguer maximum in the central part of the study area mainly results from mafic volcanic rocks of the CLGB. The Bouguer minimum in the northwest is caused by granitic rocks of the Hetta complex. The Bouguer minimum to the north of Pahtavaara mine is due to tonalitic and granodioritic gneisses of the Archean basement (Pomokaira Complex).

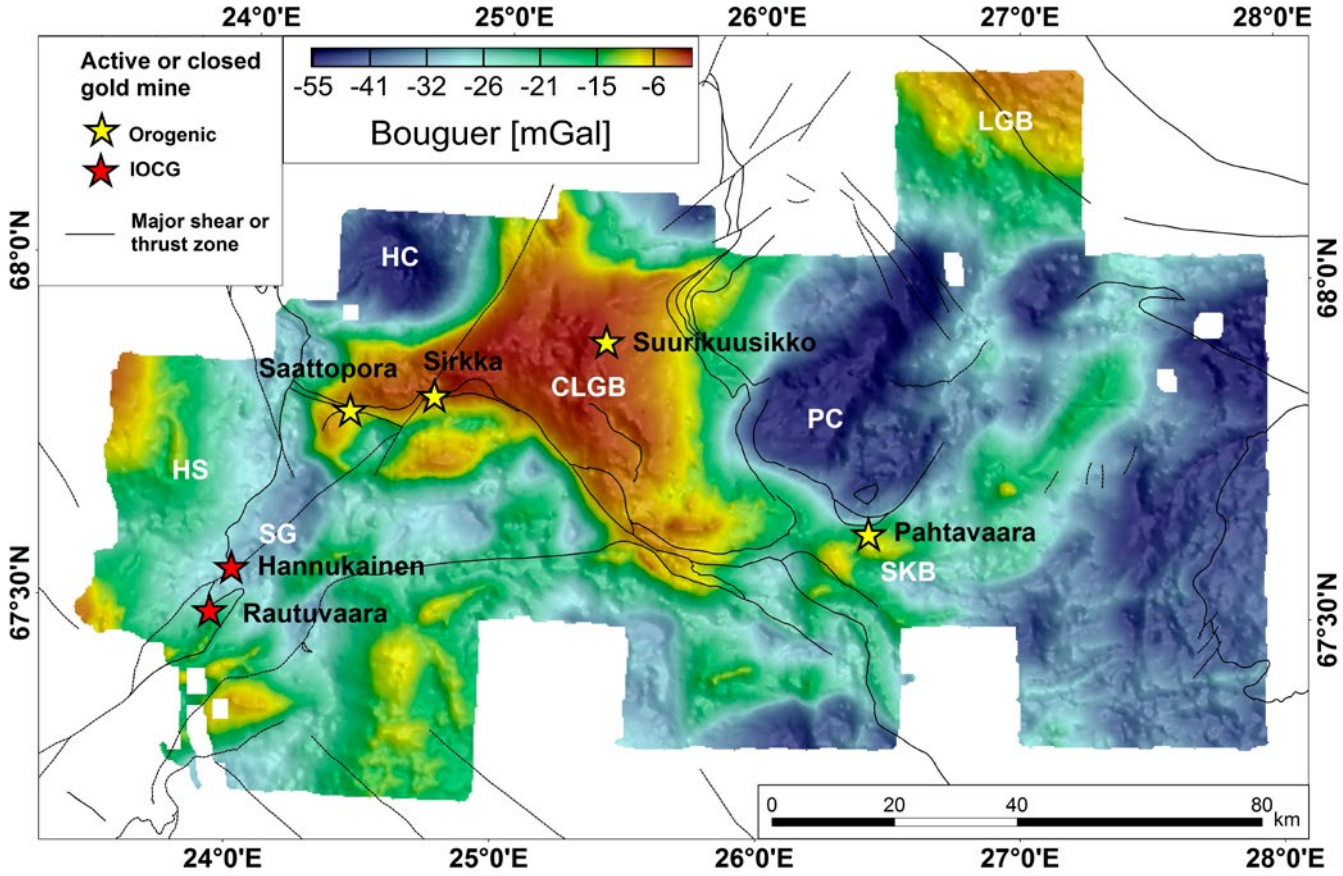

Fig. 4. Bouguer gravity map of the study area and major thrust and shear zones. Abbreviations: PC = Pomokaira Complex, SKB = Sattasvaara Komatiite Belt, CLGB = Central Lapland Greenstone Belt, HC = Hetta Complex, HS = Haaparanta Suite, SG = Sodankylä Group, LGB = Lapland Granulite Belt.

Worming

Worms were processed using the WormE wizard of the Intrepid Software v4.2. Processing was performed using 12 upward continuation levels with a multiplying factor of 1.4 times the cell size (250 m), resulting in upward continuation levels from 350 m to 14 172 m. Figure 5 shows calculated gravity worms on a grey-shaded Bouguer anomaly map. Red and blue worms represent the lowest and the highest upward continuation levels, respectively. The figure also indicates the location of the known gold deposits, prospects and active or closed mines of the study area. Mineral deposit data were acquired from the FINGOLD database (Eilu 1999, 2007) maintained by the Geological Survey of Finland. All of the known orogenic gold and IOCG deposits in the CLGB show intimate spatial correlations with shear zones of varying scale. Figure 5 illustrates that gravity worms have a clear spatial correlation with the known orogenic gold and IOCG deposits

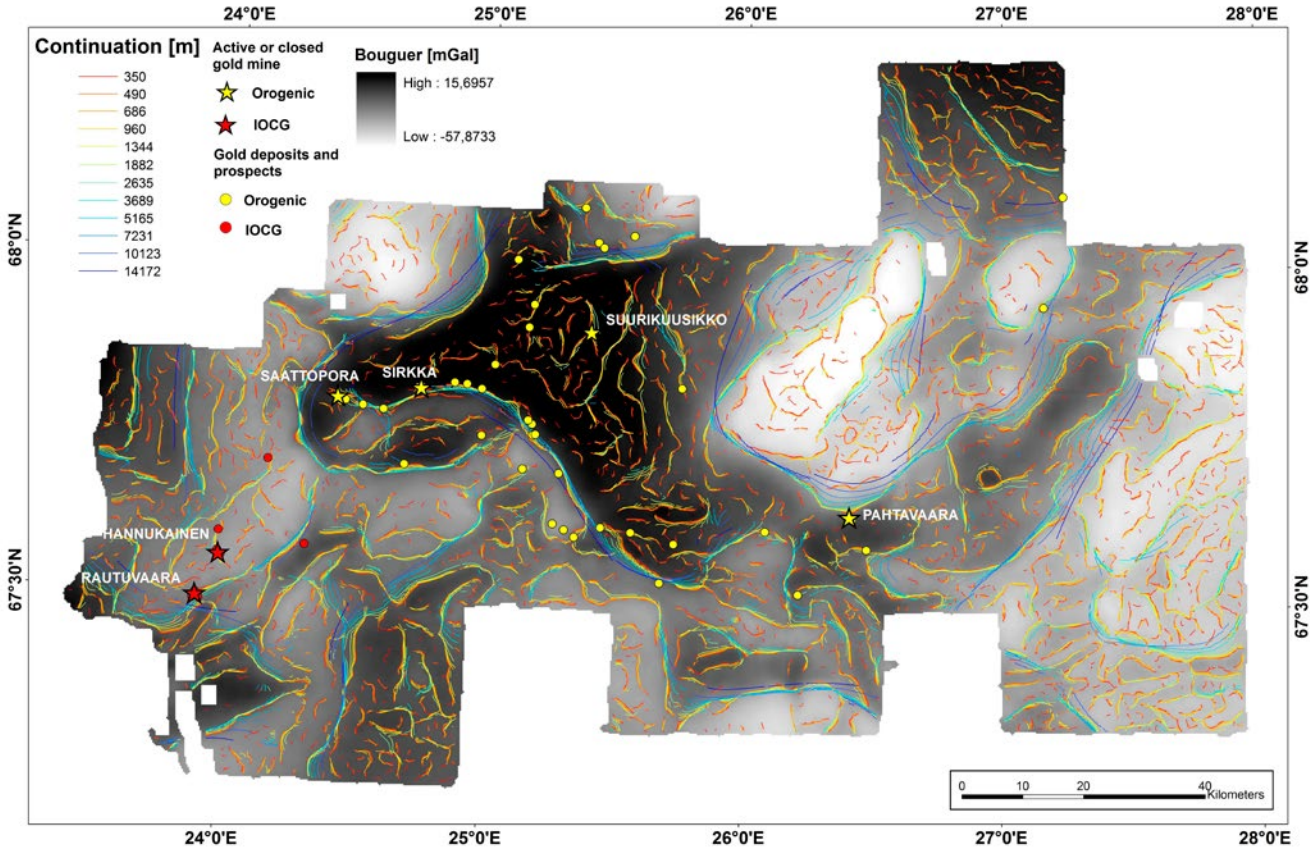

Fig. 5. Gravity worms, gold deposits and prospects of the study area. The background image is a grey-shaded Bouger gravity data.

MAIN GEOLOGICAL IMPLICATIONS

Figure 6 presents the gravity worms on a geological map of the study area. The worms highlight major geological boundaries that are also evident in the source Bouguer data and well known from previous bedrock mapping and exploration studies. One of the main advantages of worming is the capability to detect weak gravity gradients that are not clearly seen in the source data. The small-scale structures adjacent to larger ones have an important role in ore-forming processes, as they can act not only as pathways for mineralized fluids to shallow depths, but also as suitable traps for gold deposition in the study area. These worms are mainly located within the main lithological units. Several approximately N–S-trending worms are seen in the CLGB. For example, the large Suurikuusikko orogenic gold deposit and associated shear zone correlates well with the N–S-elongated worm. The worm breaks into two parts in the mining camp area (Fig. 5). To the east of the Suurikuusikko ore deposit, a number of N–S-trending worms indicate other possible prospective structures.

The major gold hosting structure in the study area is the Sirkka shear zone (Fig. 6), which is located at the southern edge of the central Lapland Greenstone Belt (Figs. 5 and 6). This shear zone contains two closed gold mines (Saattopora and Sirkka) and a number of gold deposits and prospects. Besides the shear zone itself, the gravity worm partly results from the density difference between the mafic volcanic rocks of the CLGB and the volcano-sedimentary rocks and quartzites to the south of the CLGB. The worm could be also interpreted as a lithological contact zone or tectonic boundary.

All the main structures associated with the IOCG deposits (Hannukainen and Rautuvaara) and prospects are clearly indicated by gravity worms (Fig. 5). These deposits are epigenetic in origin owing to a similar genetic link to the structures as the orogenic gold deposits. In Hannukainen and Rautuvaara, the observed worms are prob-

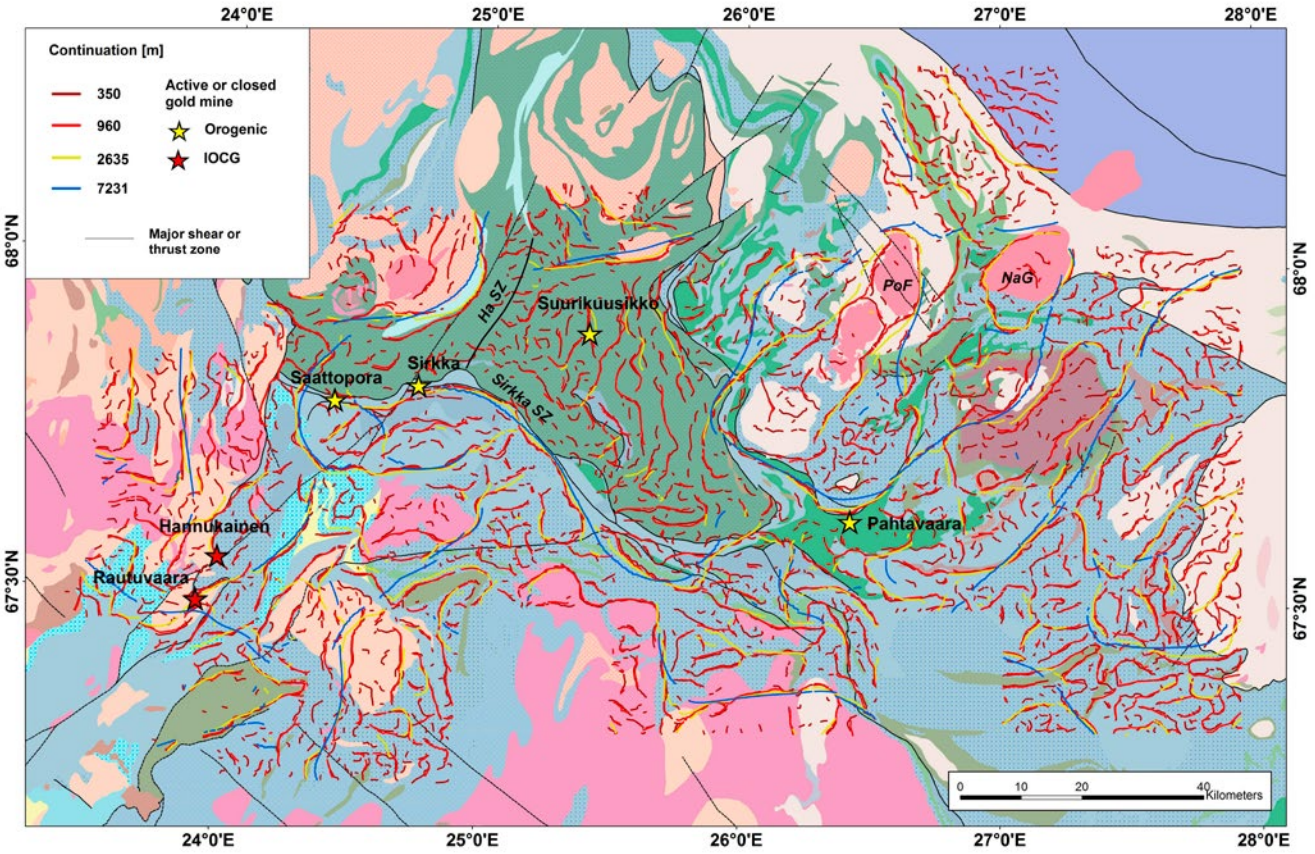

Fig. 6. Gravity worms at five continuation levels on a geological map.

ably caused by lithology, as deposits are located in the contact zone of large units of granitoids and volcanic-sedimentary rocks. However, the Rautuvaara worm extends northeastwards through volcanic-sedimentary rocks, suggesting a primarily structural rather than lithological source. Drillings performed in the target area have shown that the contact zone between the two units is tectonized in the NE–SW direction. It is therefore likely that the prolongation of the Rautuvaara worm is due to the structure that extends northeastwards. This could be a link to a minor IOCG prospect (Lauttaselkä) that is located approximately 20 km from Rautuvaara at the northeastern prolongation of the worm (Fig. 5). The observed structure might be prospective and hopefully increases confidence in area selection of IOCG exploration in the target area.

The gravity worms also indirectly reflect thrust zones, shear zones, lithological contacts, and alteration structures. For example, the presence of the major Hanhimaa shear zone (HaZ) is indicated by the truncation of worms at its location. The NE–SW-striking shear zone is marked as a black line in Figure 6. The NW–SE cross-cutting faults of the Pomokaira formation (PoF in Fig. 6) are an excellent example of the truncation of worms due to fault structures. To the east, the southern contact of the Nattanen Granite intrusion (NaG) can be traced to greater depths. Besides these, it is necessary to emphasize other sources that generate worms: the unexposed 3D geometry of geological units, density differences between adjacent lithologies (schists, granitoids, mafic volcanites, and banded iron rocks in the CLGB), and their relative displacements cause gravity worms. As the processing of worms is a straightforward technique, possible errors in worming results are mainly caused by errors in the source data and gridding of this data.

SPATIAL CORRELATION OF GRAVITY WORMS AND GOLD OCCURRENCES

For this study, the multivariate empirical approach called weights of evidence (WofE) was applied to gravity worm data. The WofE method is a Bayesian approach for combining data to predict the occurrence of events. Although the technique was initially developed as a diagnostic tool in medicine, it has been extensively used in mineral prospectivity studies (e.g. Bonham-Carter et al. 1988, Bonham-Carter 1994, Agterberg et al. 1990, Raines 1999, Nykänen & Salmirinne 2007). The method is based on the presence or absence of a characteristic feature or pattern and the occurrence of an event.

Two types of probabilities, i.e. W+ and W-, can be computed for each class in the themes of the model. For example, a class could be defined either by a high magnetic intensity or a selected proximity class from the structural lineament. For each class, a W+ probability value is computed from the presence of a feature (or training point) in the class area. In our study, gravity worms were described as a proximity map classified into 16 classes using the quantile method in GIS. The W+ probability for each class was calculated using the equation:

$$W_i^+ = 1n \frac{N(B_i \cap D) \mid N(D)}{A(B_i) \mid A(T)} \quad (1)$$

where
$N(B_i \cap D)$ = number of gold occurrences within a map class *i*
$N(D)$ = total number of gold occurrences within the study area
$A(B_i)$ = area of map class i
$A(T)$ = total study area

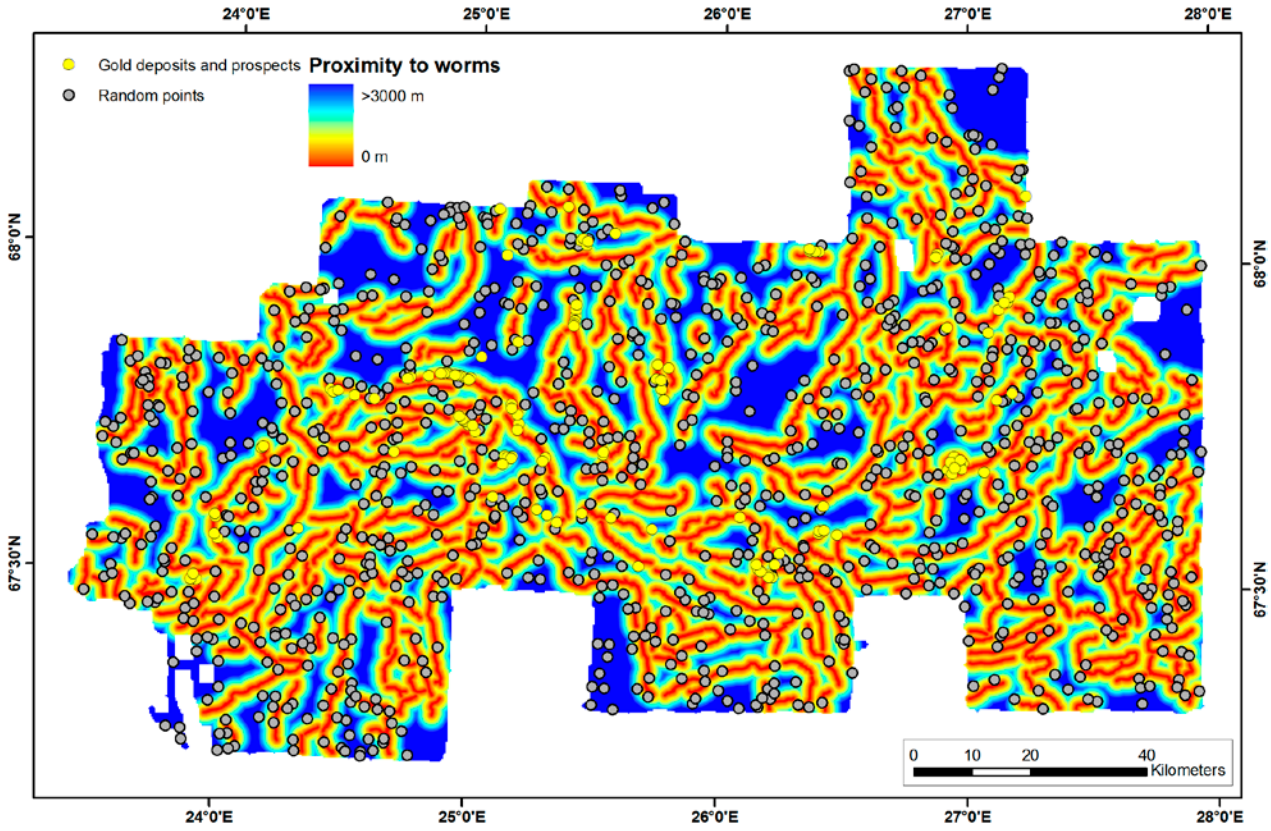

Fig. 7. Training points and proximities to the worms.

Similarly, a W^- probability value is calculated from its absence from the class area. The commonly used value is the contrast C, which is calculated from the difference between W^+ and W^-. It can be used as measure of the correlation power between the tested theme and the modeled occurrence of the feature. One of the main advantages of the WofE technique is the possibility to identify those data and data combinations that contribute most to the results.

Figure 7 presents a proximity map of the selected worms. The 119 yellow points representing the

gold occurrences were used for the calculation of weights and the 983 grey random points were used for comparison. The results of the weight calculations are provided in Figure 8.

The prospective area based on the calculation of weights is shown in Figure 9. The calculation reveals that, while the calculated worms cover only 30% of the total area, 70% of the known gold occurrences lie within this area, i.e. within 675 meters from the gravity worms. This demonstrates that gravity worms are spatially correlated with known gold deposits and prospects in the CLGB.

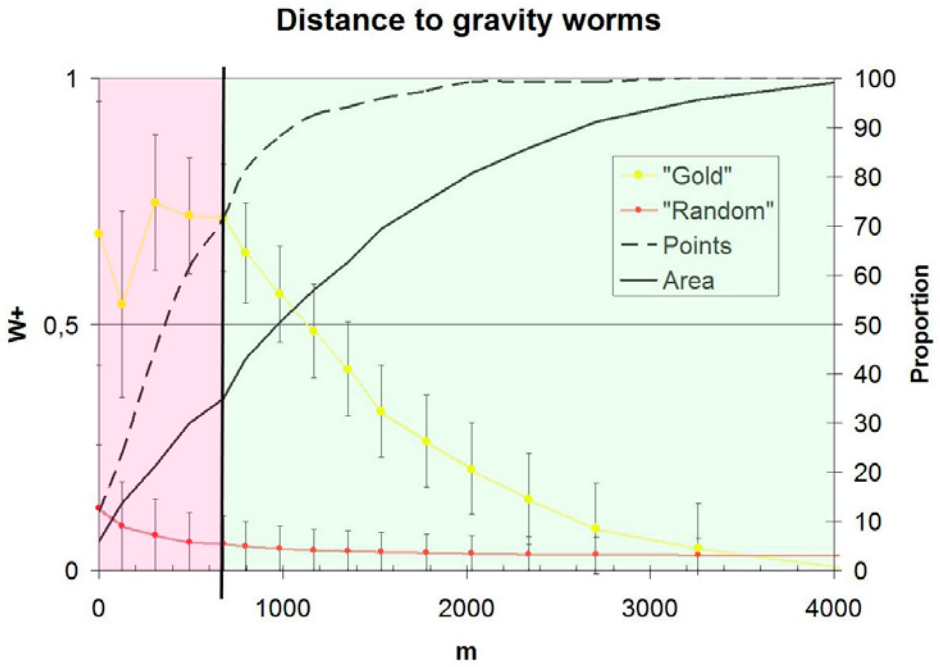

Fig. 8. Results of the calculation of weights.

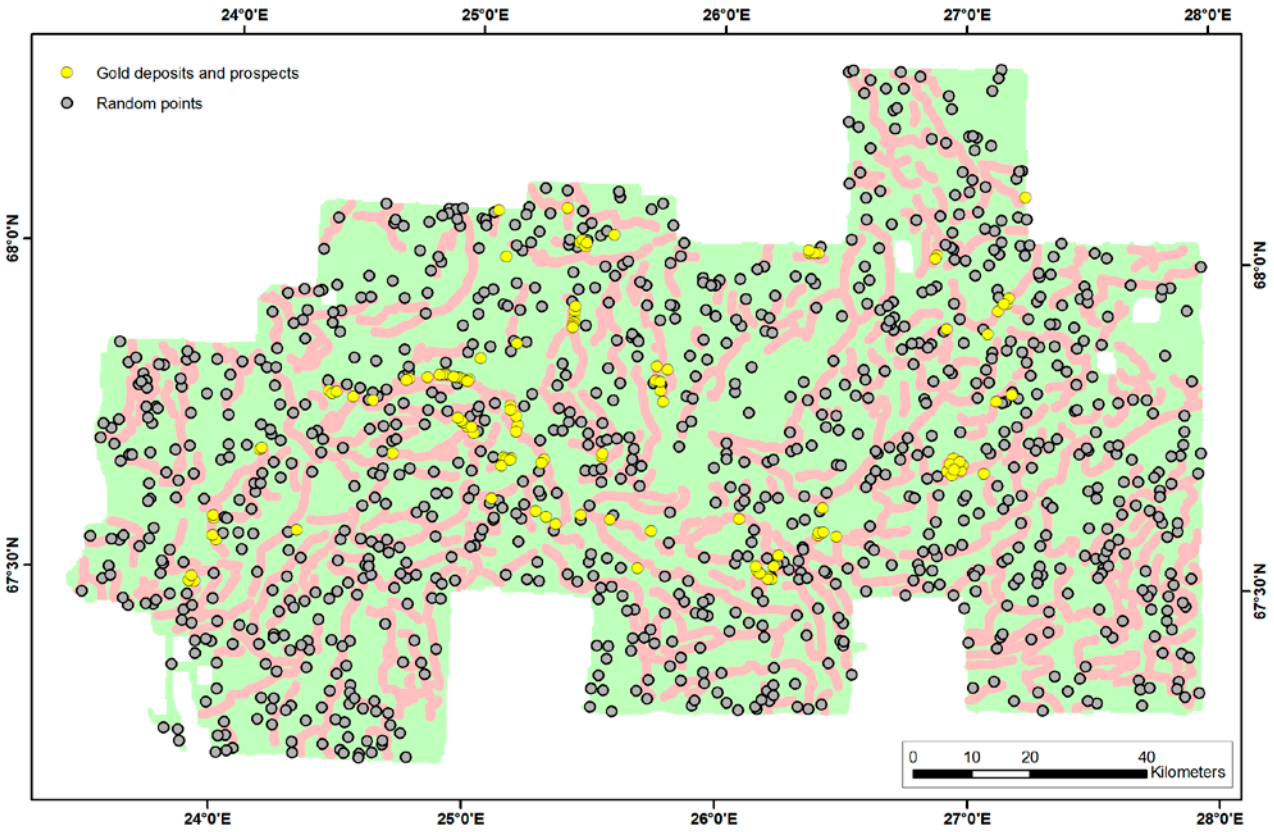

Fig. 9. Prospective area for gold based on the worms.

CONCLUSIONS

The relatively large gravity Bouguer dataset enabled us to quantitatively test the spatial correlation of gravity worms and structurally controlled gold deposits within the CLGB, northern Finland. All of the known orogenic and IOCG deposits show intimate spatial correlation with shear zones of varying scale. Gravity worms spatially correlate with known gold deposits and prospects within the CLGB. For example, the Suurikuusikko orogenic gold deposit, which is the largest known gold deposit in Europe, is associated with an N–S-trending worm in the study area. The worm breaks into two separate parts in the mining camp area. Numerous orogenic gold prospects and two closed gold mines at the Sirkka shear zone are indicated by the gravity worms. All IOCG deposits and prospects have a positive correlation with gravity worms in the study area.

WofE analysis revealed that while the calculated worms cover only 30% of the total area, 70% of the known gold occurrences lie within this area, i.e. within 675 meters from the gravity worms.

CHAPTER II.
NI PROSPECTIVITY MAPPING USING FUZZY LOGIC AND RECEIVER OPERATING CHARACTERISTICS (ROC) MODEL VALIDATION IN THE CENTRAL LAPLAND GREENSTONE BELT, NORTHERN FINLAND

Vesa Nykänen, Ilkka Lahti and Tero Niiranen

INTRODUCTION

The Central Lapland Greenstone Belt (CLGB) is located in the Northern Fennoscandian Shield, approximately 100 km north of the Arctic Circle (Fig. 10). The CLGB consists of Paleoproterozoic volcanic and sedimentary cover (2.5–1.97 Ga) on the Archean granite gneiss basement (3.1–2.6 Ga) (Lehtonen et al. 1998, Hanski & Huhma 2005). Rifting events of the Archean continent from 2.5 Ga to 1.97 Ga resulted in mostly tholeiitic mafic intrusions, dykes, and lavas. There is one operating nickel mine within the CLGB, and active nickel exploration is ongoing in the surrounding areas. Traditionally, mineral potential assessments are based on expert opinions on potential areas for a particular deposit type. However, modern digital geological maps allow quantitative analysis of data,

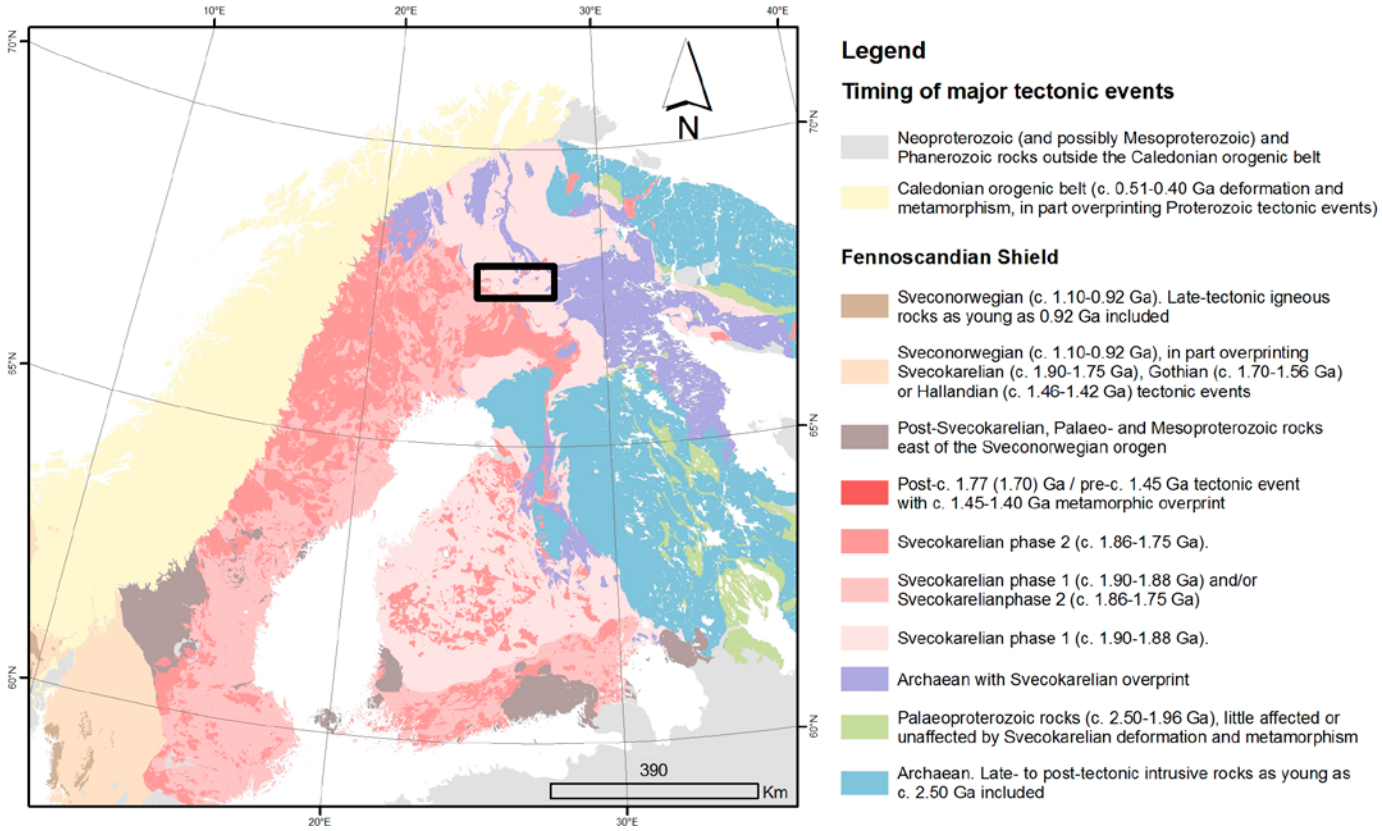

Fig. 10. Location of the study area in the Northern Fennoscandian Shield.

and thus numerical modeling for prospectivity mapping or exploration targeting. The advantage of these techniques is easy documentation of the model parameters and the possibility to refine the numeric models in an iterative manner. Therefore, it is straightforward to test several model scenarios (i.e. exploration models) with subtle or more drastic changes. There are two main approaches to performing a prospectivity analysis (Bonham-Carter 1994):

(1) The conceptual approach uses expert opinions and knowledge to re-formulate a theoretical or practical exploration model into a set of criteria that can be described by a mathematical formula. This approach is suitable for 'greenfield' mineral exploration terrains with only a limited number of known deposits available for statistical assessment. These techniques include fuzzy logic or expert weights of evidence. Unsupervised classification can also be considered to belong to this category.

(2) The empirical approach uses the known mineral occurrences within the study area as 'training points' for examining spatial relationships or correlations between the known occurrences and spatial data. These techniques are suitable for mature 'brownfield' exploration terrains with abundant data available. Supervised classification, e.g. neural networks, weights of evidence, or logistic regression, belong to this category.

The conceptual approach uses the expertise of the exploration geologists, geochemists, and geophysicists to define the threshold values for the evidential datasets. In classical set theory, the membership of a set is defined as true or false (1 or 0), whereas membership of a fuzzy set is expressed on a continuous scale from 1 to 0 (e.g. somewhere between 'anomalous' vs. 'not anomalous'). The values of fuzzy membership can be chosen based on the subjective judgment of an expert. Membership reflects the degree of truth of some proposition or hypothesis, which is often a linguistic statement such as high magnetic values are anomalous for gold deposits. To define the membership function, one needs to define the thresholds for 'not anomalous' and 'anomalous' values, and then a function describing the 'maybe – probably' values in between these two thresholds. The fuzzy membership values reflect the relative importance of each class of the maps used. The closer the fuzzy membership value is to one, the more significant is the map pattern. After defining the fuzzy membership functions for each evidential map, a variety of operators can be used to combine the membership values.

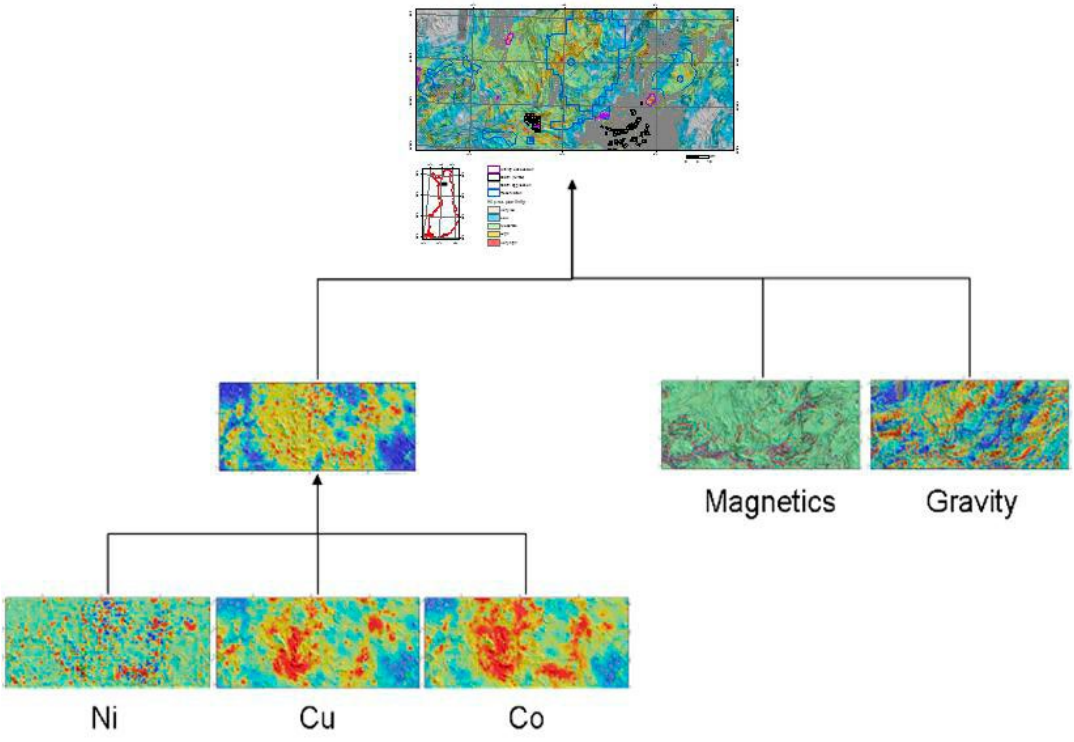

Fig. 11. Inference network describing the exploration model.

For the study reported in the present chapter, we defined a simple exploration model that integrates aeromagnetic data with data from regional gravity and till surveys. Data integration was performed using the fuzzy logic technique as described, for example, by Bonham-Carter (1994) and Nykänen et al. (2008b). This conceptual knowledge-driven method was used because there are not enough known nickel deposits within the study area to be able to carry out empirical data-driven prospectivity analysis. The selection of these data was based on the assumption that Ni deposits are related to local magnetic and gravimetric anomalies caused by Ni-critical lithologies. Since Ni is associated with sulfides, it is also assumed that these deposits would show elevated concentrations of Ni, Cu and Co in regional till assays compared to background values. Therefore, an inference network described in Figure 11 was drafted.

All the data preparation and spatial data analysis for this study was performed in ArcGIS 9.3 enhanced with the Spatial Data Modeller (SDM) toolbox (Sawatzky et al. 2009). The procedure for using these tools in mineral prospectivity mapping is extensively described by Nykänen (2008) and references therein.

DATA USED FOR MODELING

Magmatic sulfide deposits can be divided into two main groups (Naldrett 2011): 1) sulfide-rich Ni and Cu deposits, and 2) sulfide-poor PGE deposits. These deposits form from the segregation and concentration of sulfide liquid droplets from ultramafic or mafic magmas, and the partitioning of chalcophile elements into these droplets from the silicate magma forming the ultramafic or mafic rocks. These rock types typically have a higher density and magnetic susceptibility than surrounding felsic rock types, and they can therefore be seen as magnetic anomalies or gravity anomalies. Due to glacial dispersion, the outcrops of these deposits can cause elevated values of chalcophile elements in till deposits. Therefore, the exploration model we use for predicting magmatic nickel deposits defines that the host rocks of Ni deposits are characterized by local magnetic and gravimetric anomalies. A high-pass filter was applied to these data to exclude the long wavelength regional anomalies and enhance the locally derived shallow anomalies caused by possible

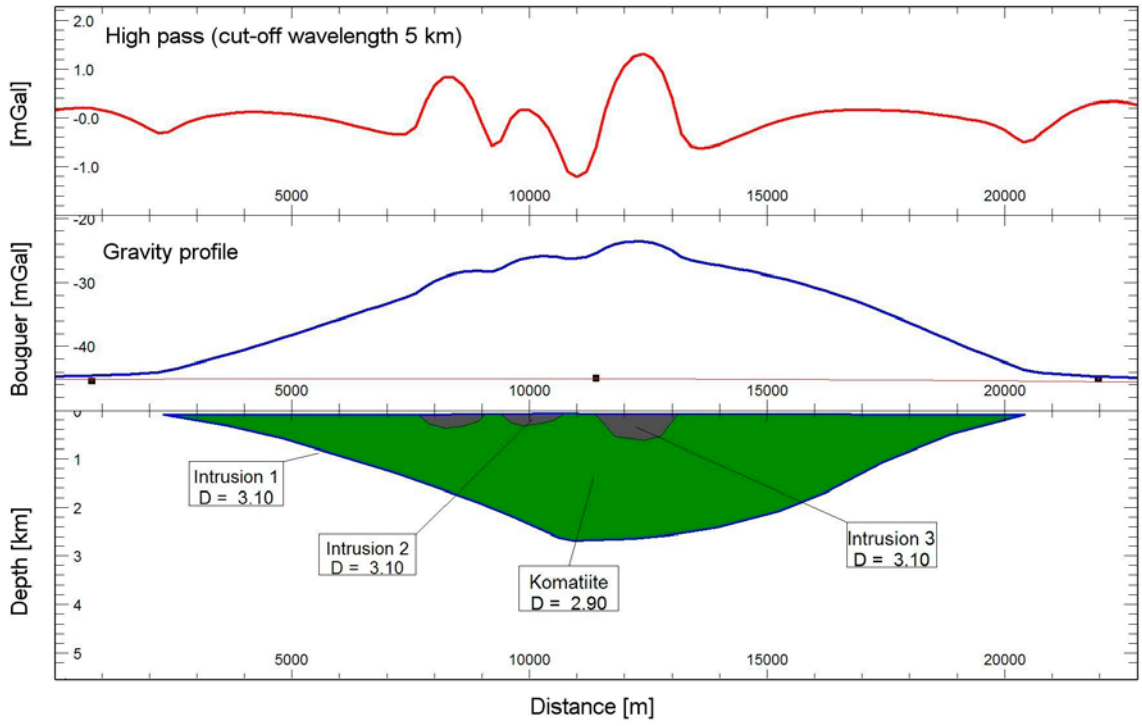

Fig. 12. Filtering of the gravity data using a high-pass filter.

mafic-ultramafic intrusions. The principle of this filtering technique is defined in Figure 12. In GIS, this filtering can be performed by using a moving window of a fixed radius across the study area to calculate the median value, which is subtracted from the original data values (e.g. Nykänen et al. 2008a). The resulting residual grid is then used as the input in the prospectivity model. This filtering was applied to the total intensity of the magnetic field (Fig. 13), regional gravity (Fig. 14), and to

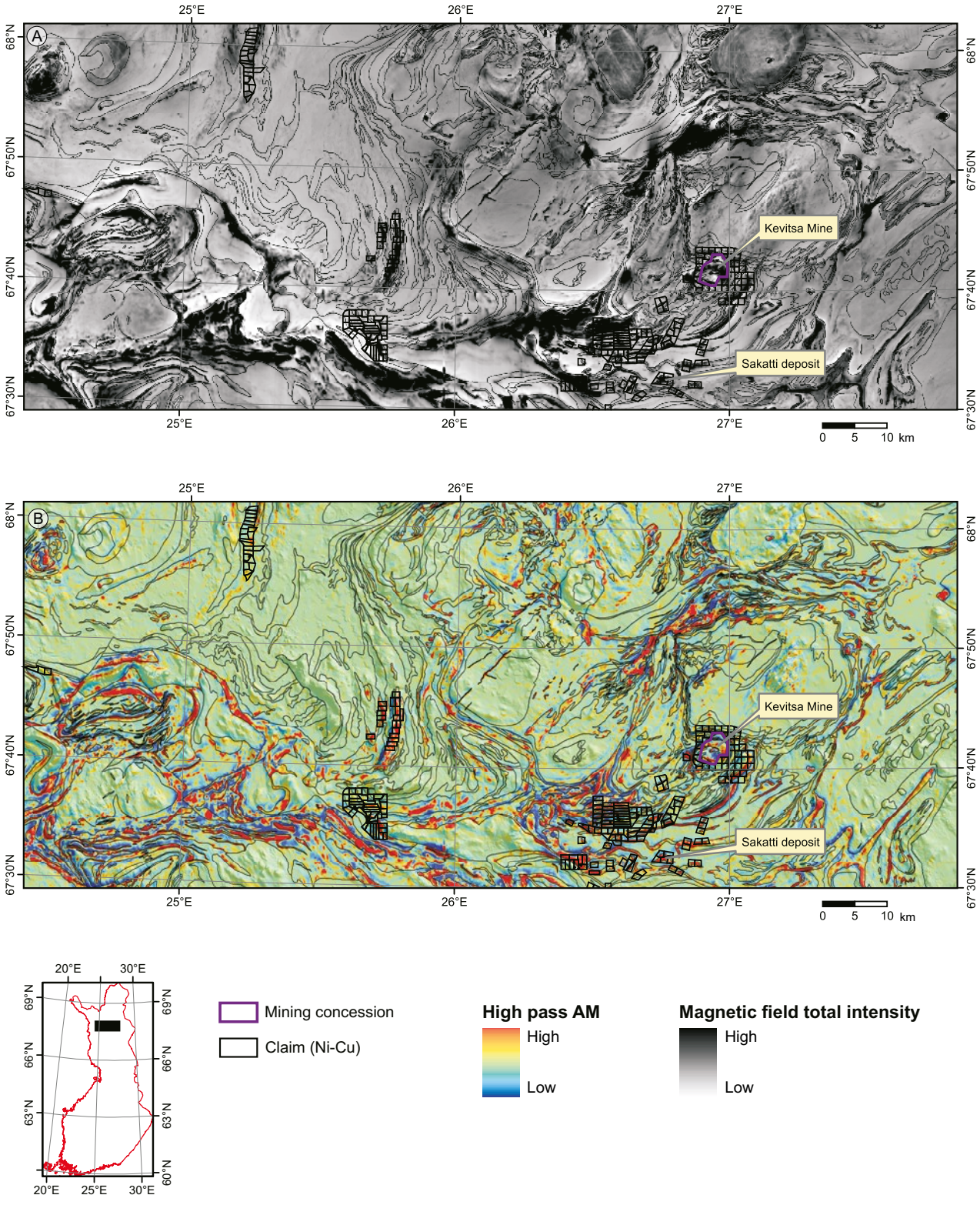

Fig. 13. A) Magnetic field total intensity. B) Residual of the magnetic field total intensity using a high-pass filter with the median value over a 2000-m-radius neighborhood. Contains data from the National Land Survey of Finland Topographic Database 03/2013 © NLS and HALTIK.

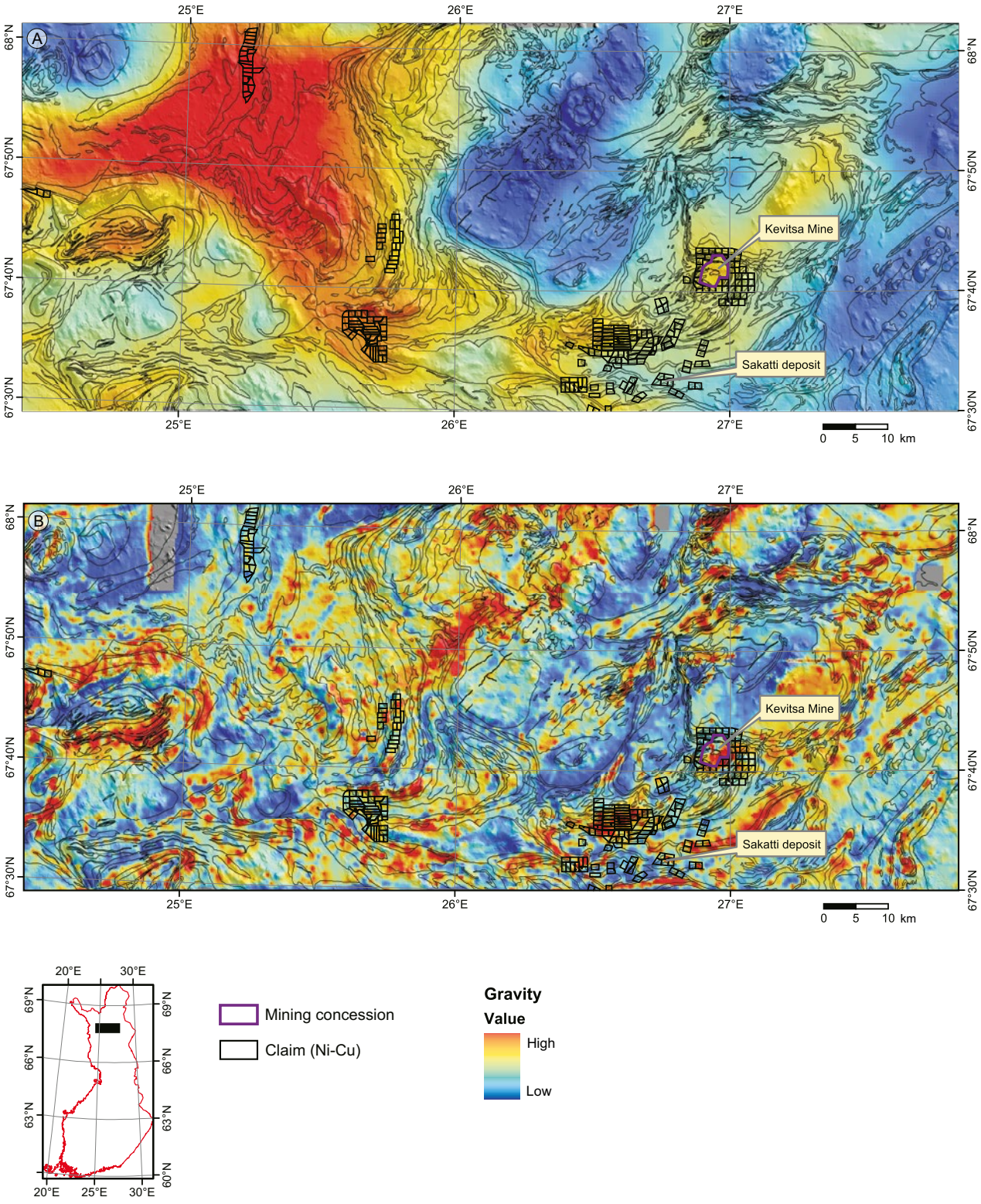

Fig. 14. A) Regional gravity Bouguer anomaly. B) Residual of the Bouguer anomaly using a high-pass filter with the median value over a 2000-m-radius neighborhood. Contains data from the National Land Survey of Finland Topographic Database 03/2013 © NLS and HALTIK.

Ni concentrations in regional till geochemistry (Fig. 15). For the geophysical data, we used a moving window with a 2000-m radius, whereas for the regional till data we used a neighborhood with a 6000-m radius. This was due to the spatial resolution, which was much coarser for the till data, with 1 sample per 4 square kilometers, when compared with the geophysical data. The airborne magnetic data were recorded using a line spacing of 200 m, and the sampling density for regional

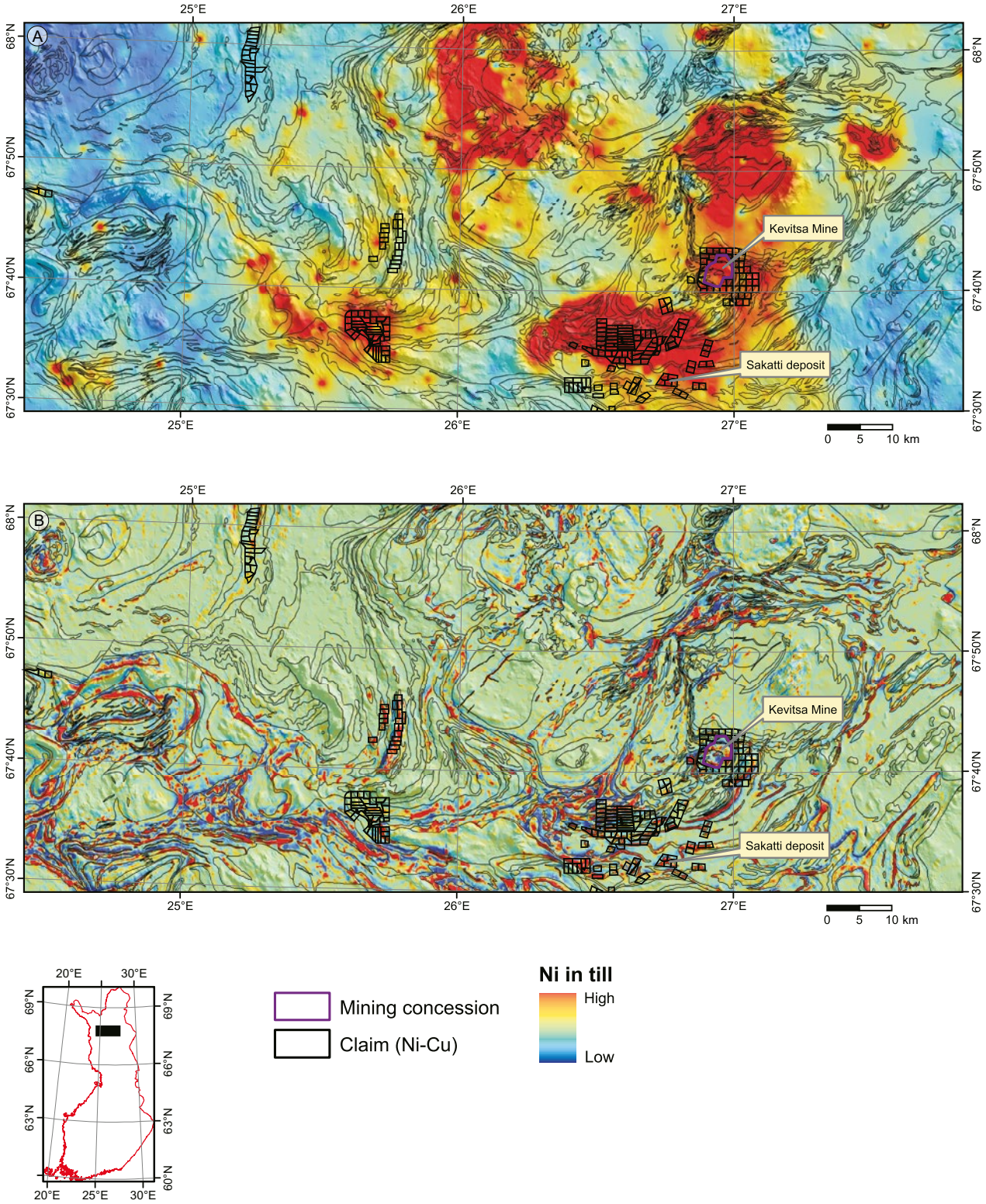

Fig. 15. A) Ni in regional till interpolated using inverse distance method in GIS. B) Residual of Ni anomaly map using a high-pass filter with the median value over a 6000-m-radius neighborhood. Contains data from the National Land Survey of Finland Topographic Database 03/2013 © NLS and HALTIK.

gravity was 1 measurement per square kilometer. The filtering enabled us to recognize the local anomalies, which would otherwise be masked by the long wavelength regional anomalies derived from deeper sources. The selection of the radius of the regional field was, however, somewhat problematic and definitely a source of uncertainty. Nickel, copper and cobalt in regional till were combined using a fuzzy AND operator (Fig. 16). This map was used as one of the inputs in the final prospectivity map described below.

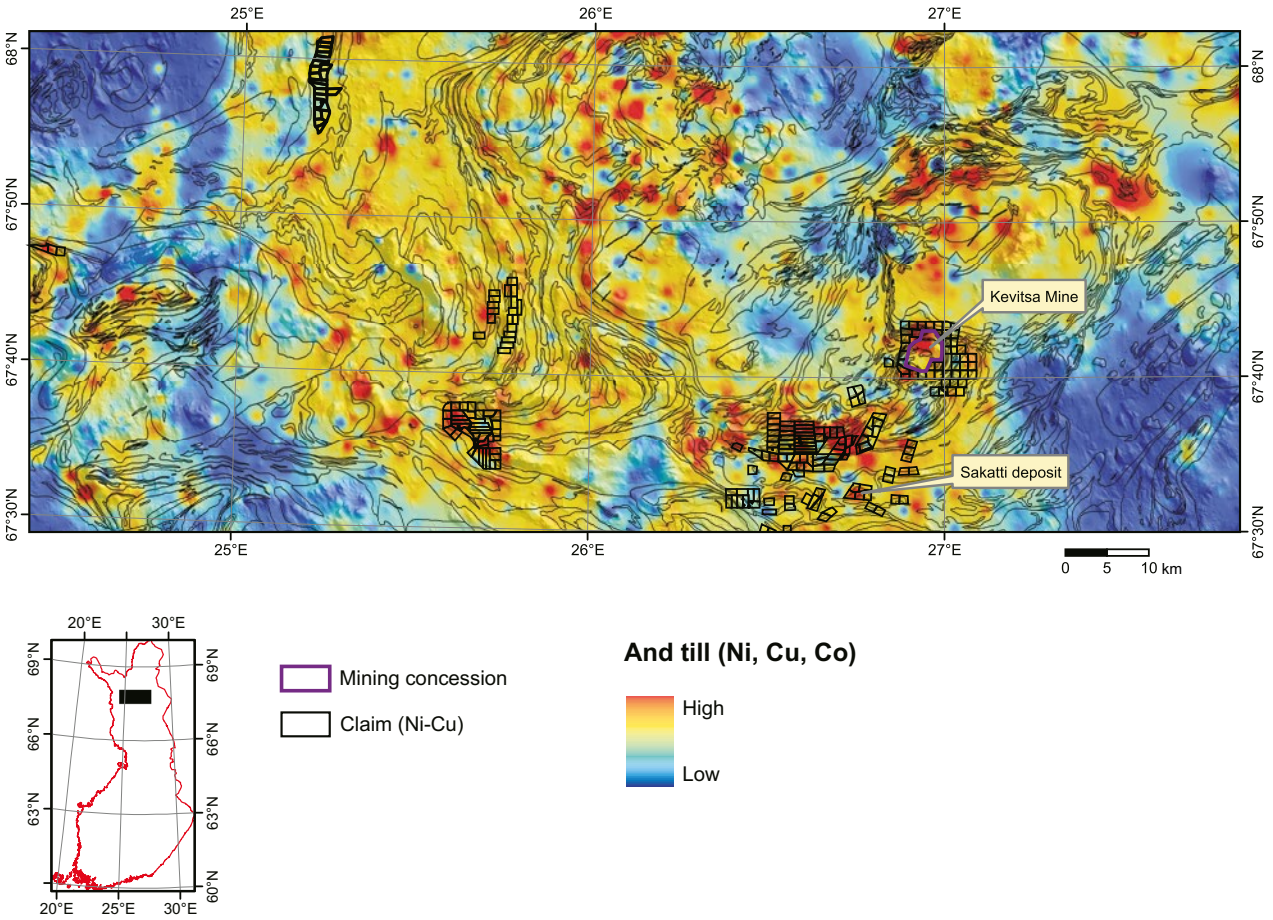

Fig. 16. Combined till geochemistry (Ni, Cu and Co). Contains data from the National Land Survey of Finland Topographic Database 03/2013 © NLS and HALTIK.

FUZZY LOGIC MODEL

Prior to data integration, the grid cell values of each map were rescaled into a common scale from 0 to 1. This was achieved by applying the fuzzy membership function Fuzzy Large (after Bonham-Carter 1994). The closer the values are to 1, the more favorable is the corresponding location for a magmatic nickel deposit. After rescaling, the input data sets were combined using the Fuzzy Gamma operator (Bonham-Carter 1994). Figure 11 defines the inference network used to combine the input maps into a single prospectivity map (Fig. 17). This map defines the most favorable areas for nickel deposits as a red color in the map. In these areas, all the exploration criteria are met. We also plotted the exploration licenses, reservations, and mining concessions related to nickel on the map. It is clear from a visual inspection that the red areas are mostly concentrated in the areas with current Ni exploration activity. The known deposits, Kevitsa and Sakatti, are also in areas with very high favorability.

The residual maps (Figs. 13–15) and the final prospectivity map (Fig. 17) also include the lithological boundaries from the 1:200 000 scale

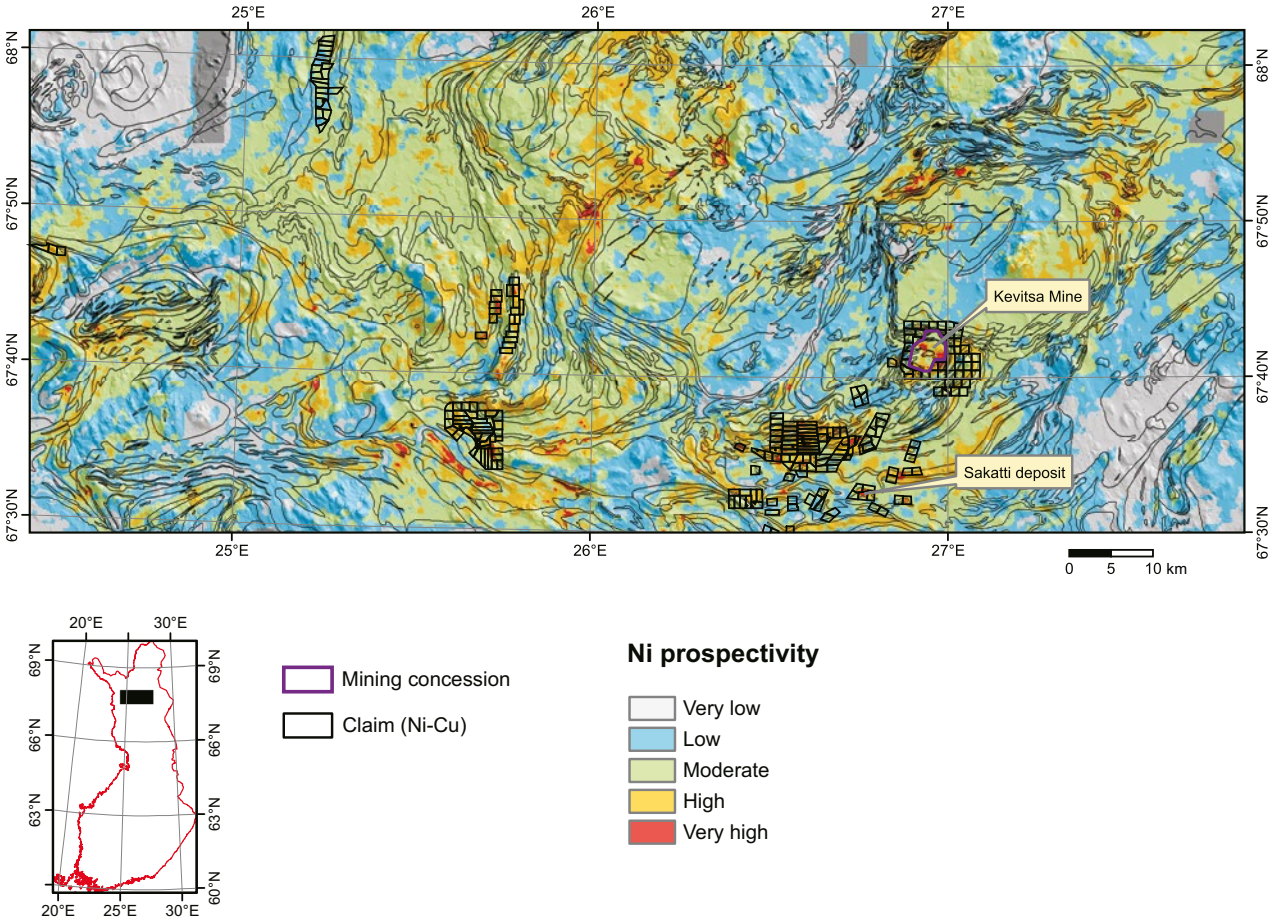

Fig. 17. Prospectivity map defining areas favorable for magmatic nickel deposits. Contains data from the National Land Survey of Finland Topographic Database 03/2013 © NLS and HALTIK.

bedrock map. The locations of the exploration license areas were used to validate the model results, because there are only two known Ni occurrences within the study area. Kevitsa is an operating Ni mine of First Quantum Minerals plc. It is clearly seen as an anomaly on all of the input maps and on the prospectivity map. The Sakatti occurrence is a prospect of Anglo American Exploration. In addition to the visual validation, we used so-called receiver operating characteristics (ROC) validation, which can be used to measure the accuracy of diagnostic systems (Obuchowski 2003) or the performance of a spatial prediction model (Nykänen 2008). An ROC curve is a plot of sensitivity (true positive rate) on the y-axis vs. 1 - specificity (false positive rate) on the x-axis. The area under ROC curve (AUC) can be used as a measure of the accuracy of a diagnostic test, and can also be used as a measure of the classification of a spatial predictive model. AUC values vary from 0 to 1. A test that results in an AUC value of 1 is perfectly accurate, having a sensitivity value of 1 and a 1-specificity value of 0 (Fig. 18). A totally random model would result in an AUC value of 0.5, and the curve would follow the chance diagonal.

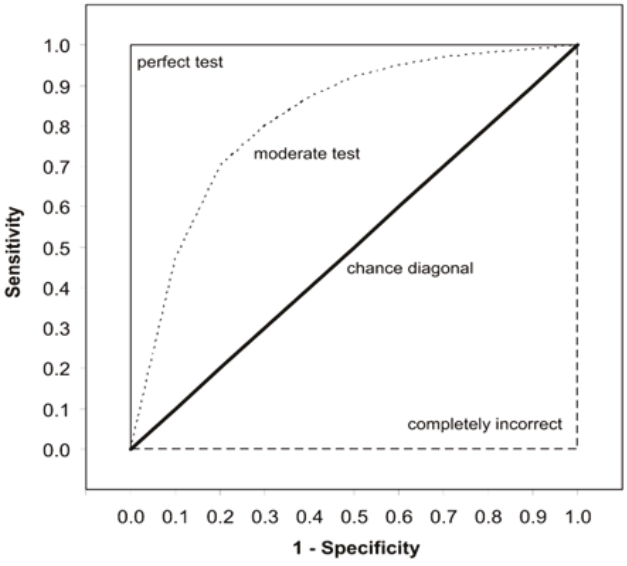

Fig. 18. ROC validation diagram.

For ROC validation we need two sets of test locations within the study area: true negative and true positive sites. The selection of true negative sites is problematic in spatial prospectivity models of this kind unless we have tested sites where we can be sure that there is no mineral deposit. We decided to use random points for this purpose. True positive sites were represented by the location of the exploration licenses for nickel exploration. This validation presented here includes a significant level of uncertainty, because not all of the claims are really Ni deposits and the true-negative sites are random points. However, this validation indicates a high level of correlation between the prospectivity model presented here and the reasoning for claiming areas for Ni exploration among the companies executing Ni exploration within the study area. Whether these high potential areas include new deposits remains to be seen in the near future, when the exploration campaigns have been executed.

The AUC values of the input data and the final prospectivity models were all above 0.5, but did not exceed 0.76 (Table 1). The 'fuzzy gamma' model performed slightly better than the 'fuzzy AND' model. The ROC curve in Figure 19 indicates that the model is not perfect, but it is definitely better than random sampling would give us. Therefore, we can conclude from these results that this prospectivity model can be used for selecting new exploration target areas for more detailed assessment.

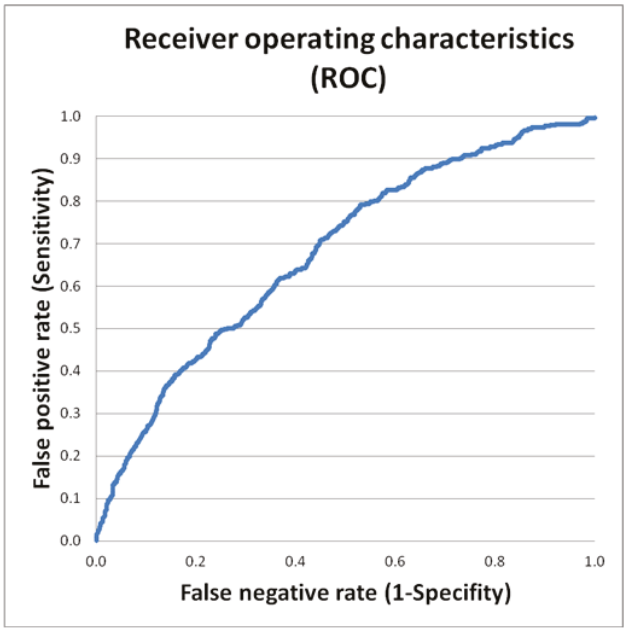

Fig. 19. ROC curve for the fuzzy gamma model. AUC is 0.68.

Table 1. AUC values of ROC tests.

Raster	AUC
Co	0.76
Cu	0.74
Combined till geochemistry	0.74
Gamma 2	0.68
AND 2	0.62
Ni	0.60
Gravity	0.55
AM	0.54

SUMMARY

This prospectivity model combined till geochemistry (Ni, Cu and Co) with airborne magnetics and regional gravity data. The data were filtered using a high-pass filtering technique, in which the long wavelength signal is removed from the data revealing local anomalies. The resulting prospectivity map identifies more than 40 targets areas favorable for Ni-Cu deposits within the study area in the northern Fennoscandian Shield. Most of these areas are under active exploration, including the Sakatti Ni-Cu deposit and Kevitsa Ni-Cu-Au-PGE mine. A receiver operating characteristics (ROC) curve was used for model validation. ROC validation indicated that the input datasets and the resulting prospectivity maps have a clear spatial association with the current Ni exploration areas defined by exploration licenses.

CHAPTER III.
3D MODEL OF THE KITTILÄ TERRANE AND ADJACENT STRUCTURES

Tero Niiranen, Ilkka Lahti and Vesa Nykänen

INTRODUCTION

The Central Lapland Greenstone Belt (CLGB) is one of the largest Paleoproterozoic greenstone belts in the world, covering an area of ca 30 000 km² (Fig. 20). The bulk of the CLGB consists of a volcano-sedimentary sequence deposited on the Archean basement during multiple episodes of rifting between 2.44–2.0 Ga. However, the mafic volcanic rock-dominated Kittilä terrane comprises the core (Fig. 20).

Economically, the CLGB is very interesting, as it not only hosts the largest gold-only deposit in Europe, namely the 7.67 Moz Suurikuusikko deposit, but also a number of other gold-bearing deposits and occurrences. The economic significance of the area was recognized in the early 1980s, and as a result of exploration and bedrock mapping, a considerable amount of geophysical and geological data has been gathered from the district. The data

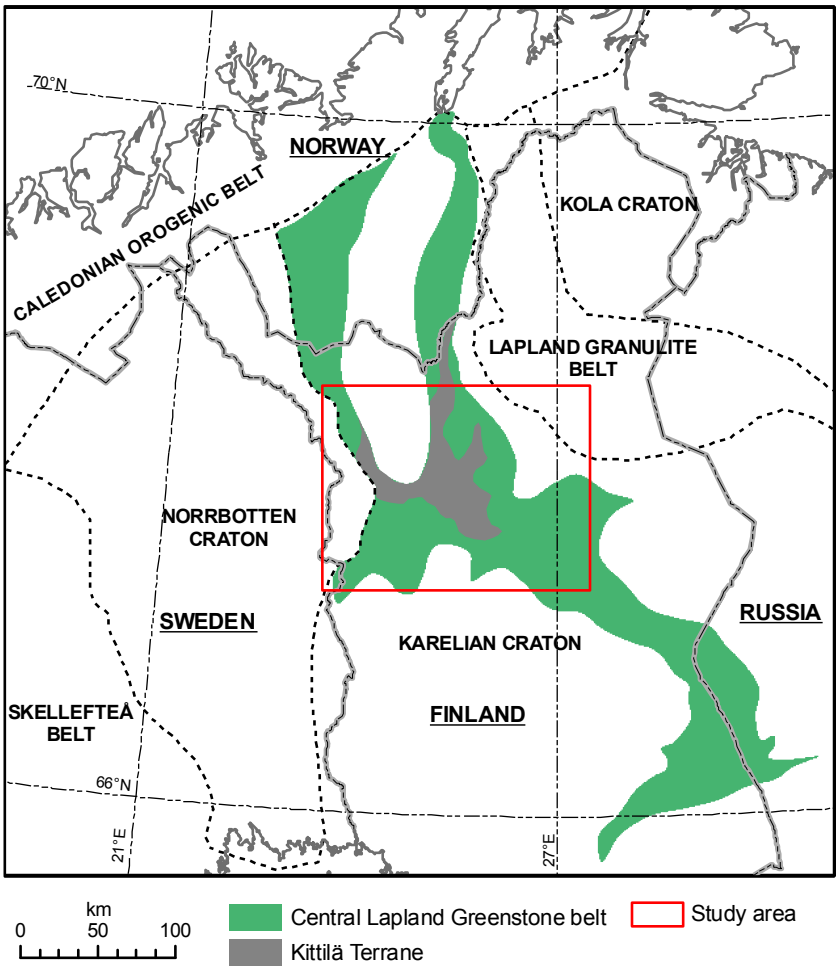

Fig. 20. Location of the study area, extent of the Central Lapland Greenstone Belt, and location of the main geological units. Contains data from the National Land Survey of Finland Topographic Database 03/2013 © NLS and HALTIK.

include high-quality airborne geophysics, ground gravity data and several seismic profiles, as well as extensive drill hole and outcrop observation datasets. A number of studies have been carried out based on the existing data. As a result, several geological interpretations have been presented as maps, cross sections, and so on. So far, the 3D interpretations have been limited to deposit-scale studies focusing on mineral resource estimates. In this chapter, we present the first regional-scale 3D interpretation of the Kittilä terrane and key structures in and around it. We also present a gold potential estimation for the area based on the 3D modeling results.

GEOLOGY OF THE STUDY AREA

The geology of the central part of the CLGB and its immediate surroundings is illustrated in Figure 21. The CLGB records a complex geological history, including a series of rifting events between 2.44 and 2.0 Ga followed by compressive tectonic events and metamorphism related to Svecofennian orogenic events at 1.91–1.79 Ga. The supracrustal rocks of the CLGB can be divided into a Karelian volcano-sedimentary sequence deposited on the Archean basement during rifting events at 2.44 Ga, 2.2 Ga, and 2.0 Ga, and a Svecofennian sequence deposited on the Karelian units during 1.89–1.77 Ga (Lehtonen et al. 1998, Hanski et al. 2001, Hanski & Huhma 2005). Hanski (1997) interpreted the Nuttio suite serpentinites near to the eastern margin of the Kittilä Group as ophiolite fragments, and suggested that the Kittilä Group represents an allochthonous unit that is at least partly oceanic in origin. This hypothesis is supported by the distinct geochemical affinity of the Kittilä Group mafic volcanic rocks, and the tectonic and/or tectonized contacts between the unit and surrounding Karelian rocks (e.g. Lehtonen et al. 1998, Hanski & Huhma 2005). The geological evolution of the CLGB culminated during the multi-stage deformation, intrusive magmatism, and metamorphism related to Svecofennian orogenic events at 1.91–1.79 Ga.

Stratigraphy

The supracrustal rocks of the CLGB have been divided into seven lithostratigraphical groups, which from oldest to youngest are the Vuojärvi, Salla, Kuusamo, Sodankylä, Savukoski, Kittilä, and Kumpu Groups (Fig. 22). In the northeastern part of the study area, the Salla Group represents the oldest unit deposited on the Archean basement. Recently, a new lithostratigraphical unit, the Vuojärvi Group, was distinguished in the southern part of the CLGB (GTK digital bedrock database 2013). The current interpretation is that the quartzites and sericite-quartzites of the Vuojärvi group overlie the Archean basement, or the Group is of Archean age.

The Salla and Kuusamo Groups predominantly consist of felsic to mafic volcanic rocks representing the earliest volcanism related to the rifting of the Archean basement. The Sodankylä Group chiefly consists of clastic sedimentary rocks with minor volcanic and carbonaceous intercalations. The Sodankylä rocks were deposited on the Vuojärvi, Salla, and Kuusamo Groups, or in some cases on the Archean basement. Widespread quartzites with locally preserved cross-bedding, herringbone and mud crack textures suggest that the depositional environment was at least locally tidal and that the rift basin was considerably widened after the cessation of volcanism related to the Salla and Kuusamo Groups (Lehtonen et al. 1998, Hanski & Huhma 2005). The Savukoski Group is lithologically complex, consisting of mixed sequences of komatiitic to tholeiitic volcanic rocks and phyllites, graphite- and sulfide-bearing schists, as well as carbonaceous rock intercalations (Lehtonen et al. 1998). In a number of locations, the volcanic rocks preserve primary pillow lava textures, indicating a sub-aqueous depositional environment.

The Kittilä Group is dominated by Fe- and Mg-tholeiitic massive lavas, pillow lavas, and pyroclastic rocks. Sedimentary interbeds and more widespread sedimentary units have also been reported within the volcanic rock units (Lehtonen et al. 1998). These consist of metagraywackes, phyllites, graphite- and sulfide-bearing schists and tuffites,

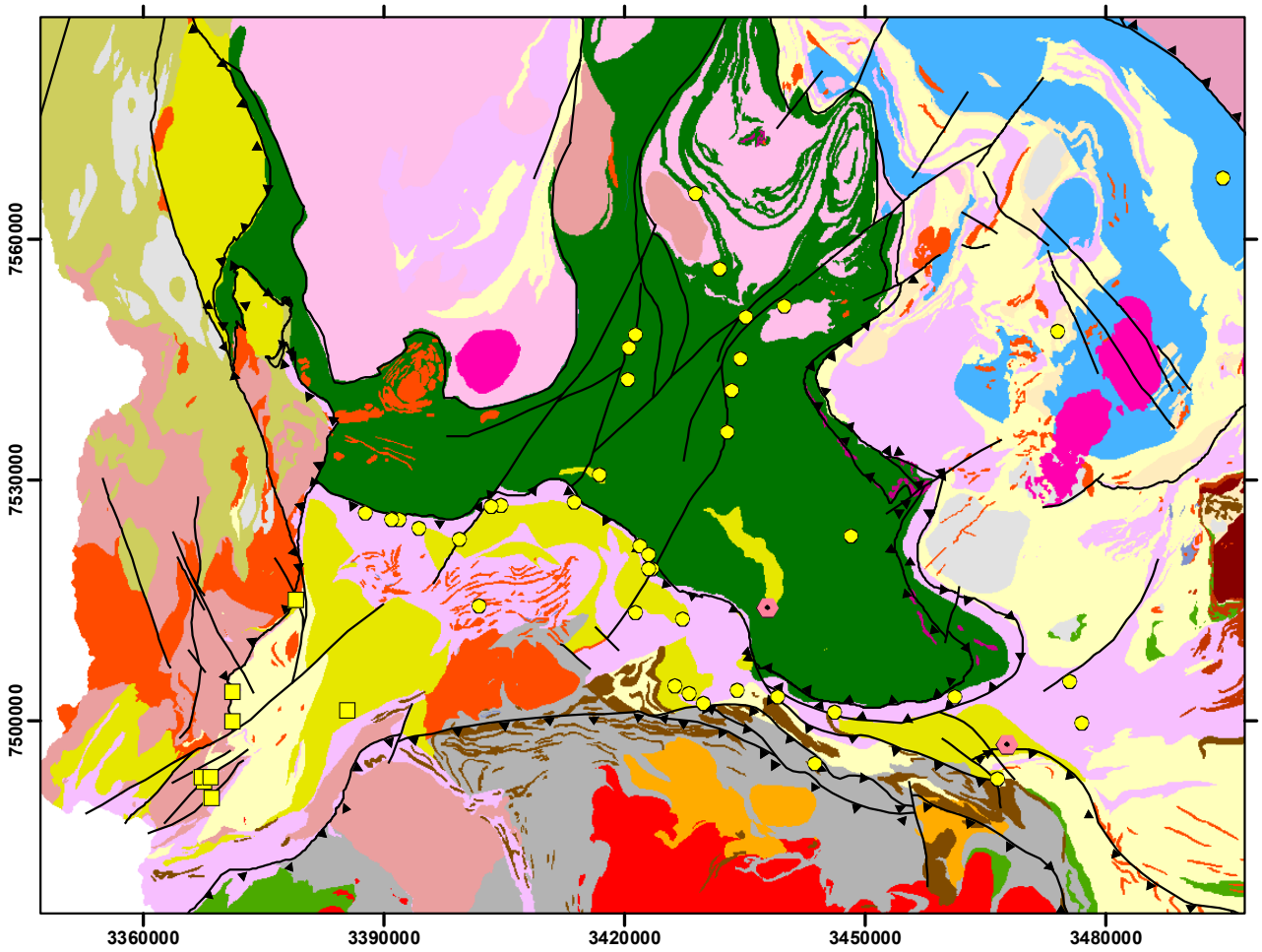

Paleoproterozoic Groups

- Kumpu Group — Quartzite, siltstone, conglomerate, intermediate to felsic volcanic rocks
- Kittilä Group — Tholeiitic volcanic rocks, graphite- and sulphide-bearing tuffite, BIF, phyllite, mica schist, graywacke
- Savukoski Group — Tholeiitic and komatiitic volcanic rocks, phyllite, graphite and sulphide-bearing schist, tuffite, dolomite
- Sodankylä Group — Quartzite, mica schist, mica gneiss, mafic volcanic rock
- Kuusamo Group — Tholeiitic and komatiitic volcanic rocks
- Salla Group — Intermediate to felsic volcanic rocks
- Vuojärvi Group — Quartzite, mica gneiss, possibly volcanic in origin

Paleoproterozoic complexes

- Lapland granulite complex
- Vuotso complex
- Hetta complex
- Central Lapland granitoid complex

Archean complexes

- Pomokaira and Muonio complexes

Paleoproterozoic supracrustal suites

- Nuttio suite
- Olostunturi suite
- Diverse lithodemes

Paleoproterozoic hypabyssal suites

- Haaskalehto gabbro-wehrlite suite

Paleoproterozoic intrusive suites

- Nattanen granite suite
- Haaparanta suite
- Nilipää granite suite
- Eastern Lapland layered intrusion suite
- Keivitsa layered intrusion suite

Major Structures

- Shear/Fault zone
- Thrust zone

Gold deposits

- Orogenic gold
- Iron oxide-Cu-Au
- Paleoplacer

Fig. 21.Geology of the Kittilä terrane and adjacent area. Location of the known gold deposits and occurrences. Modified GTK digital bedrock map database and FINGOLD.

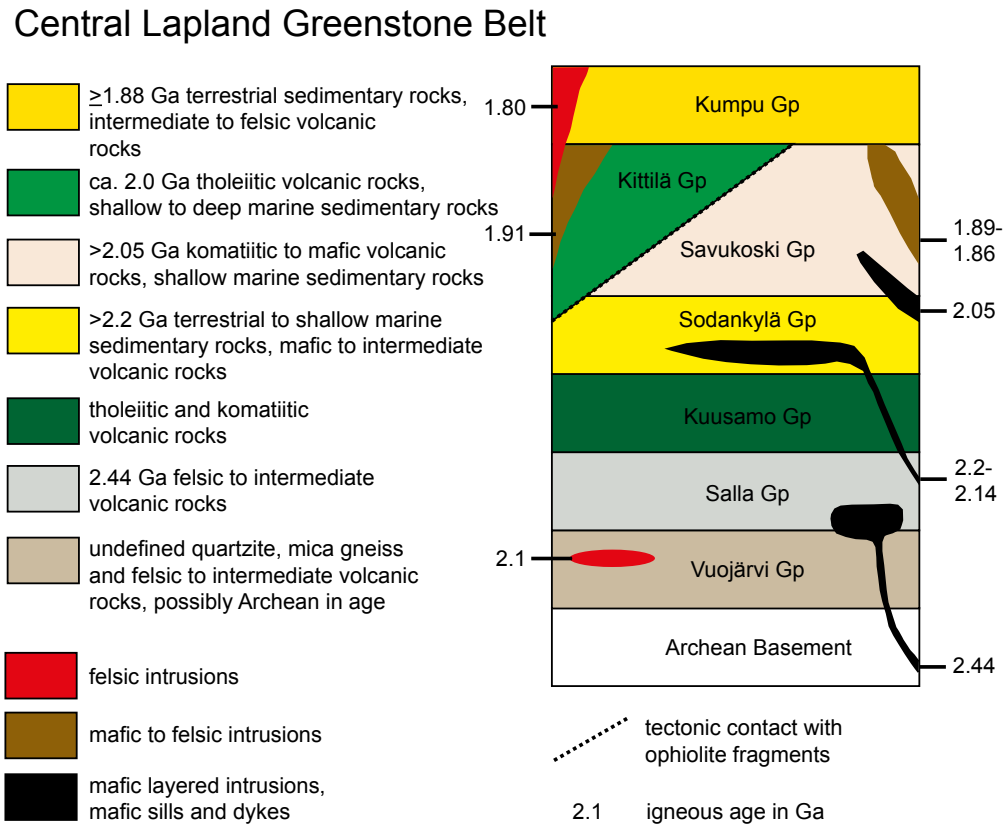

Fig. 22. Stratigraphy and igneous ages of the Central Lapland Greenstone Belt. Modified after Lehtonen et al. (1998), Hanski et al. (2001) and GTK's FINSTRATI database.

carbonate rocks, and banded iron formations. Lehtonen et al. (1998) divided the mafic volcanic rocks of the Kittilä Group into two formations: the Vesmajärvi and Kautoselkä formations. The geochemical data indicate that the former volcanic rocks have an affinity for oceanic basalts, and the latter bear characteristics of passive margin tholeiites (Lehtonen et al. 1998, Hanski & Huhma 2005). The depositional basement of the Kittilä Group rocks is unknown.

The Kumpu Group represents the youngest supracrustal unit in the CLGB. It predominantly consists of clastic, molasse-like sedimentary rocks deposited on a major stratigraphic break. Minor amounts of intermediate to felsic volcanic rocks occur in the unit in the western part of the CLGB (Lehtonen et al. 1998).

Intrusive magmatism

The early intrusive magmatism consists of 2.44 Ga and 2.05 Ga mafic layered intrusions divided into the Eastern Lapland and Kevitsa suite intrusions, respectively (Fig. 21). Abundant mafic dyke magmatism indicating repeated rifting took place at 2.22 Ga, 2.05 Ga, and 2.0 Ga (Hanski et al. 2001). The 2.2 Ga mafic dykes and differentiated sills of the Haaskalehto gabbro-wehrlite suite are the most abundant, predominantly occurring within the Sodankylä Group rocks along an E–W-trending zone south of the southern margin of the Kittilä terrane (Fig. 21). The 2.05 and 2.0 Ga magmatism predominantly consists of diabase dykes and small gabbroic intrusions, although in places coeval felsic quartz-feldspar dykes have been detected (e.g. Lehtonen et al. 1998, Hanski et al. 2001). The 1.91–1.86 Ga Haparanda Suite mafic to felsic intrusions comprise the syn-orogenic, and 1.82–1.79 Ga granitoids the late-orogenic intrusions in the area. Nilipää suite granites occur in the southern margin of the CLGB and have an enigmatic age of 2.1 Ga, suggesting that they were intruded during or between the extensional stages (e.g. Hanski et al. 2001).

Deformation and metamorphism

The CLGB records a complex multi-stage deformation history that, despite numerous investigations, is still not completely understood. The following sequence of deformation events is modified after the interpretations of Ward et al. (1989), Lehtonen et al. (1998), Väisänen et al. (2002), Tuisku and Huhma (2006), Hölttä et al. (2007), and Patison (2007). The deformation history of the CLGB area is divided into three ductile stages followed by a completely brittle stage. The main deformation stages, D_1 and D_2, lack clear overprinting relationships and geochronology, and are therefore grouped here as the $D_{1\text{-}2}$ stage. The $D_{1\text{-}2}$ stage relates to thrust tectonics and resulted in the main ductile deformation features of the CLGB. Features of the stage indicate S–SW-vergent transport and N–NE-vergent transport in the northern and southern parts of the CLGB, respectively. The S–SW-vergent thrusting in the north relates to collision of the Karelian and Kola cratons and thrusting of the Lapland Granulite belt to the SW. The northward-directed thrusting in the south involved the initial generation of the south-dipping Sirkka and Venejoki thrust zones (Fig. 23). It is currently unknown whether the two thrusting events were contemporaneous or successive.

The D_3 stage resulted in deformation features with highly variable vergence, depending on the location, and it may have consisted of several stages that do not necessary relate to each other. The D_3 deformation resulted in the generation of N- to NE-striking shear zones and local refolding

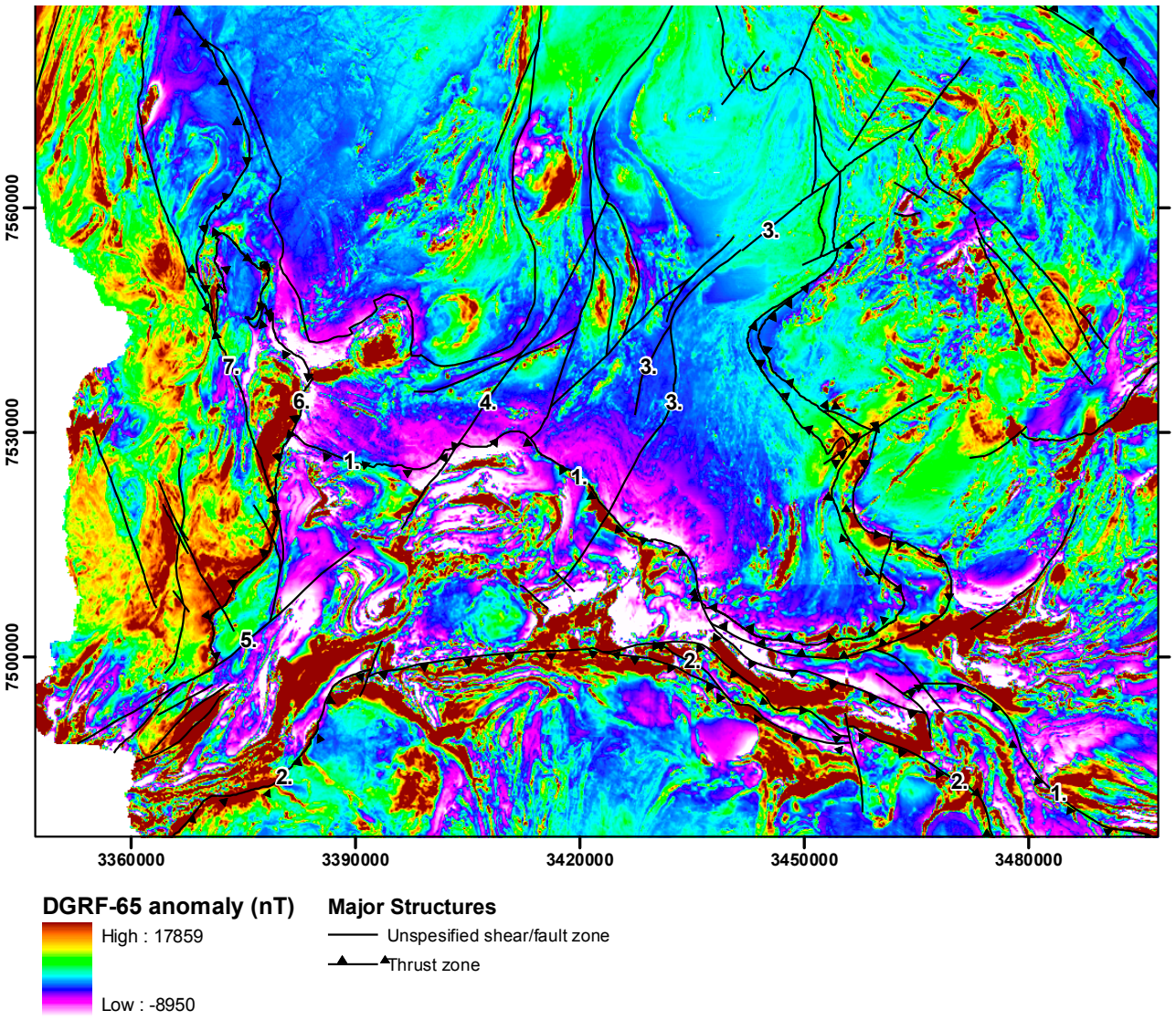

Fig. 23. Aeromagnetic map of the study area with the location of the key structures. 1. Sirkka thrust, 2. Venejoki thrust, 3. Kiistala shear zone, 4. Muusa shear zone, 5. Äkäsjoki shear zone, 6. Jerisjärvi thrust, 7. Enontekiö shear zone. GTK data.

of the earlier deformation features. In the western part of the Sirkka thrust zone, clear indications exist of reactivation of the structure during this stage (e.g. Patison 2007, Saalmann & Niiranen 2010). The external events resulting in the D_3 deformation and the robust timing of it are unknown. The minimum age and at the same time the maximum age for the following brittle D_4 stage is 1.77 Ga (Väisänen et al. 2002). The probable age frame for the D_3 is either 1.89–1.86 Ga or 1.82–1.77 Ga, and it may vary between different parts of the CLGB (e.g. Väisänen et al. 2002, Patison 2007).

The peak metamorphic conditions in the CLGB were reached during the D_{1-2} stage. A characteristic feature of the metamorphism in the CLGB is that excluding the northern and western margin, the metamorphic conditions within the Kittilä terrane are of mid-greenschist facies (Hölttä et al. 2007). The metamorphic grade increases away from the Kittilä terrane, being upper amphibolite facies in the south close to the rocks of the Central Lapland Granitoid Complex and mid-amphibolite facies in the western margin. The highest metamorphic conditions are recorded next to the Vuotso and Lapland granulite complex rocks, in which a peak metamorphic pressure and temperatures of up to 12 kbar and 800–850 °C, respectively, were reached (Tuisku & Huhma 2006). The peak metamorphic temperature estimates for the Kittilä terrane are ca. 350 °C, although no reliable pressure estimate exists for the lowest grade metamorphic area (Hölttä et al. 2007). The western margin of the Kittilä terrane has metamorphosed at a higher temperature due to heat flow from adjacent granitoids. A garnet thermobarometry from this area yields a pT estimate of 3.2 kbars and 550 °C (Hölttä et al. 2007).

DATA AND METHODS

The datasets used in this study comprised the Geological Survey of Finland's geophysical data, including airborne magnetic, EM, and radiometric data, ground gravimetric data, and various ground geophysical data sets. In addition GTK's digital bedrock database, bedrock observation data and drill core data were utilized. Much of the interpretation of deep structures relied on seismic data, for which data were utilized from the Finnish Reflection Experiment FIRE 2001–2005 and High Resolution Reflection Seismics for Ore Exploration 2007–2010 (HIRE) programs (Kukkonen & Lahtinen 2006, Kukkonen et al. 2011). The locations of the seismic profiles are indicated in Figure 24.

The data were processed in several ways. For example, potential field datasets were processed using multiscale wavelet edge detection ("worming"), described in detail in Chapter I of this volume. In addition, various derivative maps were utilized for the magnetic data to establish the contacts and dips of units and structures.

Modeling of the Kittilä terrane was based on 3D modeling of regional Bouguer gravity data and seismic data. A multidisciplinary approach was used in all modeling, and much of the modeling process was iterative. The visualization, interpretation, and modeling were carried out using Gocad™ software with Mira Mining utilities™ and GRGPack research plugins provided by the Gocad Research Group of the Nancy School of Geology.

THREE-DIMENSIONAL GRAVITY MODELING OF THE KITTILÄ TERRANE

Three dimensional gravity modeling was carried out to obtain information on the deep geometry of the Kittilä terrane and surrounding areas (Fig. 25). The Kittilä terrane is favorable for gravity modeling, as a large number of ground gravity measurements have been carried out in the area, and the belt itself produces a significant positive Bouguer anomaly of about ~45 mGal (Fig. 24). The anomaly is caused by thickness variations in the high-density mafic volcanites of the terrane in contrast to lower density surrounding felsic rocks such as granitoids, quartzites, and schists. The data and measurements used have been described in more detail in Chapter II of this volume.

The regional Bouguer gravity data (~20 000 measurements, 1–4 measurements/km^2) were

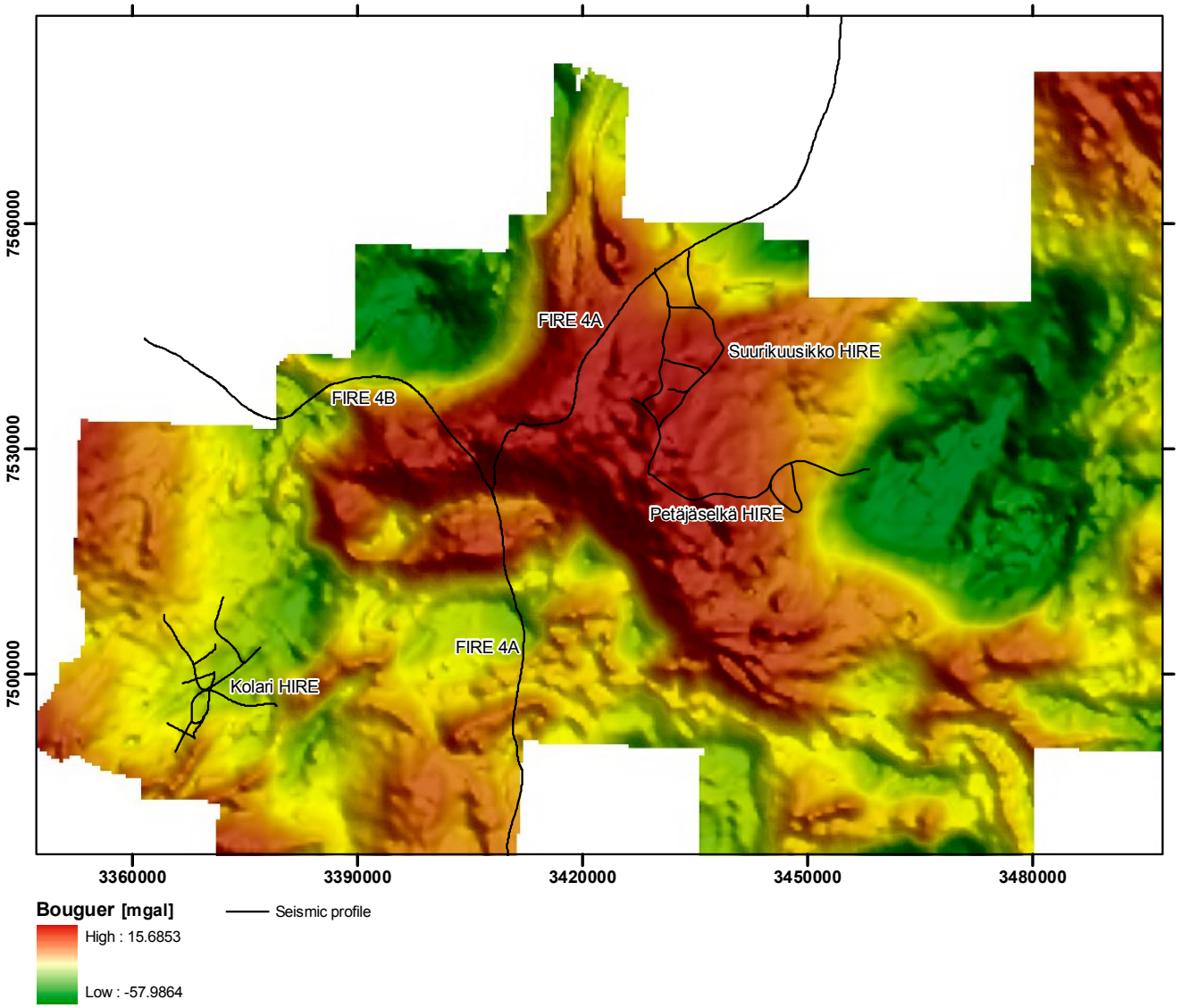

Fig. 24. Bouguer anomaly map of the study area with locations of the reflection seismic profiles used in the modeling.

gridded, and modeling lines were created by sampling the grid along 20 N–S-oriented 80-km-long lines, spaced 5 km apart. The modeling area was therefore 95 km in the E–W direction and 80 km in the N–S direction (Fig. 26). The model was constructed from a number of layer-type three-dimensional bodies shown in Figure 26. Due to the thousands of bedrock observations and drillings performed in the modeling area, the surface geology is well known. Therefore, the topmost part of the model is primarily based on the known lithology. Model densities, geometries, and the regional trend were manually modified to improve the data fit between the measured and calculated data along the modeling lines. Although such a "trial and error" modeling procedure is very time consuming, it allows the results to be checked against the geology and other geophysical results during the process. The model was revised several times in 3D using the Gocad software together with reflection seismics to obtain good agreement between the model and the seismic data. In order to gain a better final modeling result, the most significant geological units around the terrane causing positive and negative anomalies were also incorporated in 3D modeling, since the use of a single background density would yield inaccurate modeling results. The area is characterized by granitoids in the north and east, such as the Hetta, Tepasto, and Postojoki-Sovasjoki granitoids, which cause negative Bouguer anomalies. Densities of 2600–2650 kg/m^3 and thicknesses of 1–6 km were used for granitic intrusions to fit the negative Bouguer anomalies encountered in the north and east. To the south of the Kittilä terrane, more dense rock types such as schist, mica schist, and mafic–ultramafic intrusions

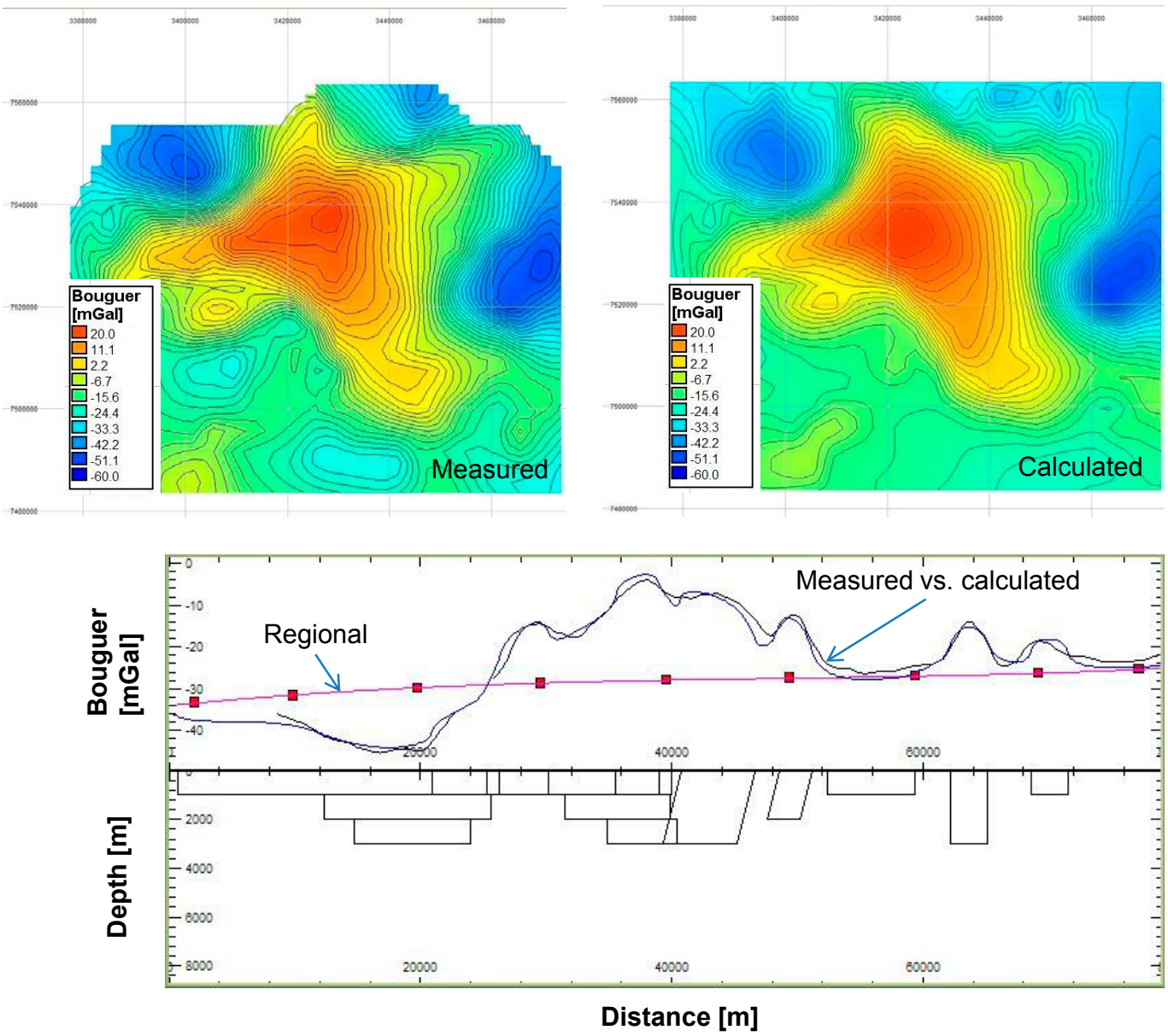

Fig. 25. 3D gravity modeling of the Kittilä terrane. Upper images show measured and modeled gravity data. The lower panel presents an example of one of the modeling profiles.

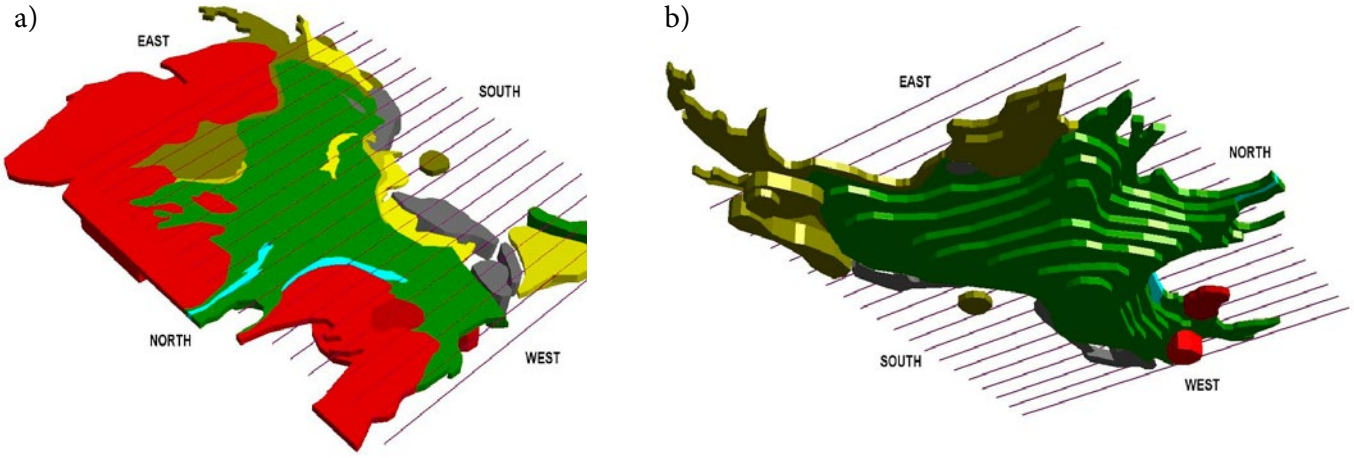

Fig. 26. a) 3D model of the Kittilä terrane and surrounding geological blocks used in the modeling. View from the northwest and b) Kittilä terrane gravity model from the northeast. Modeling profiles are presented in both images.

create short-wavelength positive anomalies. Higher density blocks (2650–3050 kg/m^3) were added in the southern part of the model. The Kittilä terrane was modeled using the density of 2950 kg/m^3, which is a representative estimate for mafic volcanites in area. The background density of 2780 kg/m^3 was assigned for the rest of the 3D model, as this value represents an average between the mafic and felsic rock types in the area. Several smaller-scale high- or low-density bodies were necessary to add in the terrane model. These anomalies are caused by banded iron formations (Porkonen), quartzites (Kumpu), and granites (Ruoppapalo).

Figure 26 presents three-dimensional perspective views of the final model. The terrane can be modeled using 8 layers, each having a thickness of 1 km. The terrane is relatively shallow (1–2 km) in the eastern and western parts, but becomes considerably thicker around the Sirkka area. The abrupt thickening is in good agreement with the reflection seismic results of the FIRE seismic profiles, which show steeply dipping reflectors in the same area (Patison et al. 2007). Although it is challenging to accurately estimate the thickness of the terrane, this modeling suggests that the thickest part occurs around the Kiistala-Lintula area.

MODELED STRUCTURES AND UNITS

Kittilä terrane

The bottom of the Kittilä terrane has been constructed on the basis of the 3D gravity model and seismic data. The surface expression is as outlined by GTK's digital bedrock map. In many locations of the FIRE profiles, there is a sub-horizontal, highly reflective unit below the Kittilä terrane that corresponds well to the base outlined by the gravity forward model (Patison et al. 2006, Niiranen et al. 2009). The contact can be also outlined relatively clearly in a number of HIRE profiles from the central and eastern part of the Kittilä terrane.

The base of the Kittilä terrane was modeled as a surface, and the terrane was also modeled as a 3D block and voxet model to calculate the volume and for further numerical estimations. The modeled base of the Kittilä terrane is presented in Figure 27. The base reaches the depth of 9500 meters in the central parts, where the unit appears to have been bulged down. This is slightly thicker than the 8 km thickness of the gravity model. However, the final

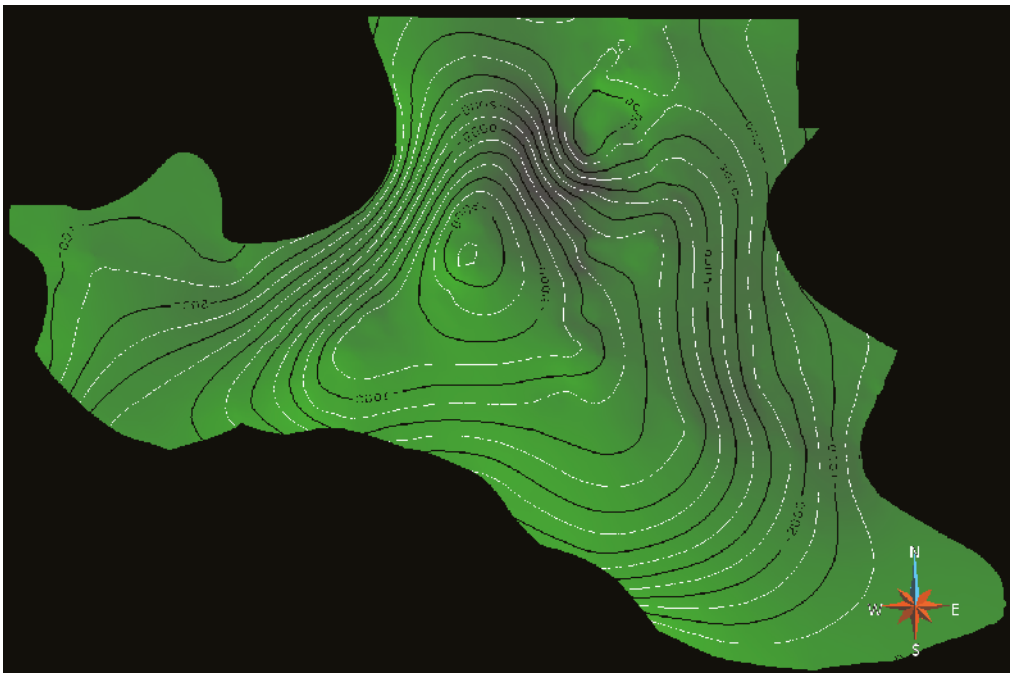

Fig. 27. The base of the Kittilä terrane with depth contours in meters below the current bedrock surface.

model is based on the combination of the gravity model and the seismic data smoothed using DSI interpolation. The lowermost 1.5 km volume covers only a small area and is in accordance with the gravity anomaly. The unit thins toward its boundaries from this location. The unit is thinnest in the western part, where the base reaches a depth of ca. 1000 m, and in SE corner, where the base surfaces.

Venejoki and Sirkka thrusts

The Venejoki and Sirkka thrusts, which form northward-directed thrust systems, were modeled as surfaces (Fig. 28). Both structures were interpreted using geophysical and bedrock maps. The FIRE 4A profile intersects both structures, and they can be seen as low reflectivity zones cross-cutting or truncating sub-horizontal reflectors (e.g. Patison et al. 2006, Niiranen et al. 2009). The apparent dips of the structures are 45 and 30 degrees for the Sirkka and Venejoki thrusts, respectively, being very close to the true dips, as the FIRE 4 profile crosses the structures almost perpendicularly (Fig. 29). The Sirkka thrust reaches a depth of at least 9 km, and the Venejoki thrust can be traced to reach the mantle at a depth of ca. 42 km (Patison et al. 2006).

Kiistala and Muusa shear zones

Kiistala and Muusa shear zones are the two strike slip systems cross-cutting the Kittilä terrane for which there was sufficient data to model them (Figs. 21, 23, and 28). They both are NE- to N-striking strike-slip structures, the Kiistala being interesting for gold, as the Suurikuusikko orogenic gold deposit is hosted by it. The Muusa shear zone appears as a low magnetic, cross-cutting linear feature on aeromagnetic map and as a sub-vertical NW-dipping transparent zone cross-cutting sub-horizontal seismic reflectors on the FIRE 4B profile (Fig. 30, Niiranen et al. 2009). There is no direct drilling or outcrop evidence of the structure, and the geological features are consequently

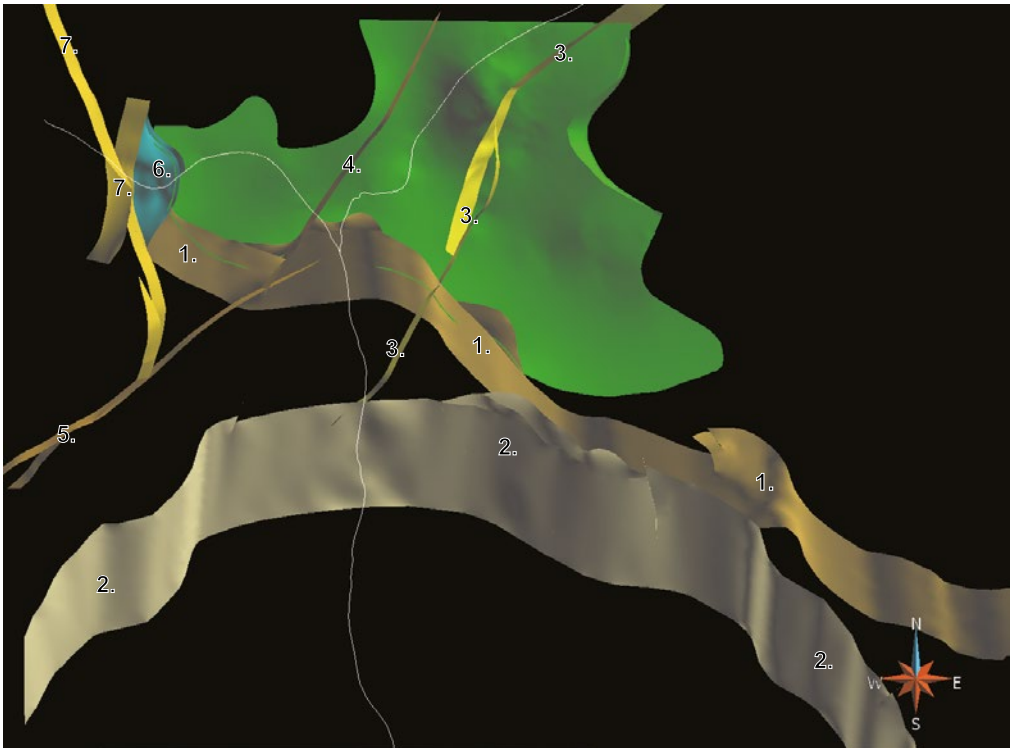

Fig. 28. Modeled key structures and the base of the Kittilä terrane (green) as surfaces. 1. Sirkka thrust, 2. Venejoki thrust, 3. Kiistala shear zone, 4. Muusa shear zone, 5. Äkäsjoki shear zone, 6. Jerisjärvi thrust, 7. Enontekiö shear zone.

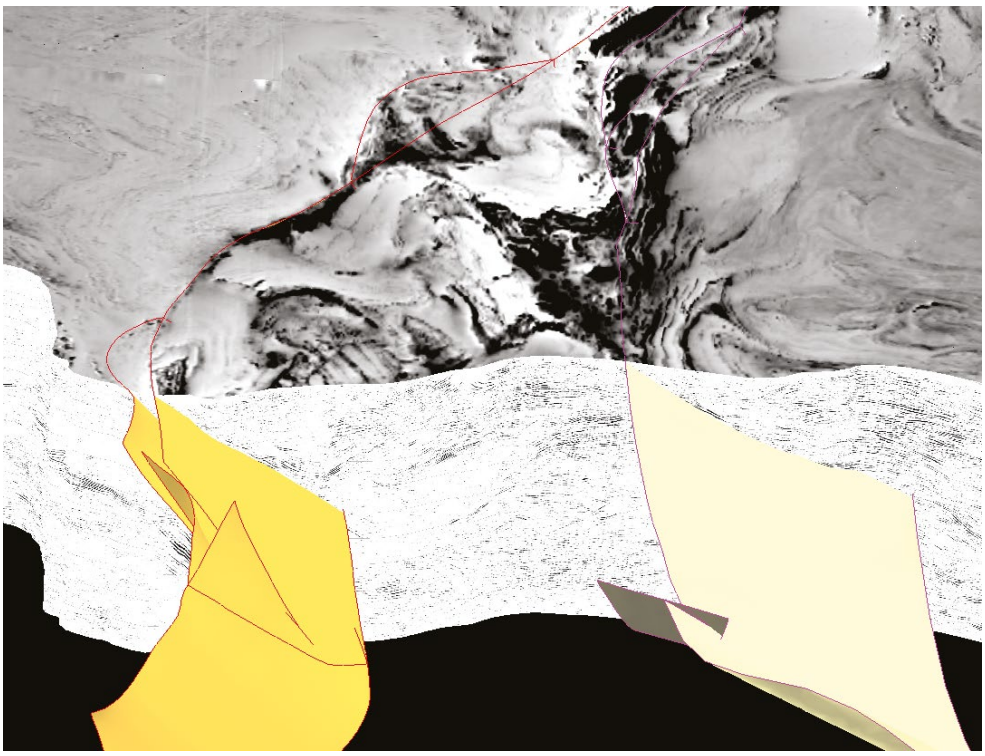

Fig. 29. Sirkka thrust (left) and Venejoki thrust (right) with aeromagnetic data and the seismic FIRE 4 profile. Oblique view from the west.

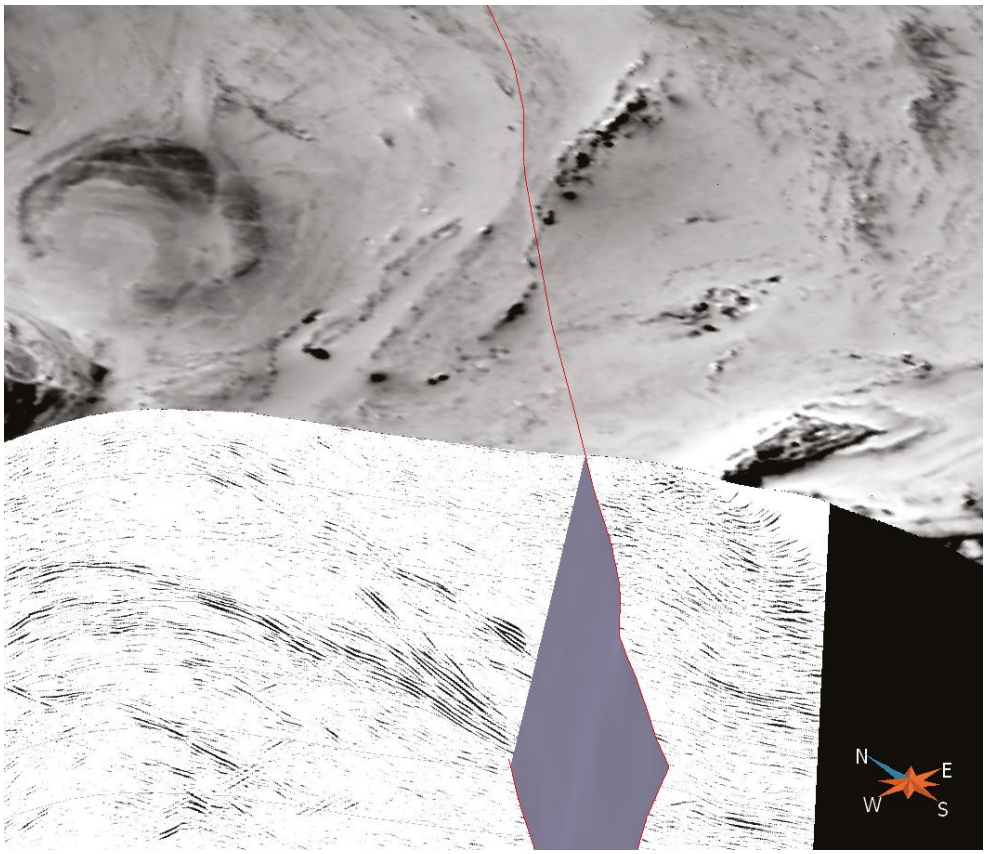

Fig. 30. Modeled Muusa shear zone (bluish gray with red borders) on the aeromagnetic map and seismic FIRE 4B profile. The structure cross-cuts the highly reflective gently dipping units on the seismic data. Also note the apparent sinistral characteristic of the shear zone on the aeromagnetic map.

unknown. Based on the aeromagnetic data, it has an apparent sinistral component.

The outcrop and drill core data of the Kiistala shear zone are mainly from the Suurikuusikko deposit and adjacent area. Patison (2007) and Patison et al. (2007) described the structure as sub-vertical strike-slip shear zone with early sinistral and late dextral movement. Based on the drilling data from the Suurikuusikko deposit, the structure extends to a depth of at least 1500 meters. On aerogeophysical maps, the structure can be outlined to extend across the Kittilä terrane, potentially reaching the Lapland granulite arc in the NE and cross-cutting the Sirkka thrust in the SW, splaying to at least two segments around the Suurikuusikko deposit (Fig. 21). The structure can be perceived on the seismic HIRE profiles from the Suurikuusikko area. However, being vertical to sub-vertical, it is not a very prominent feature. The structure is modeled as two planes, of which the southern segment dips ca. 80 degrees to the west and the northern segment 85 degrees to the east (Fig. 28).

Structures in western part of the area

Three key structures were modeled from the western part of the study area: the Äkäsjoki and Enontekiö shear zones, and the Jerisjärvi thrust zone limiting the western margin of the Kittilä terrane (Figs. 21, 23, and 28). All of these probably form part of the crustal-scale Balthic-Bothnian megashear (BBSZ), as described by Berthelsen & Marker (1986). The Äkäsjoki shear zone was modeled based on the Kolari HIRE seismic data and geophysical data, and the Enontekiö shear zone and Jerisjärvi thrust were modeled based on the seismic interpretation on FIRE 4B profile and geophysical interpretation (Patison et al. 2006, Niiranen et al. 2009).

The Äkäsjoki shear zone appears in the airborne magnetic map as a linear low magnetic zone that in places truncates magnetic low and magnetic high zones, clearly being a local-scale tectonic block boundary. It appears in the Kolari HIRE seismic data as a transparent zone that cross-cuts the gently dipping reflector packages (see Chapter IV, this volume). The modeled shear zone dips 85 degrees to the NW. There are no direct observations on the structure, although it may be a southwestern extension to the Muusa shear zone.

The Jerisjärvi thrust zone limits the western margin of the Kittilä terrane. It is most likely a northern extension to the thrust zone, extending from Hannukainen in Kolari, being truncated by the Enontekiö shear zone. In the seismic FIRE 4B profile, it occurs in a highly tectonized zone with numerous vertical to west- and east-dipping transparent zones, indicating the presence of a set of shear and thrust zones relating to the BBSZ (e.g. Patison et al. 2006, Niiranen et al. 2009). The Jerisjärvi thrust is modeled as a half bowl-shaped thrust limited at its western margin by the Enontekiö shear zone (Fig. 28). It reaches a depth of 8.5 km.

The Enontekiö shear zone appears on the aeromagnetic map as a distinct, >100-km-long, NNW-striking zone that clearly divides the area into two blocks with different magnetic patterns (Fig. 23). The structure has an apparent sinistral strike-slip component and appears to be linked to the Äkäsjoki shear zone at its southern end. Based on the seismic data, the structure is sub-vertical, dipping 80 degrees to the WSW, and reaches a depth of at least 12 km (Patison et al. 2006, Niiranen et al. 2009). The structure braids into at least two segments at its southern end and has NNE–SSW-striking conjugates next to the Jerisjärvi thrust zone (Fig. 28).

DISCUSSION

The 3D model of the Kittilä block indicates that it is considerably thicker at its thickest part than previous 2D interpretations suggested. According to Lehtonen et al. (1998), the base of the Kittilä terrane is at ca. 6 km in the Tepasto-Pomokaira area. This 2D interpretation profile is about 8 km north of the thickest part of the Kittilä terrane in our model. The base of the deepest part in our model at the location of the Tepasto-Pomokaira profile of Lehtonen et al. (1998) is 1.5 km deeper than

in their 2D interpretation. In the Kumputunturi area, the previous 2D investigation profile suggested that the Kittilä terrane is up to 5 km thick. At the corresponding location in our 3D model, the thickness is about 5.5 km, being relatively consistent with previous investigations.

The Kittilä terrane has been suggested to represent a fragment of oceanic crust obducted and emplaced to its current position during the early stages of the Svecofennian orogenic events (e.g. Hanski 1997, Hanski & Huhma 2005). The 9.5 km thickness indicated by the model is about twice the thickness of an oceanic crust. This, together with dramatic thickness variation and the 3D shape of the modeled Kittilä terrane, strongly suggests that the unit has been thickened via stacking and folding during the Svecofennian orogenic events.

A number of studies on the structural geology of the CLGB have suggested bivergent thrusting towards the Kittilä terrane: thrusting of the Lapland Granulite Belt to the SW during the collision of the Karelian and Kola cratons around 1.91 Ga, and northward-directed thrusting that was either synchronous or a subsequent event (e.g. Ward et al. 1989, Lehtonen et al. 1998, Tuisku & Huhma 2006, and Patison 2007). The 3D model of the Lapland Granulite Belt and its foreland units is described in Chapter V of this volume. The 3D model of the Venejoki and Sirkka thrusts illustrates the northward-directed thrusting systems. The exact timing and ultimate external driving force is unclear, but the thrusting most likely took place between either 1.91–1.89 Ga or 1.86–1.77 Ga (e.g. Patison 2007 and references therein). The characteristics of the Venejoki thrust are poorly known and all interpretations of this structure are based on seismic and geophysical data. In contrast to this, the Sirkka thrust has been explored for gold since the 1980s and it has been described in a number of publications (e.g. Ward et al. 1989, Lehtonen et al. 1998, Patison 2007). A cluster of 2.2 Ga dolerite dykes and sills has been detected along the Venejoki thrust, and Sattasvaara formation komatiites occur along the Sirkka thrust (e.g. Lehtonen et al. 1998). These features suggest that the Venejoki and Sirkka thrust systems may already have been initially formed during the rifting stage(s) as normal rift faults and reactivated as thrust zones during the basin inversion. In addition, there are number of indications that the Sirkka thrust was reactivated after the northward-directed thrusting as a strike-slip shear (e.g. Patison 2007, Saalmann & Niiranen 2010). If these scenarios are true, the mineral potential of these structures is even higher than has previously been considered, as many hydrothermal deposit types with structural control are most abundant in structures with a prolonged, multi-stage deformation history.

The modeled Muusa and Kiistala shear zones are just two of the several NE–SW-striking strike-slip shear zones cross-cutting the Kittilä terrane. The data on this set of shear zones suggest that they have been active during the regional D_3 stage. However, they may also have had a considerably longer history. As already suggested by Patison (2007), among others, these structures may have originally been initiated during the D_{1-2} thrusting events as transfer faults relating to the thrust zones prior to the D_3, and were multiply reactivated during the later stages. Visual examination of the 3D models presented in this volume suggest that this is a viable hypothesis, but robust timing constrains are needed to verify this.

The BBSZ, which in some publications is referred to as the Pajala Shear Zone, or Kolari Shear Zone, is clearly a significant crustal-scale feature. However, the geological evolution, timing, and external driving mechanisms of the structure are poorly known. It has been proposed to represent a collisional boundary between the Norrbotten craton in the west and the Karelian craton in the east (Lahtinen et al. 2005), although very little concrete evidence for this has been presented. Only a few indications of the timing of the tectonic evolution have been reported. From the Kolari region, Hiltunen and Tontti (1976) and Hiltunen (1982) suggested that the thrusting and shearing was coeval with the 1.89–1.86 Ga Haparanda suite magmatism, and Niiranen et al. (2007) suggested that the structures related to the BBSZ at Kolari were (re-)activated during 1.82–1.79 Ga. The cross-cutting evidence for the modeled Jerisjärvi thrust, the Äkäsjoki and Enontekiö shear zones with the Sirkka thrust and Kittilä terrane, suggests that the initial formation of the BBSZ structures postdated events in relation to the northward-directed thrusting at the southern margin of the CLGB. Clearly, more research, including robust dating, needs to be carried out before the geological evolution of the BBSZ can be unveiled.

Implication for the gold potential of the Kittilä terrane

The Kittilä terrane is an economically prospective area, especially for gold deposits, not least due to the discovery of the world-class Suurikuusikko deposit within the central part of the area. Numerous other showings and deposits are known within and in the southern margin of the terrane. All but a few of these fall into the category of orogenic gold deposits. Groves et al. (1998) presented a genetic model for orogenic gold deposits in which the metals and fluids involved are released from the country rocks during metamorphism (with or without input from intrusions) and are focused into suitable structures that act as pathways, and metals are subsequently deposited into suitable traps. Pitcairn et al. (2006) presented data from the Otago and Alpine belts in New Zealand showing a clear pattern of depletion in gold and gold-related metals from mafic volcanic and sedimentary rocks undergoing progressive metamorphism. Their work indicates that gold concentrations in sedimentary and mafic volcanic rocks metamorphosed in amphibolite facies conditions show 50–80% depletion compared with their unmetamorphosed varieties, which is in agreement with the model presented by Groves et al. (1998).

In this work, we applied the genetic model by Groves et al. (1998) and developed a scenario in which the mafic volcanic rocks of the Kittilä terrane are the dominant source for the fluids and gold, and these are released from the rocks in metamorphic reactions involving devolatization via the breakdown of hydrous silicates. In mafic rocks, the devolatization is generally strongest around the greenschist-amphibolite facies boundary at a temperature of around 525 °C.

Based on the work of Hölttä et al. (2007), the peak metamorphic temperature of the Kittilä terrane at the current erosional level is ca. 350 °C and the pressure 3.2 kbar. Using these figures and a density of 2.95 kg/dm³ for the Kittilä terrane, the temperature gradient during the peak of the metamorphism was 37 °C/km. The metamorphic peak

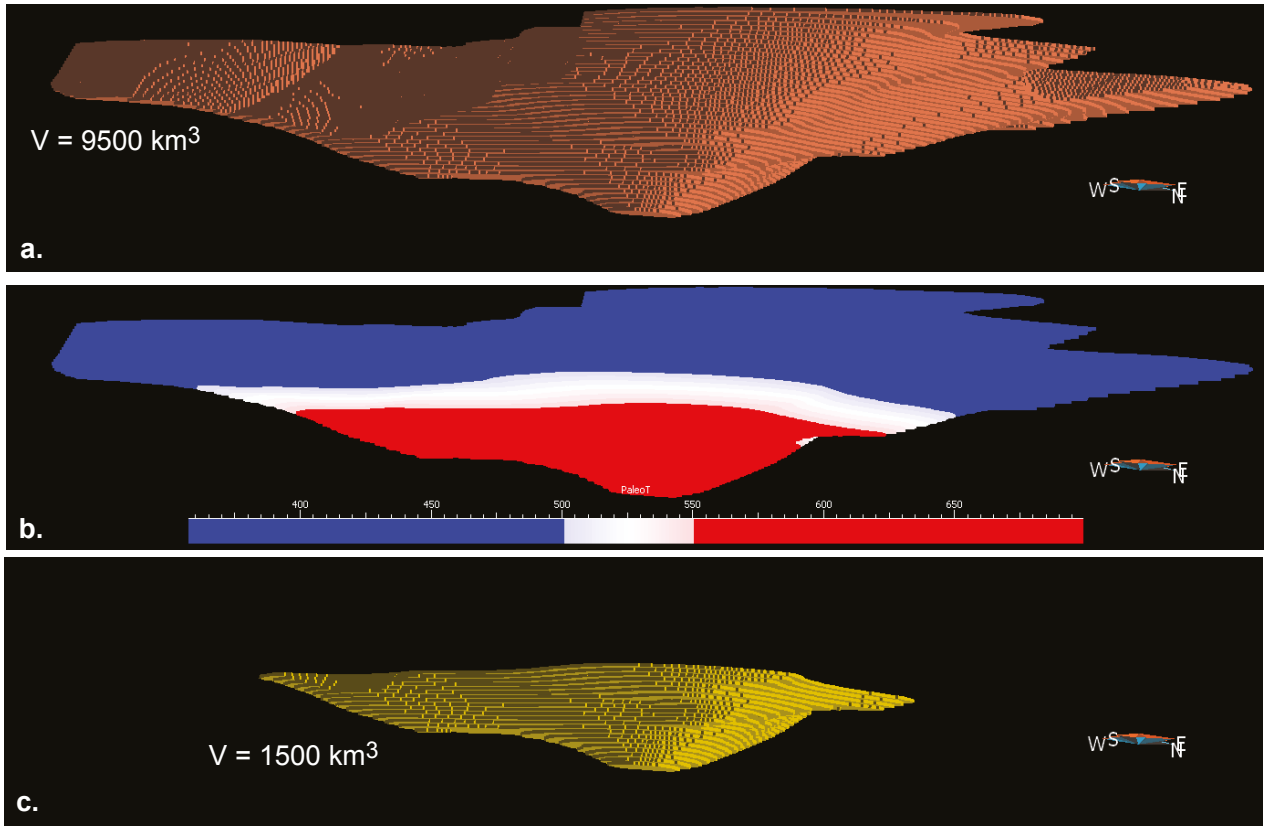

Fig. 31. a. Voxet model of the Kittilä terrane. Northern, northwestern, and westernmost high-T metamorphic zones are excluded. V is the total volume of the model. b. Calculated peak metamorphic temperature on the voxet model. The blue area is in greenschist facies, the red area is in amphibolite facies, and the white zone illustrates the transition zone between greenschist and amphibolite facies at 500–550 °C. c. Amphibolite facies part of the modeled Kittilä terrane with the calculated volume (V). Oblique view from the SE in all images. The scale is the same in all images.

temperature was calculated in a voxet model of the Kittilä terrane as a function of depth using these figures (Fig. 31). The volume of the lower part of the Kittilä terrane in amphibolite facies is 1500 km^3, and using the average density of 2.95 kg/dm^3, the total mass of this part is 4425 Bt.

Data on the background levels of Au in mafic volcanic rocks of the Kittlä terrane are lacking. However, the data from the literature suggest that the average background gold concentrations for mafic volcanic rocks vary between 0.75 ppb and 4.7 ppb, depending on the type of mafic volcanic rocks (Pitcairn, 2012 and references therein). We performed our calculations using a background concentration of 2 ppb Au. Based on this, the total amount of gold in mafic metavolcanic rocks of the Kittilä terrane subjected to amphibolite facies metamorphism was 285 Moz (8850 t). If 50–80% of this was mobilized, as indicated by the work by Pitcairn (2006), a total of 143–228 Moz gold was mobilized from the mafic volcanic rocks of the Kittilä terrane during the metamorphism. These figures are considerable compared with the currently known gold resources within the Kittilä block (Suurikuusikko and Kuotko ~7.8 Moz, Agnico Eagle data). Obviously, the gold and fluids released at depth by metamorphism need to be focused into a suitable structure such as the KiSZ, and gold needs to be precipitated in suitable trap, both events occurring with an unknown efficiency. Also, some of the gold may have precipitated above the current erosional level. Despite the numerous assumptions and hypothetical nature of the calculations presented above, it seems very likely that the undiscovered gold resources in the Kittilä terrane are potentially several tens of millions of ounces. Obviously, until the true background gold concentrations are available for refining the calculations, the above-presented figures should be considered as "blue sky" estimates.

CONCLUSIONS

The work presented above suggests that the Kittilä terrane is thicker than previous investigations have suggested. The considerable thickness variations of the terrane are due to the thrusting-related tectonics, resulting in the folding and stacking of the mafic volcanic rocks and associated sediments during the main deformation stages of the Svecofennian orogeny. The Venejoki and Sirkka thrust zones form a northward-directed thrust system. These structures may already have formed as normal fault zones during the rifting stages and may have subsequently been reactivated as thrust zones during the inversion of the basin, and yet reactivated during the later orogenic events, making them long-lived crustal-scale structures and thus highly prospective for the discovery of epigenetic metal deposits.

The Äkäsjoki and Enontekiö shear zones and the Jerisjärvi thrust zone form part of the Baltic-Bothnian megashear, which, based on the seismic data, is clearly a crustal-scale feature. Until further work on these structures is carried out, the exact nature and timing of this system remains unknown.

Based on this work, potentially up to 228 Moz gold was mobilized from the Kittilä Group rocks alone. This figure is almost 30 times greater than the total reported gold resources in known deposits in the Kittilä terrane. Although rough, our estimate shows that metamorphic processes alone can easily have liberated enough gold for the known deposits, and a considerable amount of undiscovered gold most likely remains in the terrane.

CHAPTER IV.
3D MODEL OF THE KOLARI REGION

Tero Niiranen, Vesa Nykänen and Ilkka Lahti

INTRODUCTION

The Kolari district is located in the western part of Finnish Lapland. The area has been under active exploration for decades, and some 15 iron ± Cu-Au deposits have been discovered in the area. Various genetic interpretations have been suggested for the known deposits. They have been proposed to represent metamorphosed syngenetic iron formations (e.g. Hiltunen & Tontti 1976, Mäkelä & Tammenmaa 1978, Väänänen 1998), strata-bound, intrusion-related epigenetic skarn deposits (Hiltunen 1982), or epigenetic iron oxide-Cu-Au deposits (Niiranen et al. 2007). In 2010, GTK and Northland Resources S.A., a company that is currently carrying out exploration and development of the Kolari deposits, carried out in co-operation a deep seismic profile program (HIRE) over key targets areas in the Kolari district. The data became available for research after a one-year quarantine period and were used in the Central Lapland 3D modeling program of GTK. The results of the 3D modeling and its implication for the stratigraphy of the area and the genetic interpretation of the known deposits are presented in this chapter.

GEOLOGICAL FRAMEWORK

The Kolari district forms the westernmost extension of the Central Lapland Greenstone Belt (CLGB). The bedrock of the area consist of a 2.44–2.05 Ga Karelian supracrustal sequence of rift related mafic volcanic rocks and associated sedimentary rocks, a >1.89 Ga Svecofennian sequence of clastic sedimentary rocks, 2.2 Ga dolerite dykes, 1.89–1.86 Ga Haparanda suite intrusions, and 1.82–1.77 Ga granitoids (Fig. 32, Hiltunen 1982, Väänänen 1998, Niiranen et al. 2007). The dominant Karelian rocks in the Kolari region belong to the Kuusamo, Sodankylä, and Savukoski Groups, the latter two dominating the study area (Figs. 32 and 33). These are overlain by clastic sedimentary rocks of the Svecofennian Kumpu Group.

The CLGB was subjected to multi-phase deformation and metamorphism during the Svecofennian orogenic events between 1.91–1.77 Ga. The deformation has been divided into three ductile stages, D_{1-3}, followed by a completely brittle D_4 stage (e.g. Väisänen 2002, Hölttä et al. 2007, Patison 2007). The earliest stage, D_1, resulted in bedding parallel foliation rarely visible in macroscopic observations (Lehtonen et al. 1998, Hölttä et al. 2007). The D_2 stage in the CLGB relates to thrust tectonics resulting in the main foliation in the CLGB, S_2, and recumbent or reclined F_2 folding (Väisänen 2002, Hölttä et al. 2007). The vergence of the F_2 folding varies within the area, being to the SW to W in the northern and northeastern part of the CLGB and to the N to E in the south and west (Väisänen 2002, Hölttä et al. 2007). The S_2 is in general gently dipping or flat-lying and sub-parallel to bedding. The D_2 structures were overprinted by sets of F_3 folds and late shear zones with varying orientations. The F_3 folds are upright to steeply inclined, being northward vergent in the central parts of the CLGB and eastward vergent in SW and W parts of the area (Väisänen 2002, Hölttä et al. 2007). In the eastern and northern part of the

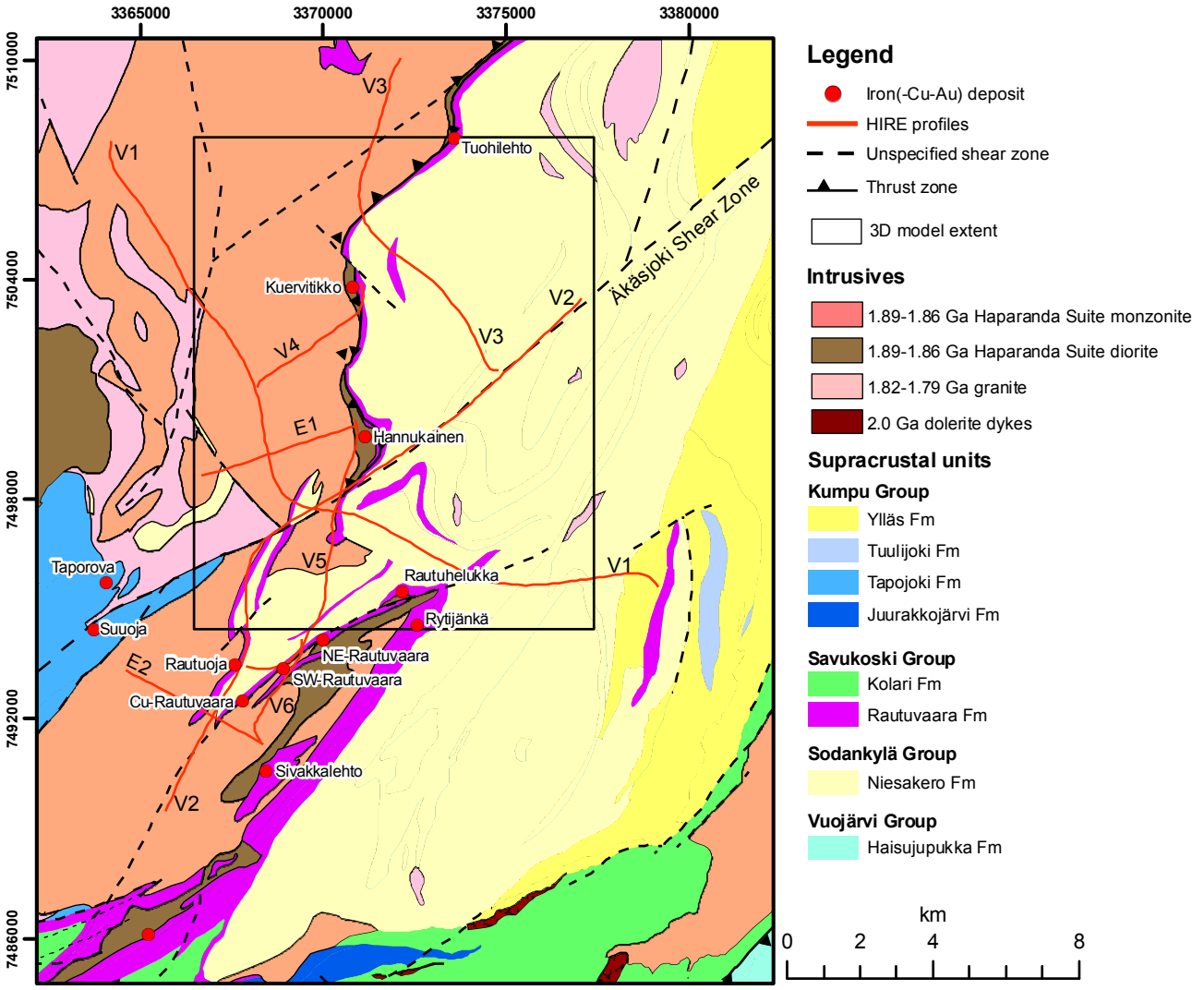

Fig. 32. Geological map of the study area with the location of the known Fe ± Cu, Au deposits, seismic profiles, and the extent of the 3D model. Geological map modified after Bedrock of Finland – DigiKP.

CLGB the vergence is to the west. D_2 took place between 1.91 Ga and 1.86 Ga, and D_4 is younger than 1.77 Ga (Väisänen 2002, Hölttä et al. 2007, Patison 2007). D_3, which most likely consists of several sub-stages varying in age in different parts of the CLGB, took place between 1.89 Ga and 1.77 Ga (Patison 2007). The peak metamorphic conditions vary from upper amphibolite to mid-greenschists facies and were reached prior to the development of D_3 shear zones (Hölttä et al. 2007). In the Kolari district, the peak metamorphic conditions are of mid-amphibolite facies conditions (Hölttä et al. 2007).

Stratigraphy of the study area

The initial detailed stratigraphy of the Kolari region was laid out by Hiltunen and Tontti (1976) and Hiltunen (1982). According to these works, the lowermost unit, the Niesakero-Kuertunturi quartzite complex, consists of quartzite, arkosite, conglomerate and mica gneiss, with thin amphibolite intercalations (Fig. 33). These rocks are correlated with the >2.2 Ga Sodankylä Group rocks. The Niesakero-Kuertunturi quartzite complex is overlain by the Rautuvaara and Kolari greenstone Formations, representing the Savukoski Group in the area (Fig. 33). The Kolari greenstone and Rautuvaara Formations have similar lithology consisting of mafic volcanic rocks, graphite-bearing

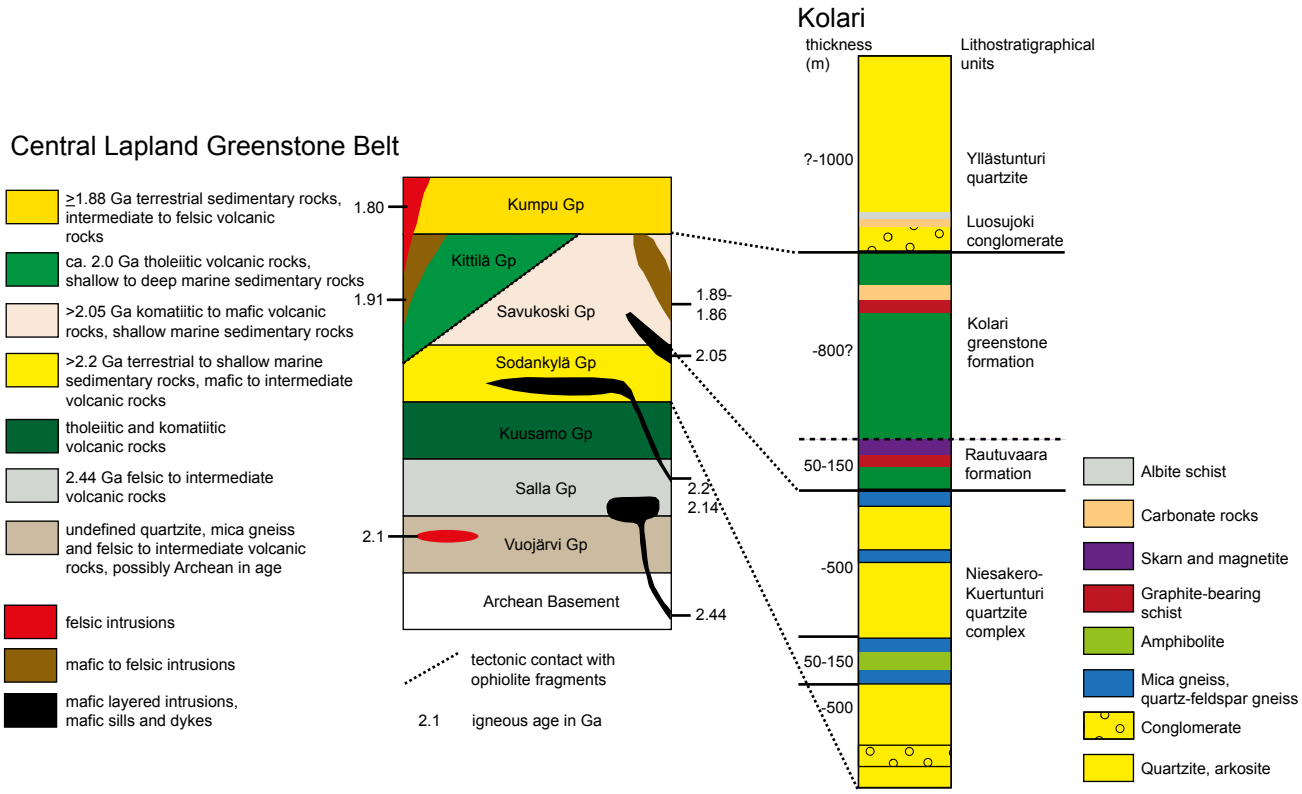

Fig. 33. Stratigraphy of the Central Lapland Greenstone Belt (modified after Lehtonen et al. 1998, Hanski et al. 2001, and GTK's FINSTRATI database) and the Kolari region (redrawn after Hiltunen 1982).

schists and carbonate rocks (Fig. 33). The Rautuvaara Formation is separated into its own formation based on the occurrence of skarn rocks and magnetite ore in it (Hiltunen 1982). In geophysical maps, it can be followed as magnetic highs and locations where iron ± Cu-Au deposits are known (Fig. 34). The uppermost units in the Kolari area consist of Luosujoki conglomerate and Yllästunturi quartzite units, which correlate with the <1.89 Ga Kumpu Group (Fig. 33). The stratigraphical scheme of Hiltunen (1982) has changed very little during the past 30 years, with only minor changes in the nomenclature and separation of the Kumpu Group into four separate formations (Fig. 32).

Recent unpublished GTK age data from western Lapland suggest the presence of a previously unrecorded unit of clastic sedimentary rocks that have a maximum depositional age of ca. 1.91 Ga, which is slightly older than the Kumpu Group age of <1.89 Ga. One of the dated samples of the 1.91 Ga unit is from the sillimanite quartzite taken from ca. 6 km E of the Rautuvaara Formation, representing the Niesakero Formation (Niesakero-Kuertunturi quartzite complex in Fig. 33). These results indicate that the correlation of the Niesakero Formation with the Sodankylä Group is most likely correct, and that the quartzites in the eastern part of the study area overlie the Rautuvaara and Kolari Formation rocks and are overlain by the Kumpu Group rocks (Fig. 32).

Structural features

Hiltunen (1982) described the structural pattern in the Kolari region as a series of synclines and anticlines with axial trace striking NE to N, with discontinuity at the Äkäsjoki shear zone (ÄSZ) dividing the area into two tectonic domains (Fig. 32). In the northern domain, the layering dips gently to the west, whereas in the southern domain the dips are steeper (e.g. Hiltunen & Tontti 1976, Hiltunen 1982). A characteristic feature of the Kolari area is SW-plunging folding with the fold axis plunging 20–55 degrees to the SW (Hiltunen 1982, Väisänen 2002). A pronounced stretching lineation has been recorded in the district, having a similar SW-plunging orientation to the F_2 fold axis.

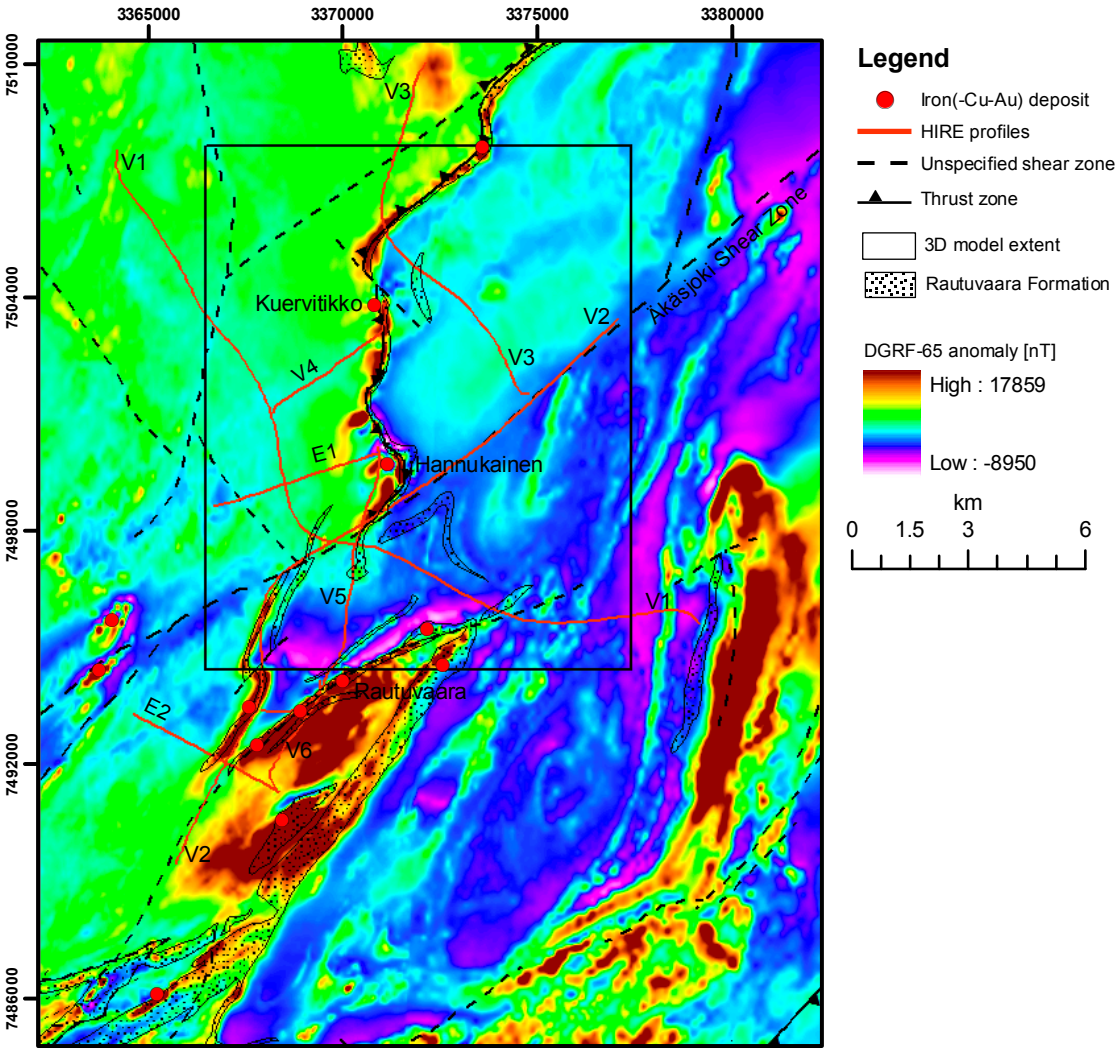

Fig. 34. Aeromagnetic map of the study area with shear zones, seismic profiles, and known deposits. The Rautuvaara Formation is as in Figure 1.

Northeast-, east-, and southwest-vergent folding has been reported in the broader Kolari area, the first of which is probably the youngest generation and relates to the regional D_3 stage (Hiltunen 1982, Väisänen 2002, Hölttä et al. 2007).

Several shear and thrust zones have been outlined in the Kolari region (Fig. 32). These comprise the crustal-scale Baltic-Bothnian megashear zone (BBMZ) in the Kolari area, sometimes referred to as the Pajala Shear Zone, or Kolari Shear Zone (Berthelsen & Marker 1986). This N–S-striking shear zone system reaches from Kalix in Sweden in the south through western Finnish Lapland up to the Norwegian Caledonides in the north, being about 400 km in length and up to 75 km in width. Lahtinen et al. (2005) proposed that the BBMZ represents a cratonic boundary between the Norrbotten craton in the west and the Karelian craton in the east.

Fe ± Cu-Au deposits

About 15 Fe ± Cu-Au deposits are known from the Kolari district. The deposits are located near to the contact zone between the 1.86 Ga Haparanda Suite monzonite and diorite intrusions and the Savukoski and Kumpu Group supracrustal rocks, being structurally controlled by thrust and shear zones (Hiltunen 1982, Niiranen et al. 2007). The deposits consist of lenticular to tabular disseminated to semi-massive magnetite bodies that host the Cu-Au mineralization (Hiltunen 1982, Niiranen et al.

2007). The typical metal association in the Kolari deposits is Fe-Cu-Au, with locally elevated Co and LREE. The size of the deposits ranges from 110 Mt to about 1 Mt (Hiltunen 1982, Risto et al. 2010). Multi-stage and -style alteration is associated with the deposits. Early, pervasive albitization occurs around all deposits, and this is overprinted by calc-silicate (skarn) alteration that envelopes most of magnetite bodies (Hiltunen 1982, Niiranen et al. 2007).

THE DATA AND METHODS

The modeling utilized GTK's aerogeophysical, digital bedrock (DigiKP), bedrock observation, and drill core databases. Old Rautaruukki maps and cross sections were used, in addition to the previously mentioned data sets. Much of the modeling relied on the reflection seismic profiles generated in the High Resolution Reflection Seismics for Ore Exploration 2007–2010 (HIRE) program (e.g. Kukkonen et al. 2011). The HIRE data on Kolari consist of a total of 80 km of lines in 8 profiles (Fig. 32) (see Kukkonen et al. 2011, for further details of the seismic data).

The visualization, interpretation, and modeling were carried out using Gocad™ software with Mira Mining utilities™ and GRGPack research plugins provided by the Gocad Research Group of the Nancy School of Geology. The key horizons were interpreted on the geological and geophysical maps, cross sections, and seismic profiles in Gocad as lines and point sets. The surfaces were interpolated from interpreted lines and point sets using the GRGPack StructuralLab plugin using methods described by Caumon et al. (2007). A 3D block model was generated from the surfaces using Gocad inbuilt tools.

INTERPRETATION OF THE SELECTED HORIZONS AND 3D MODELING

The seismic section E1 at Hannukainen (Fig. 35) shows three highly reflective, gently dipping units stacked on top of each other. The thickness of these units varies between 200 and 250 m. The uppermost of the highly reflective units can be correlated with the mafic volcanic rock that hosts part of the ore at Hannukainen and correlates with the Rautuvaara Formation. Comparison with the E1 profile and cross section of the Hannukainen deposit demonstrates that the Laurinoja ore body also shows up as a reflector on top of the Rautuvaara Formation reflectors in the seismic data (Fig. 36). The second, lower highly reflective unit (B in Fig. 35) correlates at its upper part with the mica schist and quartzite unit below the Rautuvaara Formation at Hannukainen. Drilling has not, however, extended through this unit, and the composition of the lower part is therefore unknown. There are no drilling or outcrop data that would indicate the lithology of the lowermost C unit.

The stacked highly reflective units can be traced from section to section, thus making them ideal key horizons for 3D modeling. Of the key structures, only the ÄSZ has been modeled. It appears as a set of transparent zones that cross-cut the reflectors, a feature that is clearest in seismic sections V1 and V5, which cross-cut the shear zone at steep angles (Fig. 37). The gently dipping to horizontal A, B, and C units appear to steepen on both sides of the shear zone, although no dramatic vertical shift in these units can be seen. The ÄSZ, albeit clearly a zone of fractures with an approximate thickness of a few hundred meters, is modeled as a plane.

The modeled three highly reflective units (A, B, C in Fig. 35) form a broad open fold plunging approximately 30 degrees to the SW, the ÄSZ being located in the axial plane of the fold (Fig. 38). The internal form of the fold structure shows small-scale dome and basin structures, suggesting buckling and bulging of the A, B, and C units during the folding events. The projected surface geology of the horizons A and B correlates well with the geological maps for the north of the Äkäsjoki shear zone. The A unit correlates with the Rautuvaara Formation mafic volcanic rock unit and B with the Sodankylä Group quartzites. The quartzite-mica schist sequence south of the ÄSZ, interpreted in geological maps to represent

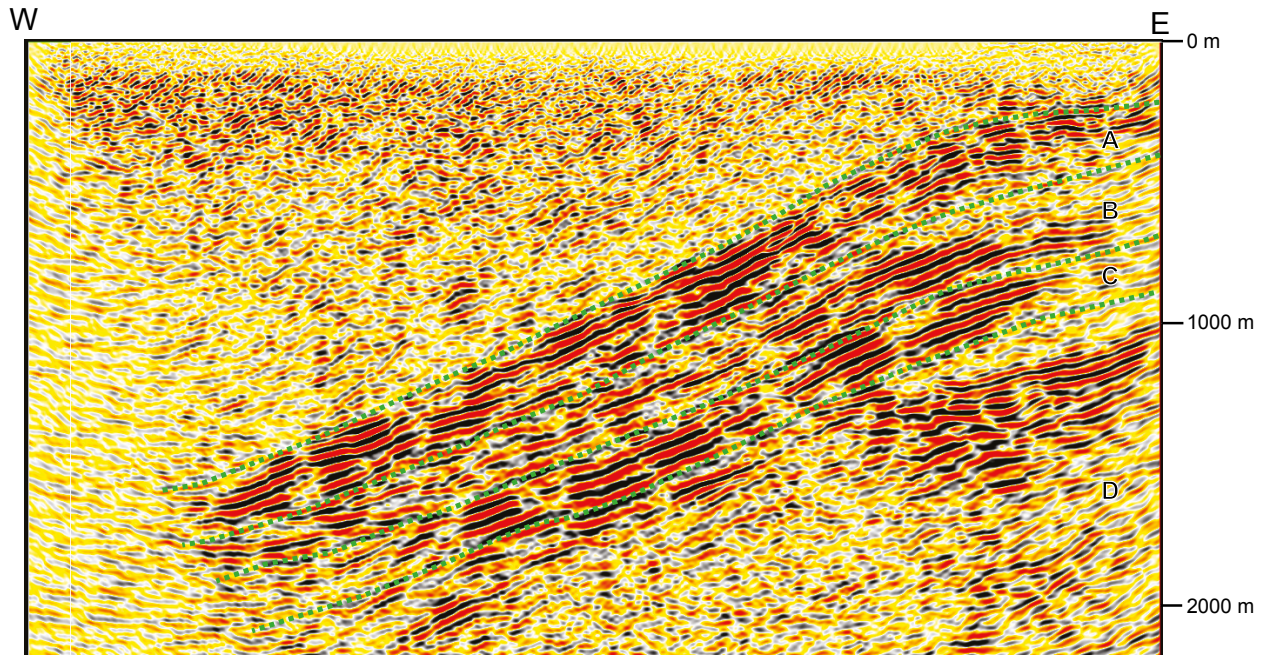

Fig. 35. Seismic E1 profile from Hannukainen with interpreted units (dashed green lines). See Figures 32 and 34 for the location of the profile.

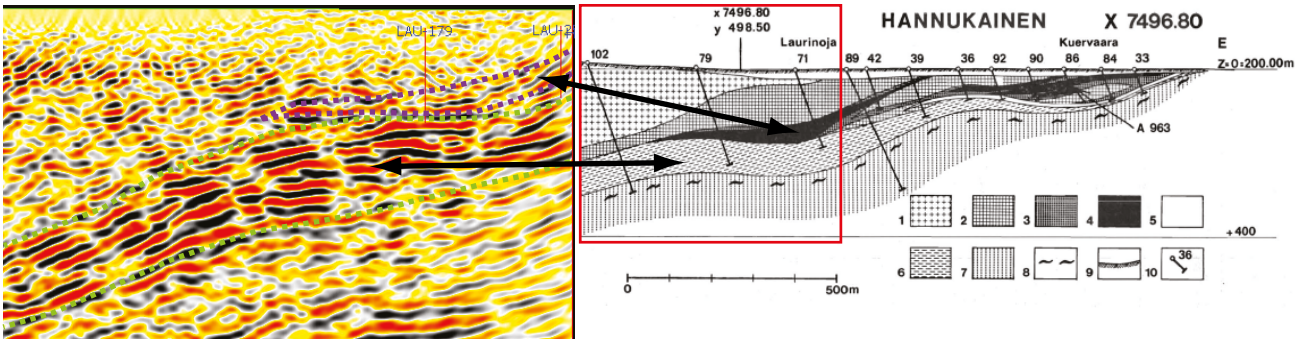

Fig. 36. Comparison of the geological cross section (Hiltunen 1982) and the E1 seismic profile spatially coinciding with the geological profile. The western part of the Laurinoja semi-massive magnetite ore shows up as reflectors, as well as the highly reflective mafic volcanic rock footwall unit. Legend for the geological profile: 1. monzonite, 2. diorite, 3. skarn rock, 4. magnetite ore, 5. quartz-feldspar schist, 6. mafic volcanic rock, 7. quartzite, 8. mica gneiss, 9. ground surface, 10. drill hole.

Sodankylä Group rocks, correlates with a 300- to 500-m-thick, weakly reflective topmost sequence on the eastern segment of seismic profile V1. It appears to be discordant with the modeled A and B units, suggesting that contrary to the current geological interpretation, the quartzite-mica schist unit is younger than the Sodankylä Group sedimentary rocks. This interpretation is further supported by new age data for the sedimentary rocks (see above). The aeromagnetic map of the area (Fig. 34) shows that there appear to be two different domains within the Sodankylä quartzite unit in the geological map. The domain north of the ÄSZ appears relatively monotonous and moderately magnetic, whereas the domain south of the ÄSZ is considerably more complex, consisting of alternating magnetic lows and highs. Based on seismic data and the geophysical characteristics of the two domains, the quartzite-mica schist unit south of the ÄSZ is modeled as a Svecofennian unit discordantly overlying the modeled A, B, and C units, and the northern domain is considered to represent the Sodankylä Group rocks.

The seismic reflectors become discontinuous, weak, and difficult to interpret in the southeastern corner of the modeled area and in the Rautuvaara

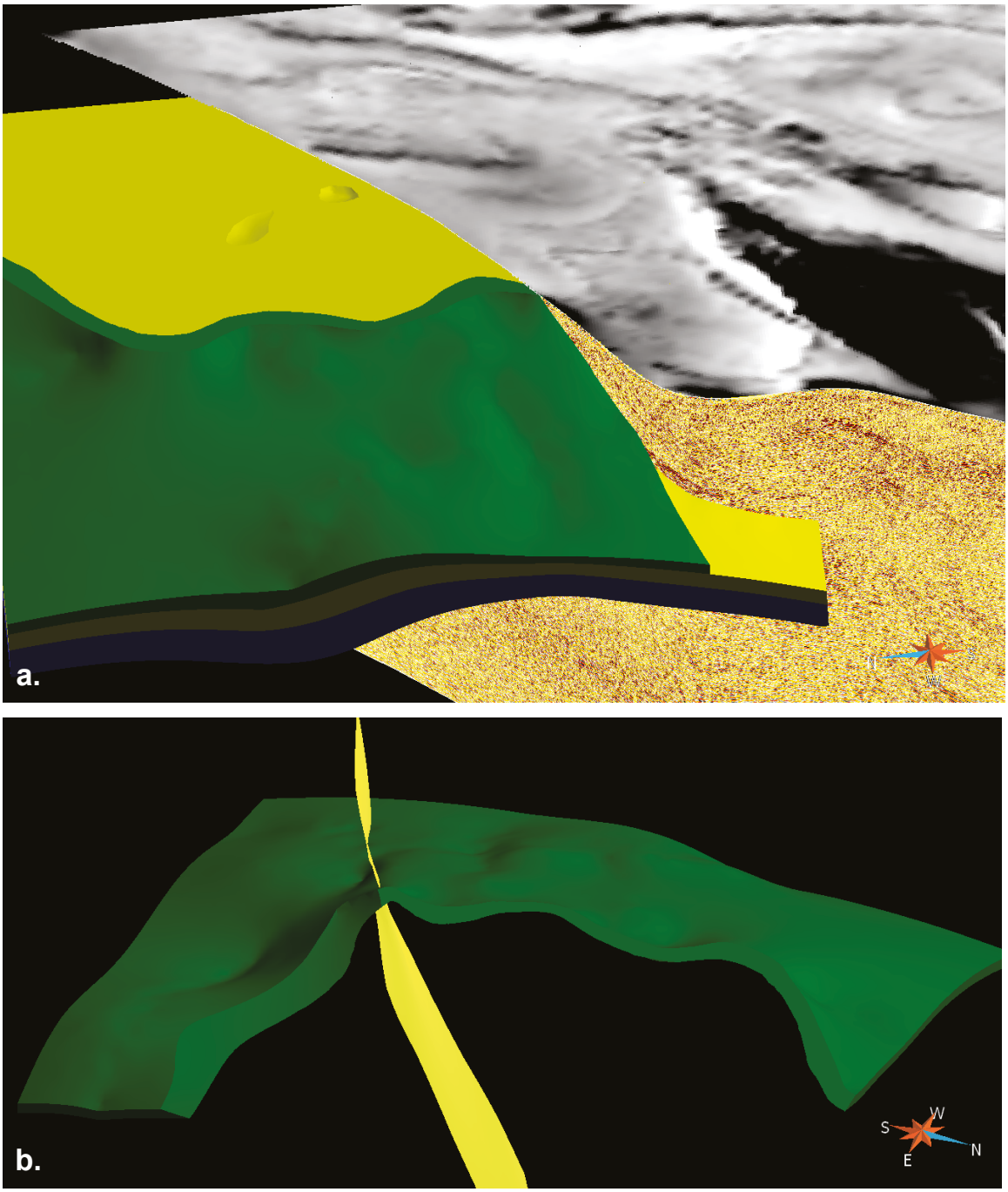

Fig. 37. A. Modeled three highly reflective units with seismic profile V2 and the aeromagnetic map. The uppermost green unit corresponds to the Savukoski Group mafic volcanic rock at footwall at Hannukainen, the yellow unit to the quartzite below it. Oblique view from west. B. Modeled uppermost highly reflective unit and Äkäsjoki shear zone as the plane (yellow). Note the folded geometry and the small-scale bulging and buckling of the mafic volcanic rock unit. The Äkäsjoki shear zone appears to be developed in the axial plane of the fold structure.

area. This may be due to steepening of the structures in this part, or the abundant monzonite intrusions that cut the units and cause the discontinuity, or both. Therefore, we modeled the intrusions and the small mafic volcanic rock units in this area as a single block referred to as the Rautuvaara complex. Other units modeled include the 'basement' on which the A, B, and C units overlie, and the low reflectivity unit north of the ÄSZ correlating with the monzonite, diorite, and granite intrusions west of Hannukainen. The complete model is presented layer by layer in Figure 39.

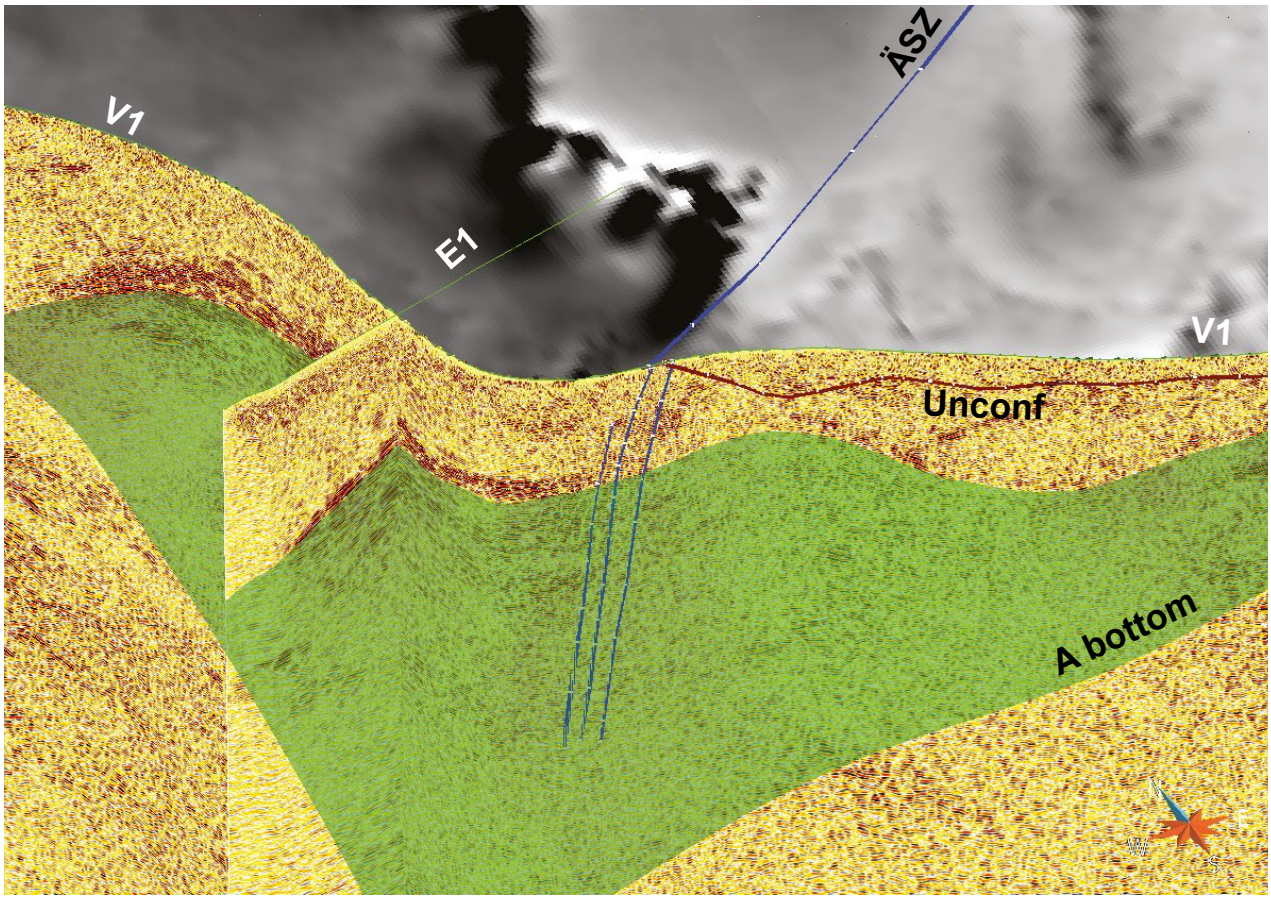

Fig. 38. The Äkäsjoki shear zone, which shows up as a set of subvertical transparent zones (blue lines) cross-cutting the subhorizontal reflectors on seismic profiles. The transparent green plane is the modeled bottom of the A horizon of Figure 37. The brown line indicates the unconformity on the Karelian units (see text). The gray-scale aeromagnetic map is presented as a reference on the surface.

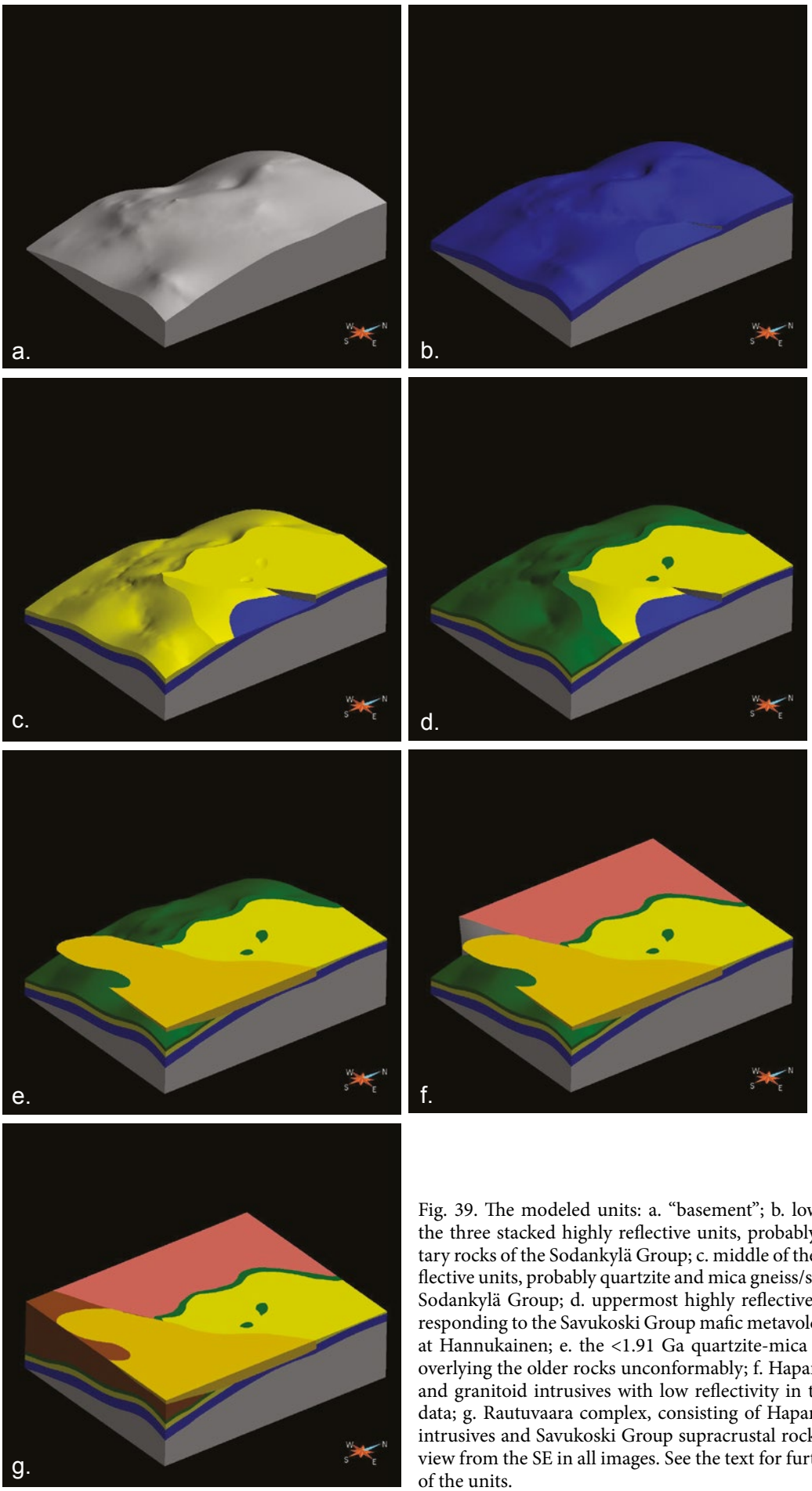

Fig. 39. The modeled units: a. "basement"; b. lowermost of the three stacked highly reflective units, probably sedimentary rocks of the Sodankylä Group; c. middle of the highly reflective units, probably quartzite and mica gneiss/schist of the Sodankylä Group; d. uppermost highly reflective units corresponding to the Savukoski Group mafic metavolcanic rocks at Hannukainen; e. the <1.91 Ga quartzite-mica schist unit overlying the older rocks unconformably; f. Haparanda suite and granitoid intrusives with low reflectivity in the seismic data; g. Rautuvaara complex, consisting of Haparanda suite intrusives and Savukoski Group supracrustal rocks. Oblique view from the SE in all images. See the text for further details of the units.

DISCUSSION AND CONCLUSIONS

The uppermost highly reflective unit that correlates with the Savukoski Group mafic volcanic rock at Hannukainen forms a broad open fold structure plunging ca. 25 degrees to the SW, which is consistent with the observed folding data from the outcrops. In the Rytijänkä and Rautuoja areas, the top of this unit is respectively at 1500 m and 3000 m below the current bedrock surface. Although the model does not extend to the Rautuvaara area, it is clear that the same unit that partly hosts the deposits north of the ÄSZ cannot be exposed at the surface in the Rautuvaara area, and that the present interpretation of the Rautuvaara Formation in current maps is not correct.

The proposed strata-bound nature of the known deposits has been somewhat dubious, as some of the deposits are partially hosted by the Haparanda-type diorite intrusions and younger Kumpu Group rocks (e.g. Hiltunen 1982, Niiranen et al. 2007). The seismic data show that even the deposits that in current 2D geological maps are hosted by the so-called Rautuvaara Formation cannot be within the same stratigraphic level. Thus, the strata-bound model for the deposits is very unlikely, as already suggested by Niiranen et al. (2007). The division of the Savukoski Group at Kolari into the Rautuvaara and Kolari formations in previous interpretations was mainly based on the presence of skarns and iron deposits in the former, the lithology being otherwise the same. The seismic data do not support the presence of a uniform stratigraphic layer that could be connected through the area. Therefore, there remains no justification for separating the Savukoski Group into two separate formations in the Kolari area.

The highly reflective unit below the modeled Savukoski Group mafic volcanic unit is somewhat problematic. Based on the drilling data, the upper part of this consist of quartzites and mica gneiss and the unit outcrops at the location where the bedrock has been interpreted to represent Sodankylä Group rocks in current bedrock maps. However, the new age data combined with the seismic data indicate that the Niesakero-Kuertunturi quartzite complex south of the ÄSZ is an early Svecofennian unit overlying the older supracrustal rocks. The possible scenarios for nature of the quartzite north of the ÄSZ are: a) it belongs to the Sodankylä Group as it is mapped and shown in our model, b) it belongs to the same Svecofennian unit as the rocks south of the ÄSZ, and the Savukoski Group rocks in the Hannukainen area and parts north of it have been thrusted on top of the quartzite, or c) the mafic volcanic rocks that host the deposits at Hannukainen are also Svecofennian in age. We consider option c to be very unlikely. The difference between the two quarzite-mica-schist domains in aeromagnetic maps suggests that the first option would be the most viable, although further age dating would be required to verify this. The lowermost highly reflective unit C cannot be correlated with any known exposed rocks. If the B unit belongs to the Sodankylä Group, it is very likely that the C unit represents the lower part of the same group.

The results of this work provide some interesting insights into the tectonic evolution of the area. The broad open fold shape of the modeled Savukoski Group and orientation of the fold axis coincides with the previously measured fold axis. Hiltunen and Tontti (1976) suggested that this was the earliest folding event in the area, and that it predates or is synchronous with the intrusion of the 1.89–1.86 Ga Haparanda suite rocks. The fold axis orientation suggests that the dominant compression was NW–SE-oriented at this stage. Väisänen (2002) presented evidence of NE-vergent thrusting from the SW part of the Kolari area, and the very prominent SW-plunging stretching lineation supports this. The small-scale dome and basin structures observed in the modeled Savukoski and Sodankylä Group units may result from refolding during the D_3 stage thrusting. However, this is somewhat uncertain, as the doming may already have taken place during the D_2 folding event.

The modeled Äkäsjokisuu shear zone appears to have been developed into the axial plane of the broad fold structure, supporting the earlier interpretations of Hiltunen and Tontti (1976) for the generation of the NE-striking shear zones in the area. This suggests that there was a shearing component during the early folding event or that the NE-striking shear zones were developed during the following NE vergent thrusting.

The unconformity between the modeled <1.91 Ga quartzite-mica schist unit and the lower supracrustal units suggest that there was a hiatus between the two supracrustal sequences. The outcrop data and the geophysical map of the <1.91 Ga quartzite-mica schist unit indicate that it is folded,

and that the folding appears to have taken place in the same stage as when the Savukoski Group rocks were folded. Nevertheless, the Karelian rocks appear to have been tilted prior to the deposition of the younger sedimentary rocks on them.

CHAPTER V.
THE LAPLAND GRANULITE BELT 3D MODEL

Tero Niiranen, Vesa Nykänen and Ilkka Lahti

INTRODUCTION

The Central Lapland greenstone belt (CLGB) is bound at its NE end to a tectonized zone consisting of the Hetta and Vuotso complexes intermingled with Karelian Salla, Sodankylä, Savukoski, and Kittilä group rocks (Fig. 40). The Lapland Granulite Belt (LGB) comprises the northeasternmost unit of the tectonized zone. The LGB has been interpreted by several authors as a SW-vergent thrust zone related to the continent–continent collision of the Kola craton in the NE and the Karelian craton in the SW (e.g. Marker 1988, Gaál et al. 1989, Korja et al. 1996, Tuisku et al. 2006). Many of the main tectonic features of the CLGB have been interpreted to be related to compression from the NE and linked to LGB thrusting, making the area one of the key locations in understanding the structural evolution of the CLGB (e.g. Ward et al. 1989, Väisänen 2002, Hölttä et al. 2007, Patison 2007). Several 2D interpretations of the area have been presented based on the magnetotelluric, gravity and seismic POLAR and FIRE data (e.g. Elo et al. 1989, Gaál et al. 1989, Korja et al. 1989, Patison et al. 2006). This chapter presents a 3D visualization of the part of the LGB closest to the CLGB.

GENERAL GEOLOGY

The LGB has been divided into the Kuttura and Saariselkä suites (Fig. 40). The Saariselkä suite consists of garnet-sillimanite gneisses, originating from pelitic to psammitic sediments. The Kuttura suite consists of concordant sheets of anortosites and arc-type noritic to enderbitic intrusions. The detrital zircons of the Saariselkä suite sedimentary rocks fall within the range of 1.94–2.9 Ga, clustering around 1.97 and 2.2 Ga, and the age data for intrusions of the Kuttura suite norite-enderbite series indicate that they were intruded into the Saariselkä suite sediments at ca. 1920–1905 Ma (Tuisku & Huhma 2006). The bedrock adjacent to the southwest of the granulite consists of Vuotso complex arcositic gneisses and amphibolites and mafic to ultramafic intrusions intermingled with rift-related 2.44–2.0 Ga Salla, Sodankylä, and Savukoski group supracrustal rocks. Further southwest to these are the Hetta complex granitoids and mafic metavolcanic rocks of the 2.0 Ga Kittilä Group, the latter of which are referred here as the Kittilä Terrane (e.g. Lehtonen et al. 1998). The ca. 1.77 Ga Nattanen granite intrusions and Salla and Laanila dykes cross-cut these rocks and comprise the youngest rocks in the area.

The LGB and Vuotso complex rocks comprise the highest metamorphic grade rocks of northern Finland. The data for the LGB sedimentary rocks indicate a clockwise metamorphic path, with peak pT conditions of 5.5–8.0 kbars and 800–850 °C. The peak metamorphic conditions for the Vuotso complex rocks, at the SW margin, reach ca. 12 kbars and 650 °C (Tuisku et al. 2006). The metamorphic conditions decrease to the SW, being 7.4–9.9 kbars and 600–690 °C around the Hetta complex and the NE corner of the Kittilä Terrane, and decreasing to 3.2 kbars and 350–400 °C for

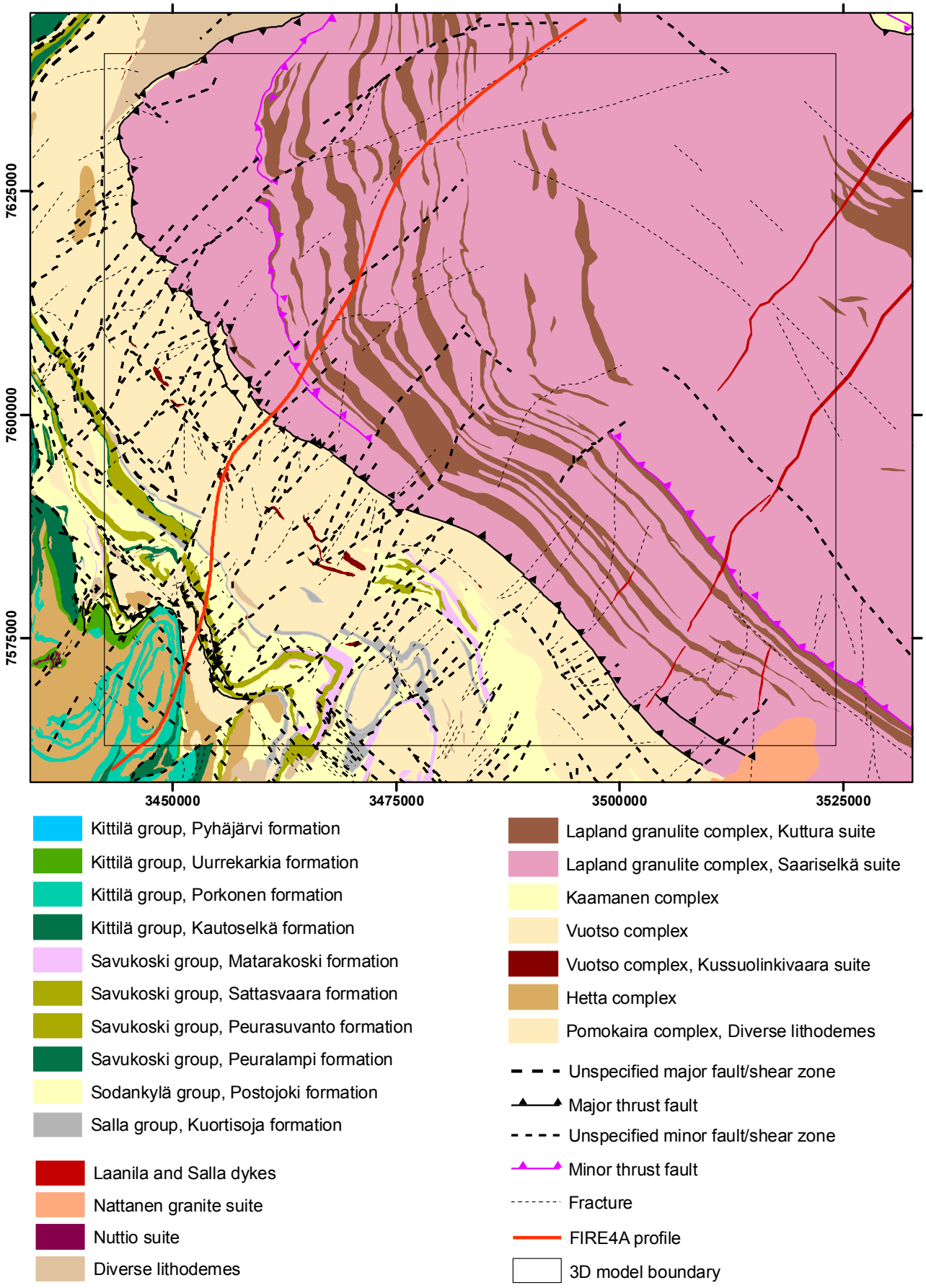

Fig. 40. Bedrock map of the study area with the location of the 3D model boundary and the FIRE4A seismic profile. After Bedrock of Finland – DigiKP.

the central and eastern parts of the Kittilä terrane (Hölttä et al. 2007).

Based on the metamorphic and age data for the LGB, Tuisku et al. (2006) and Tuisku and Huhma (2006) divided the evolution of the LGB into several stages: burial and heating of the metasediments after ca. 1.94 Ga, high-T metamorphism and migmatization at ca 1.91 Ga, accompanied by emplacement of norite-enderbitic intrusions at ca. 1.92 Ga, thrusting, erosion, and cooling of the whole LGB sequence from ca. 1.91–1.88 Ga, and final crystallization of leucosomes and exhumation to upper crust in 1.89–1.88 Ga. Tuisku et al. (2006) considered high-strain rocks of the Vuotso complex as a foreland slab related to the LGB thrust.

MATERIAL AND METHODS

The study was based on the airborne geophysical, bedrock observation and digital bedrock databases of GTK. In addition, seismic data from the Finish Reflection Experiment 2001–2005 (FIRE, see Kukkonen & Lahtinen 2006) were used in modeling. The modeling was carried out by interpreting the lithological units on geological and geophysical maps as well as on the seismic FIRE 4A profile. The visualization, interpretation and modeling were performed using Gocad™ software with Mira Mining utilities™ and GRGPack research plugins provided by the Gocad Research Group of the Nancy School of Geology. The surfaces were interpolated from these using the GRGPack StructuralLab plugin following methods described by Caumon et al. (2007). A 3D block model was generated from the surfaces using Gocad inbuilt tools.

INTERPRETATION OF THE KEY HORIZONS

In airborne magnetic maps, the LGB shows up as variable thick bands of magnetic low and high zones with a general strike of NW–SE (Fig. 41). The bands are cut and locally displaced by NE–SW-striking magnetic low lines interpreted as fault or shear zones in geological maps (e.g. Fig. 40). The area SW of the LGB representing the Vuotso complex rocks has similar characteristics in airborne magnetic maps, although the banding is less clear. The LGB and Vuotso complex rocks appear as highly reflective units in the seismic section, with the reflectors having a gently NE-dipping listric pattern (Fig. 42a). The reflectors correlating with the LGB and Vuotso complex rocks flatten out at depth, and based on the seismic data, the interpreted base of the southwesternmost Vuotso complex rocks reach a depth of ca. 12.5 km. The seismic pattern of these units correlates with the interpreted SW-directed thrust. However, the listric thrust pattern extends further SW on the seismic profile, the southwesternmost listrict reflectors reaching the surface at the northeasternmost margin of the Hetta complex (Figs. 40 and 42a).

Based on seismic, aeromagnetic, and bedrock data, a total of 9 tectonic blocks were distinguished (Figs. 42 and 43). The LGB in the modeled area is divided into four tectonic blocks separated by discontinuities in the seismic data, which appear as tectonic features (thrust planes). For the Vuotso complex, three tectonic blocks were distinguished on a similar basis. In addition, one small tectonic slice was outlined, correlating with Vuotso complex rocks on the surface, and the last unit in the seismic profile consists of Kittilä terrane material (Figs. 42 and 43).

The apparent dips of the seismic reflectors of the thrust zones closest to the surface level vary between 18 and 32 degrees to the NE along the thrust zone. As the seismic profile is almost perpendicular to the lithological banding, the dips on the seismic data are relatively close to the true dips. This is further supported by the bedrock observation data. GTK's databases include a total of 712 foliation measurements from the LGB and Vuotso complex rocks within the modeled area and its close proximity. We divided these measurements into three groups based on their spatial distribution: measurements in the NW, central, and E part of the model (Fig. 44). The average dip orientations of these groups are in agreement with

apparent dip data measured from the seismic profile. This also shows that the dips appear to steepen when moving from the NE to the E along the LGR and Vuotso complex units, a feature that has also previously been reported (e.g. Tuisku et al. 2006). This at least partly explains the apparent thickening of the lithological units moving to the NE.

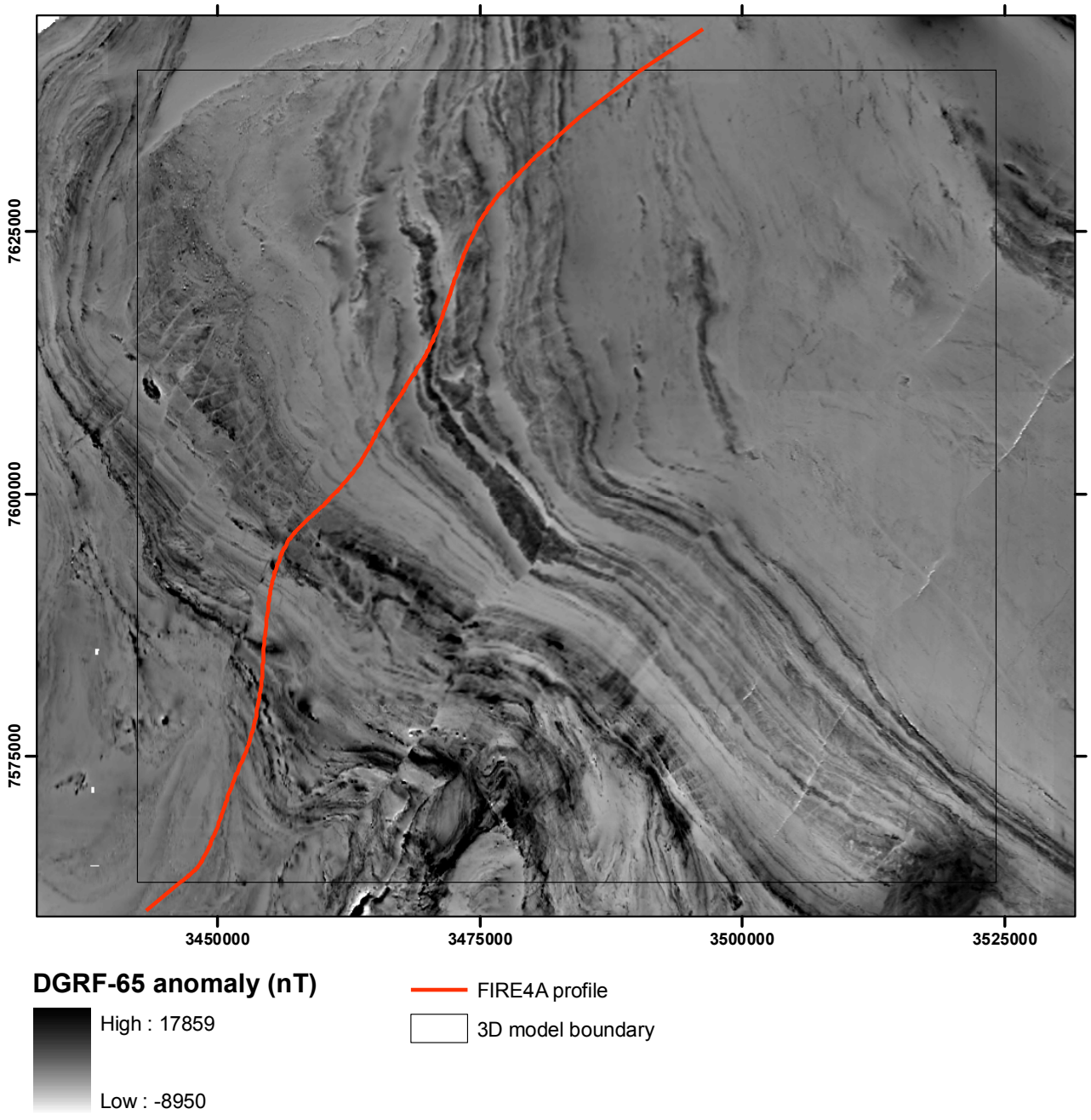

Fig. 41. Airborne magnetic map of the study area with the location of the 3D model boundary and the FIRE4A seismic profile. GTK data.

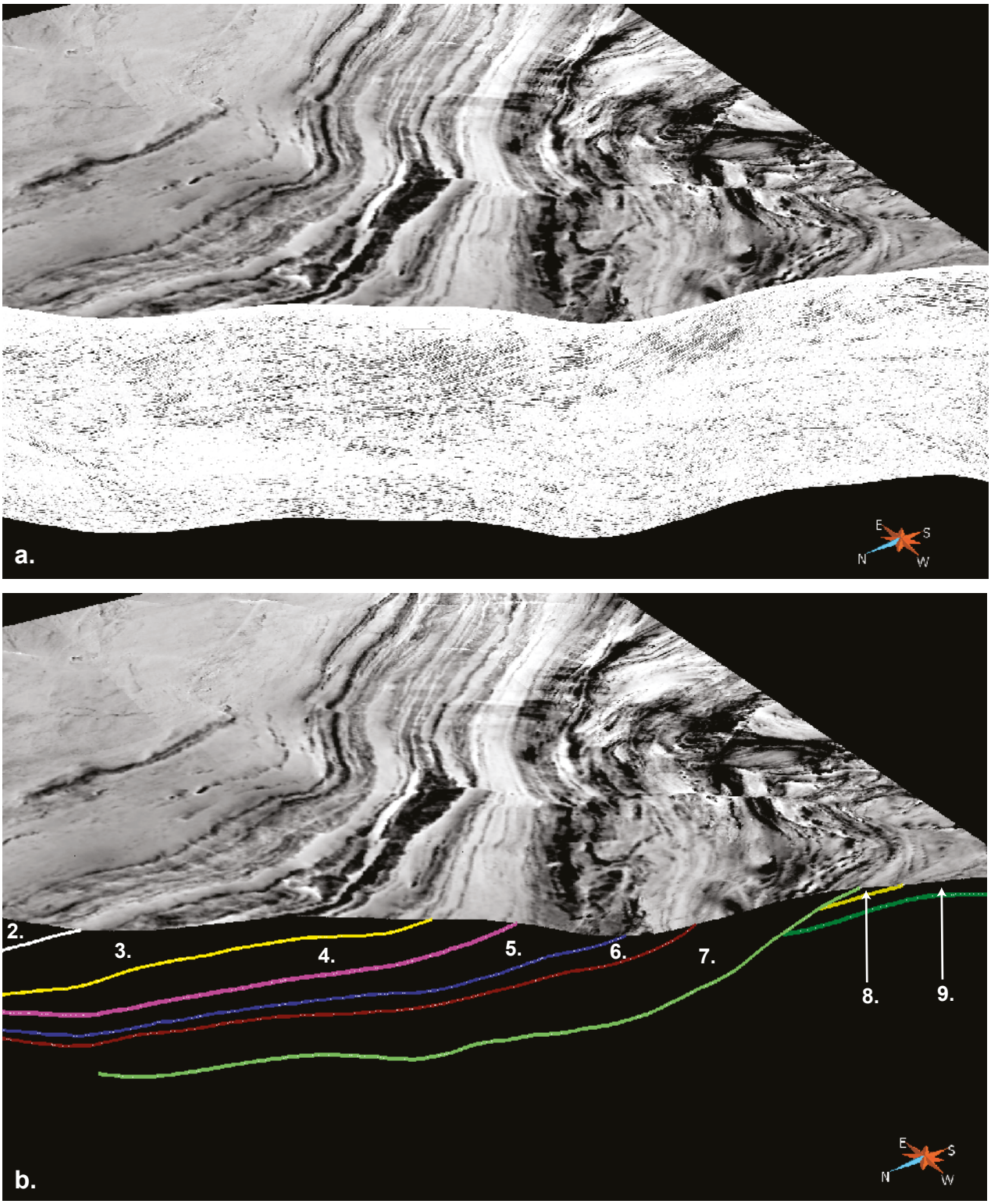

Fig. 42. a. Airborne magnetic map and the FIRE4A seismic profile. The bottom of the seismic profile is at 20 km depth. Oblique view from the NW. b. The tectonic blocks, interpreted based on the seismic data. The same view as in a. See Figure 43 and the text for an explanation of the numbering.

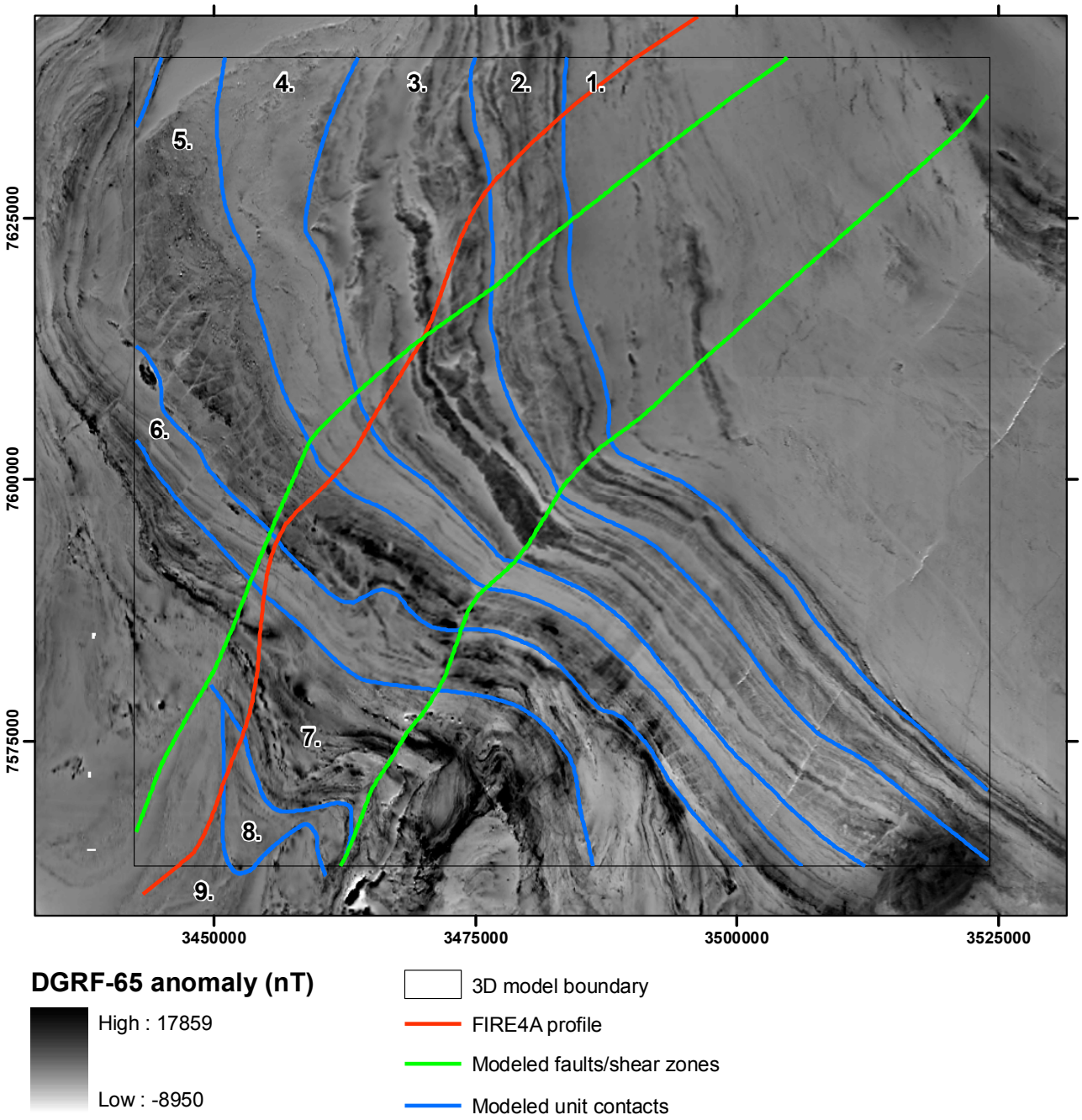

Fig. 43. Interpreted tectonic block boundaries (blue) and modeled faults (green) on the airborne magnetic map. Units 1–4 comprise the LGB blocks, 5–7 the Vuotso complex blocks, 8 Hetta complex rocks, and 9 Kittilä terrane rocks (cf. Figure 1).

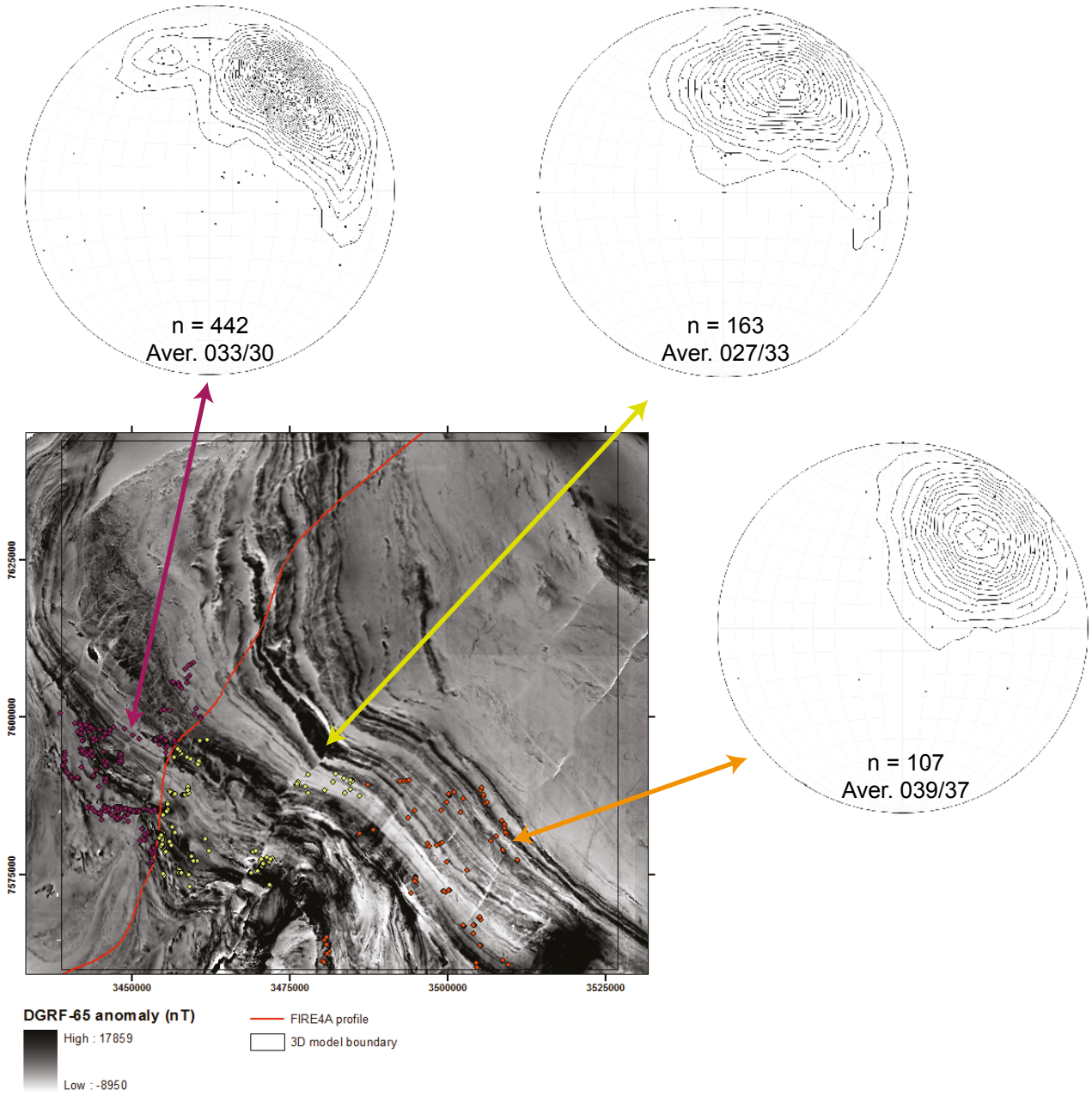

Fig. 44. Location of the foliation measurement data and the average foliation orientations in different parts of the study area. Dip orientation vectors as points on the lower hemisphere, equal area projection.

The 3D model

Based on the interpreted boundaries presented in Figures 42 and 43, and the foliation measurement data, the thrust planes limiting units 1–6 were constructed as surfaces, and from the surfaces the units representing the four LGB tectonic and 2 Vuotso complex blocks were built as 3D blocks (Fig. 45). The two most significant NE–SW-striking faults were constructed in the model as planes. However, as there are no direct dip data, the faults were assumed to be vertical. The modeled units are presented in Figure 46. The vertical extent of the model is 10 km.

Based on the modeled units, all tectonic blocks are relatively uniformly thick along their horizontal axis, the apparent thickness variation observable on their surface expressions relating to the variation in dips. The true thickness of units 2–4 varies between 2.5 and 3 km. They thicken towards

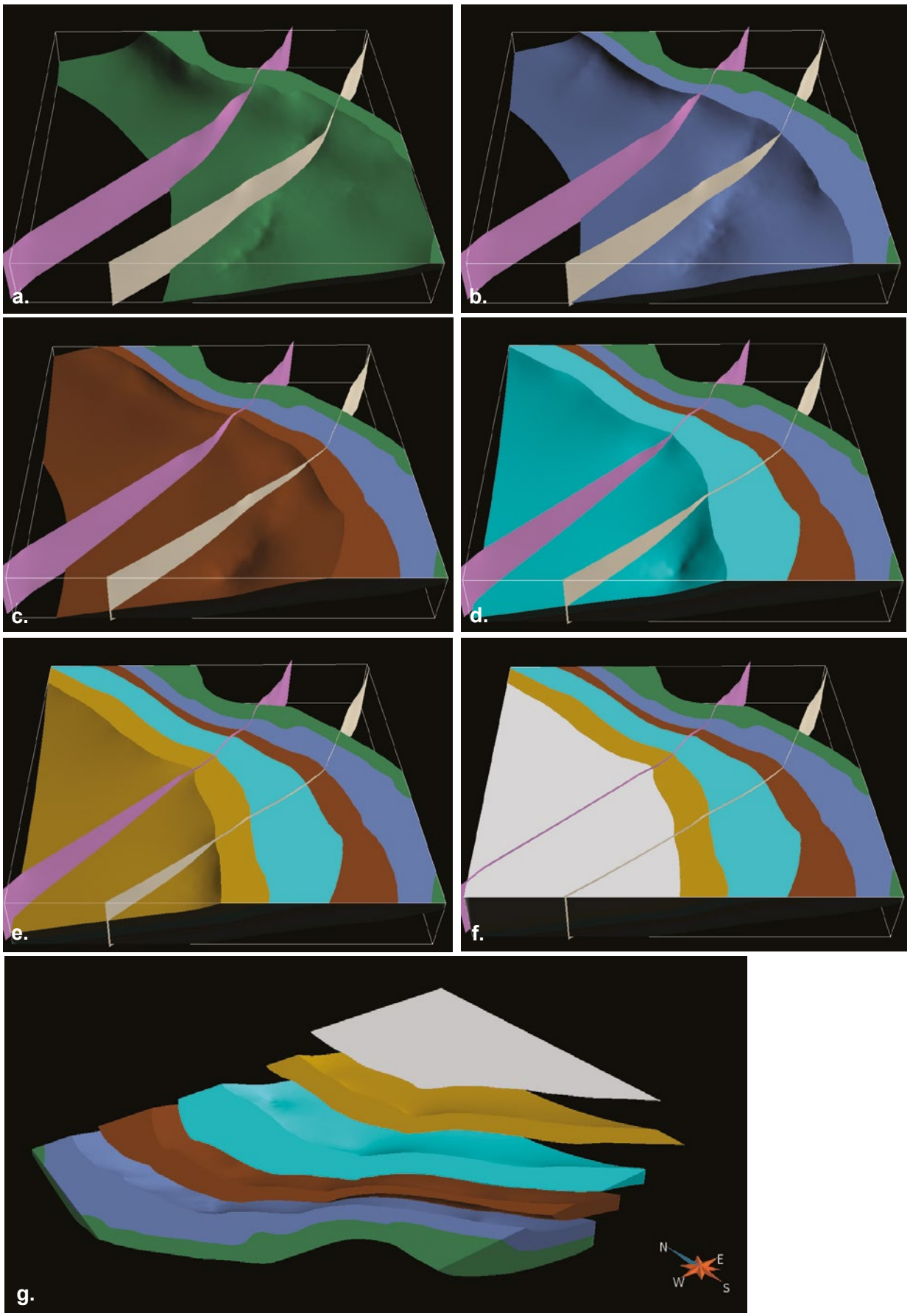

Fig. 45. 3D model of the study area. a.–d. are the LGB tectonic blocks (1–4 in Fig. 43), e.–f. the Vuotso complex tectonic blocks (5–6 in Fig. 43). The two planes are modeled NE–SW-striking faults. Oblique view from the N. g. All modeled tectonic blocks in an "exploded" view. Oblique view from the SW.

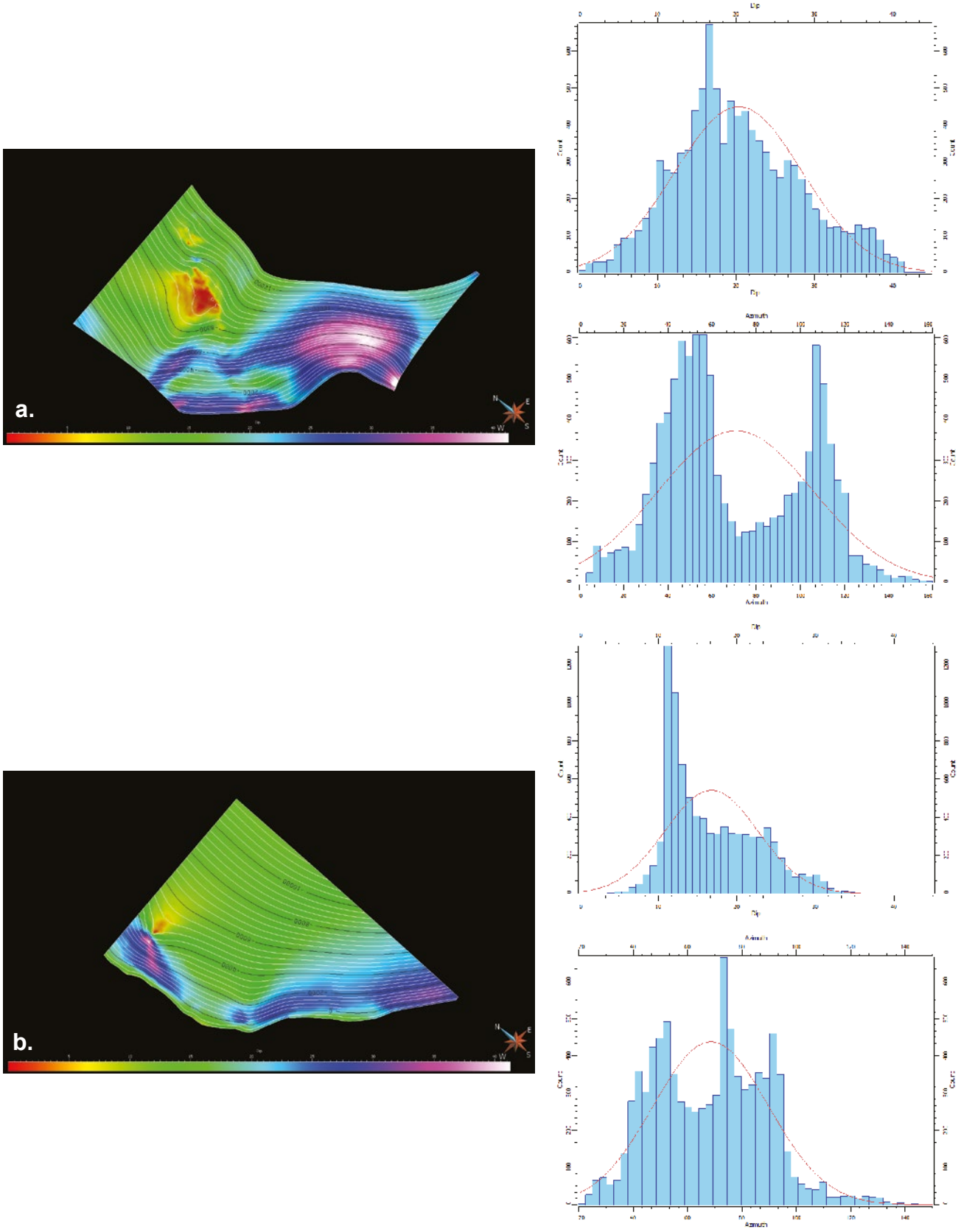

Fig. 46. The variations in the dip of the base of the modeled tectonic blocks. a. Block 6; b. block 1. Histograms of the dips and strikes for each node in the corresponding planes.

the top at the locations where their dips steepen. A similar pattern exists with units 5 and 6, representing Vuotso complex rocks. However, there is also thickness variation along the horizontal axis in these units. The spatial variation in dips of the base of units 1 and 6 is presented in Figure 46. This illustrates the flattening of the modeled units at depth, the steepest parts generally being close to the surface.

DISCUSSION

The constructed 3D model shows classical features of a thrust front with listric thrust planes, being in good agreement with the previous studies on the LGB. The NE–SW-striking shear or fault zones probably represent tear or transfer faults relating to the thrust planes. Clearly, the thrust front extends a considerable distance to the SW from the LGB rocks, including all of the Vuotso complex rocks, and the effects of the SW-directed thrusting events extend further SW to the Kittilä terrane rocks.

Based on the metamorphic data, Tuisku et al. (2006) and Tuisku & Huhma (2006) estimated that the high-pressure assemblages of the LGB were formed at depths of ca. 28 km, and the melting and crystallization of the leucosomes took place at ca. 7 km depth some 30 Ma later. The highest peak metamorphic pressure estimates come from the Vaulo area, which corresponds to the modeled block 5. For these, the metamorphic assemblages indicate pressures of ca. 11 kbar, corresponding to a depth of ca. 40 km (Tuisku et al. 2006). Tuisku et al. (2006) presented a model for LGB metamorphism in which the sedimentary rocks were deposited into a trench environment and were subsequently obducted by a subducting slab into the mantle, where they were subjected to high-pressure high-temperature metamorphism. The subsequent low-pressure assemblages were formed via post-peak metamorphic thrusting and exhumation of the LGB rocks.

Based on the seismic data and the 3D model presented here, the thrusting of ca. 40 km of the LGB rocks in a horizontal direction would have resulted in a ca. 10 km change in depth if the shape of the LGB had been the same as at present. This suggests that an approximately 18-km-thick sequence of rocks had to be exhumed from the top of the LGB rocks, and ca. 30 km from the Vuotso complex rocks. These figures are clearly too high to be explained by simple erosion and uplift, and the tectonic transport during the later stages of evolution has clearly accounted for much more than the 10 km uplift. The dramatic peak pressure differences between the Vuotso complex and the LGB data indicate that the depth difference of these units was more than 10 km during the formation of the peak pressure assemblages. Hence, there were probably considerable differences in transport distances between the different tectonic blocks within the thrust belt.

CHAPTER VI.
THE SAATTOPORA Au-Cu DEPOSIT 3D MODEL

Tero Niiranen, Vesa Nykänen and Ilkka Lahti

INTRODUCTION

The Saattopora Au(-Cu) deposit was discovered in 1985 by Outokumpu Oyj and was subsequently mined during 1988–1995 from two open pits and underground workings. The total amount of gold produced was 6279 kg, and 5177 tonnes of copper was produced as a by-product. The deposit is located in the municipality of Kittilä, in Northern Finland. The Saattopora is one of several gold deposits discovered along the E–W-trending Sirkka thrust, although it is the only one that has been under full-scale mining. In 2008, Outokumpu Oyj delivered much of the existing data from the Saattopora deposit to GTK. This was the early stage of the 3D modeling project on the Central Lapland Greenstone Belt, and it was soon decided to use the data to construct a deposit-scale 3D model of the Saattopora. The aims were to test the suitability of Gocad software in deposit modeling, to evaluate the possible continuation of the mineralization to depth, and to assess whether the modeling would provide new insights into the geological setting of the deposit, including its relation to the regional deformation.

GEOLOGICAL BACKGROUND

The Saattopora deposit is located in the western part Central Lapland Greenstone Belt (CLGB), next to the major, crustal-scale Sirkka thrust zone (Fig. 47). The deposit consists of two roughly E–W-trending lodes that are hosted by variably altered mica schists, phyllites, komatiites, mafic tuffs and mafic lavas of the >2.2 Ga Savukoski Group (Fig. 48). The intrusives in the area consist of 2.2–2.0 Ga diabase dykes and 2.0 Ga felsic porphyry dykes, the former of which occur in the ore hosting sequence. The mineralization consists of N–S-striking, sub-vertical to vertical quartz-carbonate-sulfide-gold veins, vein arrays, and hydrothermal breccias (Fig. 49). The total size of the deposit is 2.163 Mt and the average grades are 3.29 g/t Au and 0.28% Cu (Lahtinen et al. 2005).

The host rock sequence was subjected to polyphase deformation and metamorphism during the Svecofennian orogenic events in 1.91–1.79 Ga. The earliest ductile deformation stages, D_{1-2}, relate to thrusting from the south and northeast, and the last D_3 stage in the western part of the CLGB relates to thrusting from the west or southwest (e.g. Ward et al. 1989, Hölttä et al. 2007, Patison 2007). The regional metamorphic grade at Saattopora is of mid-greenschist facies and the peak conditions were reached during the D_{1-2} stage (Hölttä et al. 2007). The Saattopora deposit is structurally controlled by second or lower order structures relating to the Sirkka thrust, which was initially formed during the northward-directed thrusting in the D_{1-2} stage and subsequently re-activated during D_3 as a strike-slip shear (Patison 2007, Saalmann & Niiranen 2010).

Multi-stage and -style alteration has been detected at Saattopora. The earliest alteration stage is a regional-scale albitization that was folded in D_3 and possibly already during D_{1-2} (e.g. Patison 2007, Saalmann & Niiranen 2010, Niiranen et al. 2012). At Saattopora, the albitized rocks are overprinted

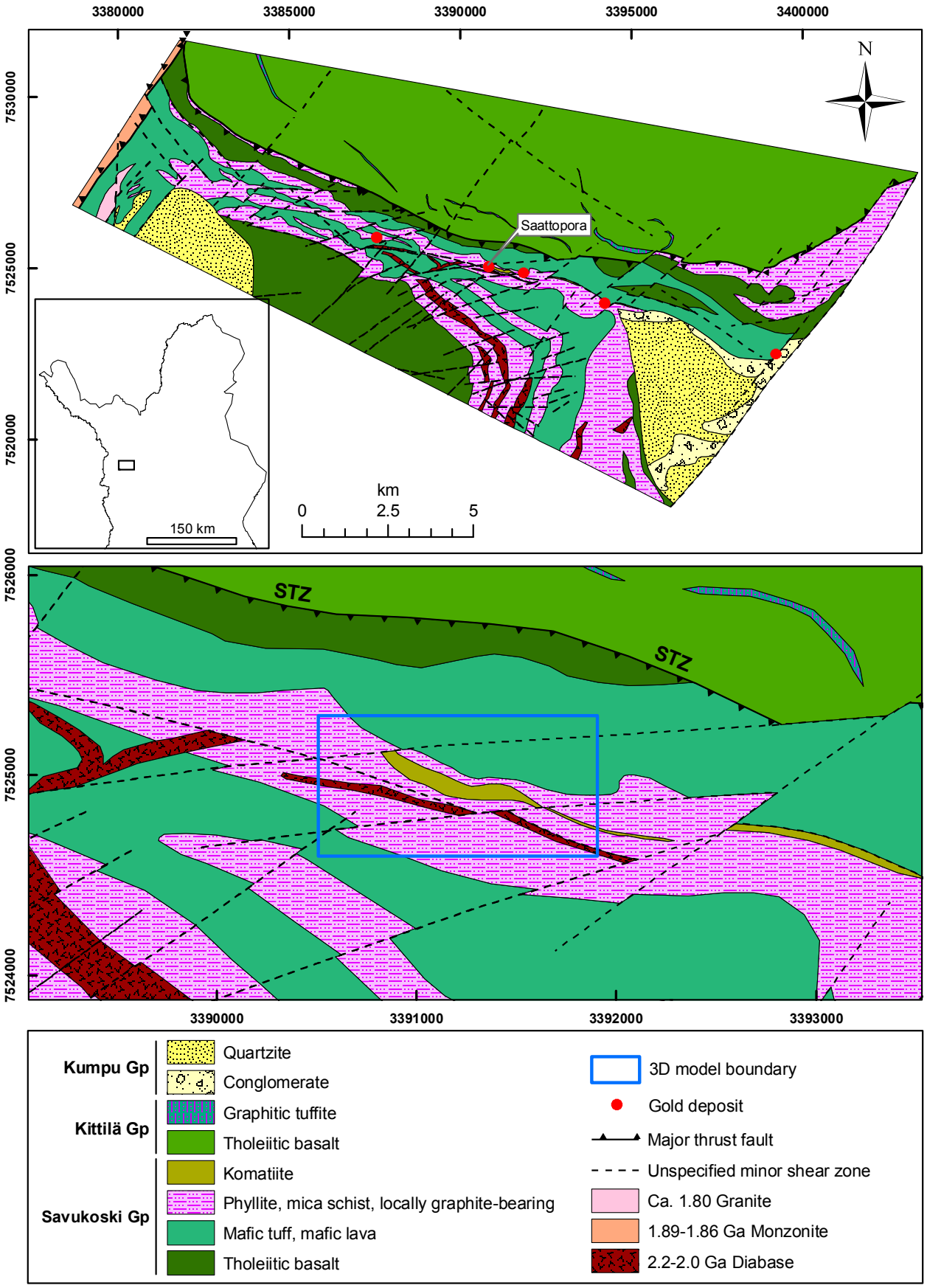

Fig. 47. New geological map of the Saattopora-Pahtavuoma region with the location of known orogenic gold deposits. Location of the mapping area in the inset (upper part). Detailed view of the Saattopora area geology and location of the 3D model extents. STZ = Sirkka thrust zone. Lithostratigraphical units after Lehtonen et al. (1998). Contains data from the National Land Survey of Finland Topographic Database 03/2013 © NLS and HALTIK.

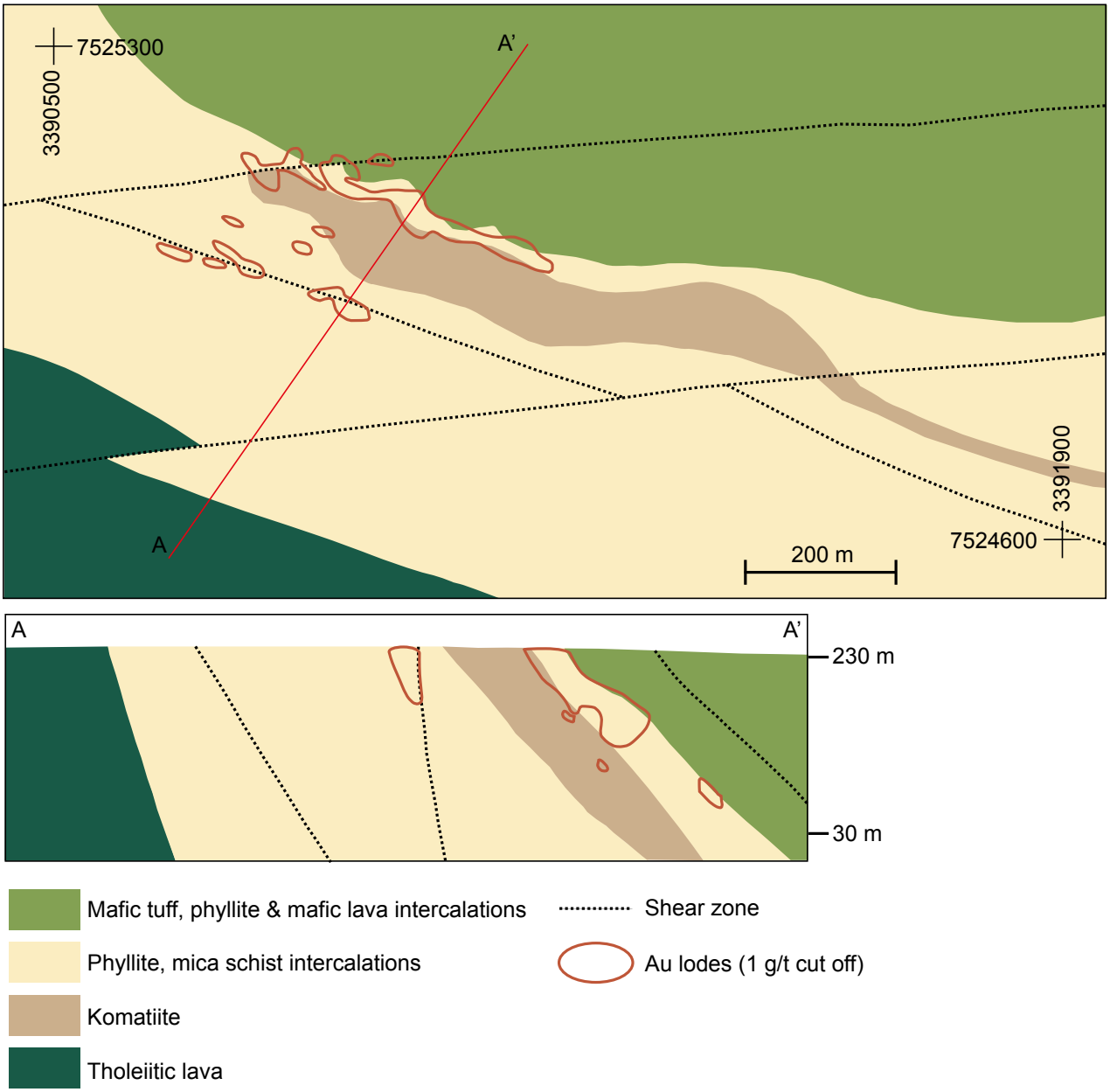

Fig. 48. Geology of the Saattopora deposit with 1 g/t Au envelopes. Redrawn after the generated 3D model.

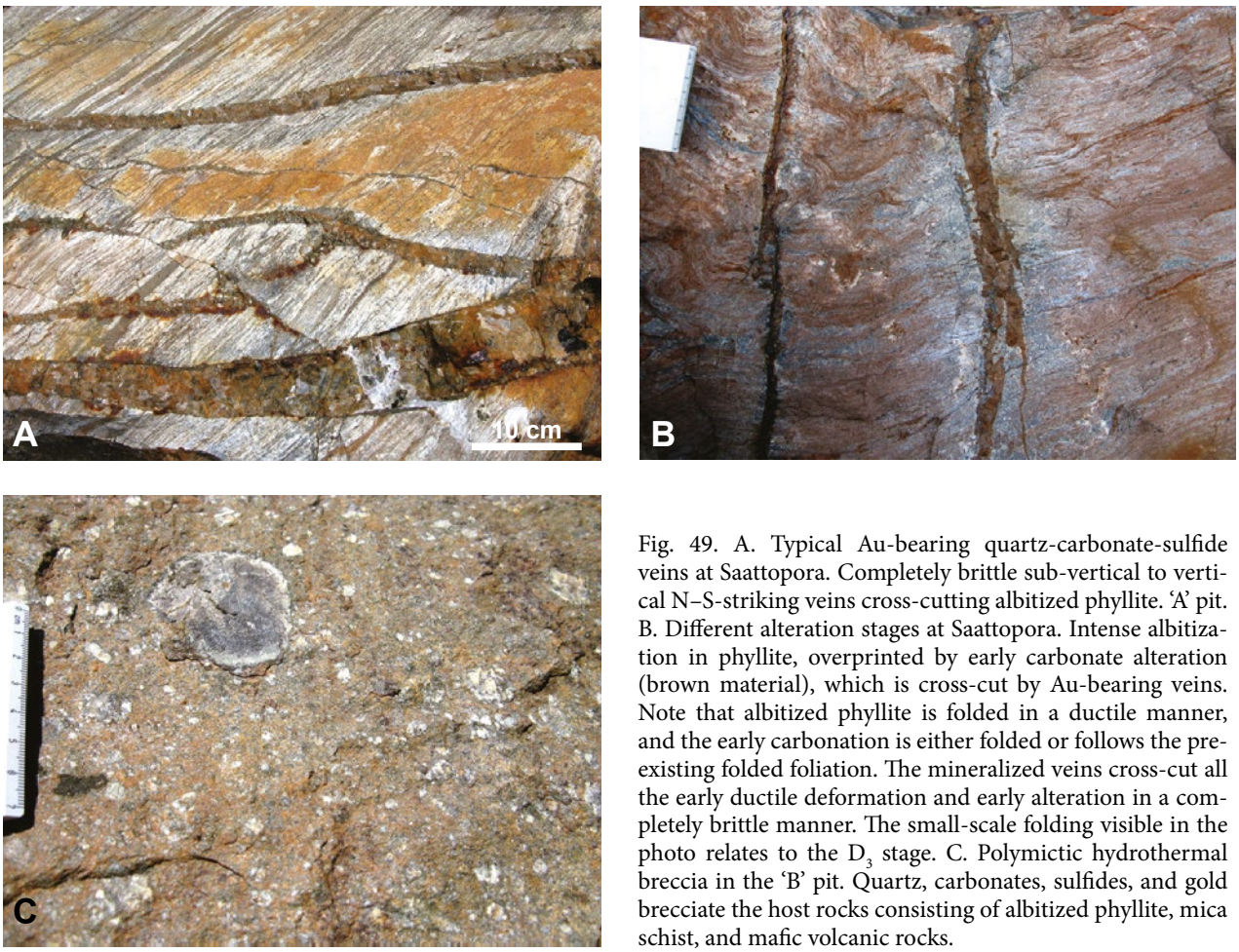

Fig. 49. A. Typical Au-bearing quartz-carbonate-sulfide veins at Saattopora. Completely brittle sub-vertical to vertical N–S-striking veins cross-cutting albitized phyllite. 'A' pit. B. Different alteration stages at Saattopora. Intense albitization in phyllite, overprinted by early carbonate alteration (brown material), which is cross-cut by Au-bearing veins. Note that albitized phyllite is folded in a ductile manner, and the early carbonation is either folded or follows the pre-existing folded foliation. The mineralized veins cross-cut all the early ductile deformation and early alteration in a completely brittle manner. The small-scale folding visible in the photo relates to the D_3 stage. C. Polymictic hydrothermal breccia in the 'B' pit. Quartz, carbonates, sulfides, and gold brecciate the host rocks consisting of albitized phyllite, mica schist, and mafic volcanic rocks.

by carbonation, which was either folded in the D_3 stage or follows the foliation folded in the D_3 stage (Fig. 49b). The mineralized veins crosscut these early alteration stages, as well as all ductile deformation features in the area. Other alteration styles reported are chlorite and talc-chlorite alteration detected in mafic and ultramafic rocks. However, they may be a regional feature related to the development of thrust and shear zones, as they have been reported from well outside the mineralized zone along the Sirkka thrust zone (e.g. Saalmann & Niiranen 2010). Sericite alteration has been also reported from the felsic host rocks, although it is unclear how it is related to the mineralization.

Fluid inclusion data from the mineralized quartz-carbonate veins indicate that the aqueous-carbonic mineralizing fluid was moderately saline (ca. 9% $NaCl_{eq.}$) and the mineralization took place at 300–350 °C (Niiranen et al. 2012). Fluid inclusion data also suggest that the mineralization was most likely due to phase separation between the aqueous and carbonic phases of the gold-carrying fluid, a feature that is further supported by the presence of hydrothermal breccias (Fig. 49c).

The general features of the Saattopora deposit fit the categorization of an orogenic gold deposit with atypical metal association outlined by Groves et al. (1998).

DATA AND PROCESSING

In the modeling, all available regional geological, geophysical, and digital elevation data of GTK were utilized, including the bedrock observation database and airborne geophysics. Ground geophysical data provided by Outokumpu, including magnetic, VLF-R, and gravity data, were additionally used (further details in Lahtinen et al. 2005). Based on these data and new field observations

recorded during the project, a revised 2D geological map was constructed covering the Saattopora and adjacent areas (Fig. 47). The 3D model is mostly based on the drill core data and geological maps available in the reports of Outokumpu Oyj (e.g. Korkalo et al. 1988, Korvuo 1995).

The drill core data package used in modeling consists of a total of 227 drill holes covering 19 727 meters of drill core. A total of 6212 rows of assay data were available in the data sets, including 2183 whole rock assays. The sample lengths of the assays varied between 0.15 and 6.01 meters, being 1.40 meters on average. The original lithological data consist of 7514 rows of data with lithological data in two columns, one with the lithology and the other with the respective abbreviation.

Much of the lithological data, especially on altered rocks, is reported using up to three index minerals in order of increasing abundance in front of the lithological name that refer to the rock texture, e.g. "carbonate quartz chlorite rock" or "quartz carbonate chlorite schist". This method, common prior to the computerized processing of drill core data, essentially means that all geological data (lithology, alteration, texture, volumetric proportions of minerals etc.) are embedded into a single cell, from which they have to be extracted prior to use in modeling. The use of the above-mentioned method for describing lithological data resulted in 199 different lithologies in the data set. By applying several methods, the lithology list was simplified for the modeling, focusing on extracting the original protolith for the altered rocks and extracting different alteration styles, textures, and structural styles into separate columns. The following key lithologies were extracted: phyllite, mica schist, mafic tuff, mafic lava, diabase, and komatiite. During the modeling process, these data were further simplified into mafic tuff, mafic lava, komatiite, and phyllite units, the last of which included both phyllite and mica schists.

THE 3D MODELS

Two types of 3D models were constructed: a lithological and a voxet model. The lithological model covers an area of 1500 m x 800 m x 240 m (length, width, height) and shows the major lithological units and the key structures as blocks and planes. The voxet model covers the same volume as the lithological model. The volume is divided into 5 m x 5 m x 5 m cells, into which the Au and Cu grades were interpolated from the drill core data and also the lithological data based on the modeled lithological boundaries.

Lithological model

Based on the drill core data, old geological maps, and geophysics, the following planes were modeled: three key shear zones, the surface of the bedrock, the surface of the earth, and four key lithological contacts (Fig. 50). The earth surface is based on the digital elevation model, the surface of the bedrock on the drill core data, and both surfaces were interpolated from the point data using the discrete smooth interpolation (DSI) method of the Gocad modeling software. DSI was selected because it aims to reduce the error between the data and the object that models the data while keeping the object as smooth as possible. The shear zones and lithological contacts were modeled using contact data from the drill cores and digitized contact data from the available lithological maps. In many cases, these data were insufficient for the software to produce geologically reasonable surfaces with the DSI method, and geological interpretations were thus carried out on cross sections and horizontal sections using expertise and the best judgment of the geologist. The reliability of the created surfaces depends on the density of the available data and complexity of the geology. The modeled surfaces are most complex and reliable in areas where the drilling data are dense. Some surfaces (e.g. the southernmost lithological contact) are only based limited drilling data. In turn, the northernmost contact of the komatiite unit is the most detailed, as most of the drill holes relating to the 'A' ore body were drilled through this.

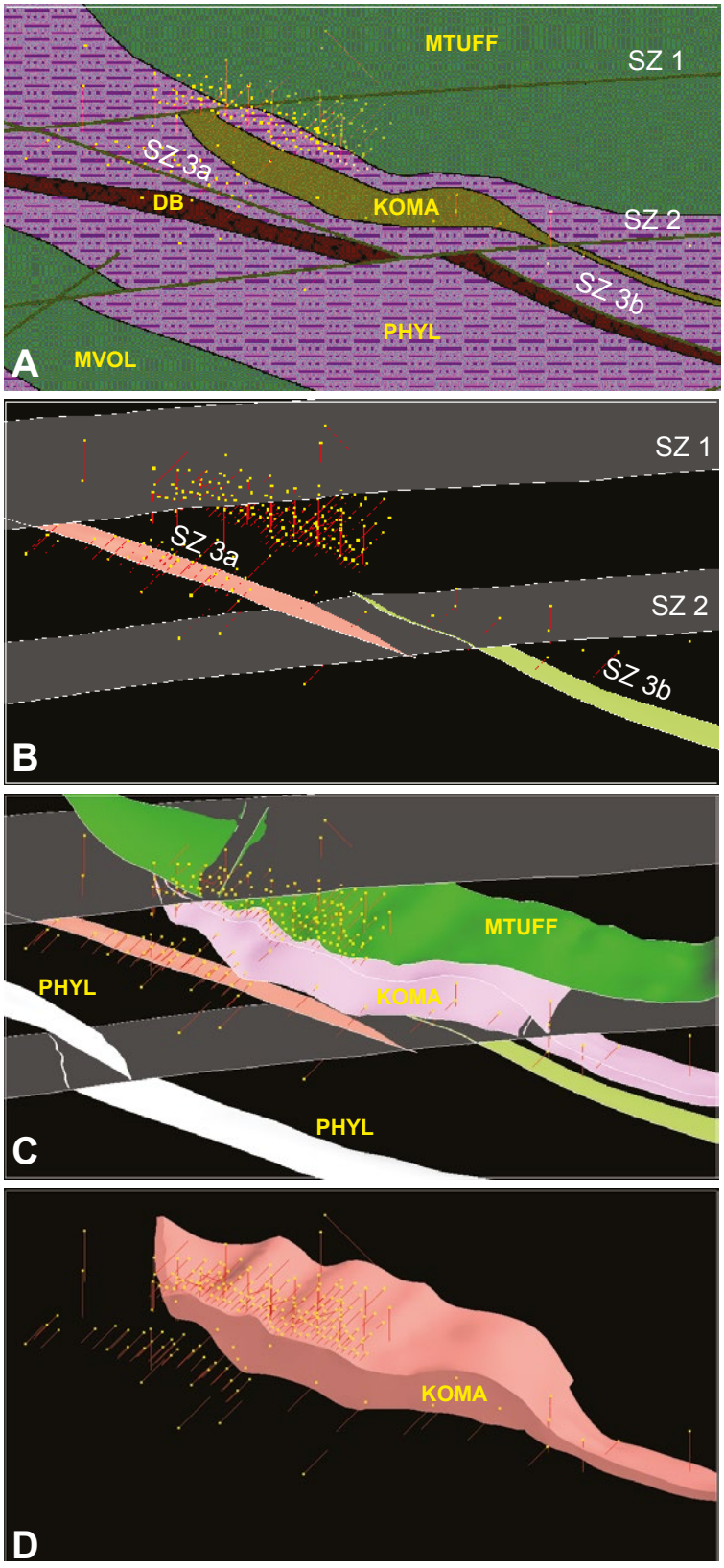

Fig. 50. Schematic figure of the modeling process. Same view angle for all images A–D. A. Geological map with the location of drill holes and the main lithological and structural units to be modeled. SZ = Shear Zone, MTUF = mafic tuff, Koma = komatiite, DB = diabase, PHYL = Phyllite, MVOL = mafic lava. The drilling data were inconsistent with the 2D interpretation of the diabase. Although there were thin intercepts of diabase in the drill core data, no continuation from drill hole to drill hole could be envisioned. Therefore, the unit was omitted from the final interpretation. B. Main shear zones interpreted as planes. C. Contacts between the lithological units interpreted as planes. D. Komatiite unit generated from the interpreted surfaces as a 3D block. Note the folded character of the unit: the fold axis plunges 45 degrees to 050, coinciding with the measured f_3 fold axis orientation in the close vicinity of the deposit (see text).

Volumetric blocks of the main geological units were generated using the modeled surfaces. These blocks enable better visual estimation of the geology. Although the volumes of each unit can be calculated and properties (e.g. density, susceptibility) can be assigned to each unit, their use in numerical modeling is limited.

Voxet model

The voxet model was generated to estimate the size, grade, and 3D extent of the ore. Furthermore, the lithological units were generated in the voxet model using the surfaces generated for the lithological model. The voxet model of the ore was calculated using search ellipsoids and the inverse distance gridding method. We emphasize that the generated model is not according to the international resource modeling standards (e.g. NI43-101 or JORC). However, the results are relatively consistent with the available production data of the Saattopora deposit.

The resource model was calculated separately for the 'A' and 'B' ore bodies. Search ellipsoid dimensions of 15 m x 15 m x 5 m were used in both cases. Orientations of 020/45 and 020/85 for the search ellipsoid were used for the 'A' and 'B' ore bodies, respectively. Initial orientations of the search ellipsoids were visually estimated, and the optimal values were determined by trial and error. The inverse distance method with a fall-off of three was used in calculations for both ore bodies. The ore bodies were separated into regions using cut-offs of 1 g/t Au and 1.5 g/t Au (Fig. 51). Cu grades were calculated for the voxet model using the same search ellipsoid values as for the gold. The calculated grades and tonnages, as well as statistics for the Au and Cu grades, are provided in Table 2. As density data on the ore blocks were lacking, the original estimate in Korkalo et al. (1988) of a bulk density of 2.9 g/cm^3 was used. The total tonnages and average grades for 1.0 g/t and 1.5 g/t Au cut-off values are summa-

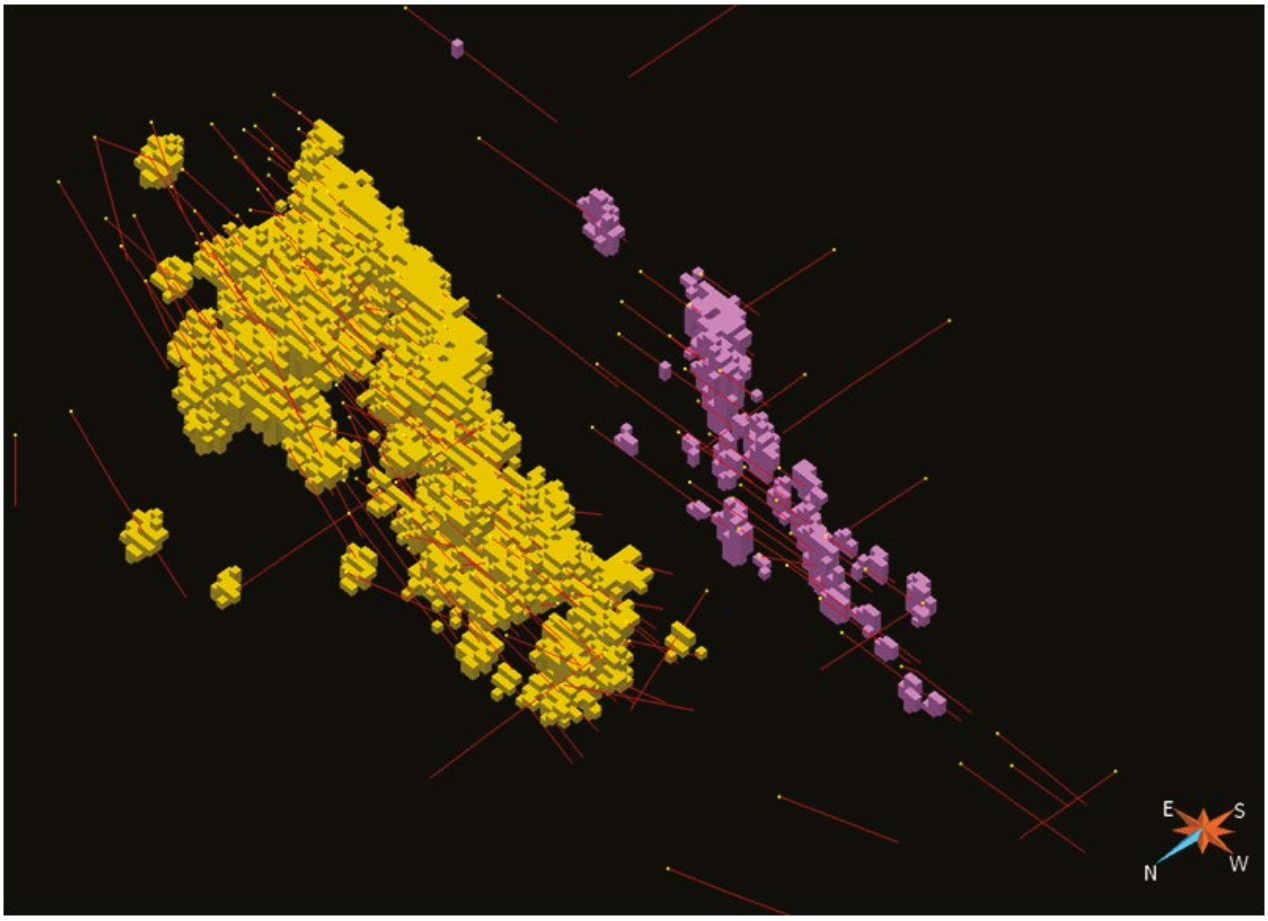

Fig. 51. Voxet model of the 'A' (yellow) and 'B' (purple) ore bodies with the drill holes. 5 x 5 x 5 m block size, 1 g/t Au cut off. Oblique view from NW.

Table 2. Resource calculations and basic statistics of the ore blocks of the A- and B-ore bodies.

	A-body		B-body	
1 g/t cut off	**Au g/t**	**Cu %**	**Au g/t**	**Cu %**
Minimum:	1.00	0.01	1.00	0.00
25th percentile:	1.33	0.11	1.24	0.08
Median:	1.79	0.16	1.60	0.16
75th percentile:	2.72	0.24	2.66	0.24
Maximum:	192.20	2.61	93.02	1.47
Mean:	2.54	0.20	2.64	0.19
Std. deviation:	3.51	0.16	4.57	0.16
Volume m3	1232250		186375	
Mass Mt	3.57		0.54	
Number of ore blocks	9858		1491	
1.5 g/t cut off	**Au g/t**	**Cu %**	**Au g/t**	**Cu %**
Minimum:	1.50	0.01	1.50	0.00
25th percentile:	1.84	0.11	1.81	0.08
Median:	2.37	0.16	2.47	0.14
75th percentile:	3.36	0.24	3.65	0.23
Maximum:	192.20	2.61	93.02	1.47
Mean:	3.28	0.20	3.80	0.19
Std. deviation:	4.21	0.16	5.91	0.18
Volume m3	790750		102625	
Mass Mt	2.29		0.30	
Number of ore blocks	6326	5990	821	

Block size of 5 x 5 x 5 meters was used
Density of 2.9 g/cm^3 was used in calculating the mass

rized together with the total amount of ore mined with average grades in Table 3.

The resource modeling results calculated for the 1.5 g/t Au cut-off are remarkably consistent with the production data with respect to the average Au grade, the average Cu grade being somewhat lower than in the production data (Table 2). The 2.61 Mt resource is comparable with the production data, suggesting that about 0.5 Mt of Au ore is left unmined. A marked tonnage increase occurs with the lower Au cut-off, but the Au grade decreases to 2.56 g/t. The original resource estimate was carried out using the 1.5 g/t Au cut-off, although the cut-off value was adjusted during the mining process (0.5 to 2.0 g/t) depending on the location and whether the ore was mined from an open pit or underground (Korkalo et al. 1988, Lahtinen et al. 2005). The average cut-off grade used during the mining operations is unknown.

Table 3. Total resources and average grades with actual production data.

	Size Mt	Au g/t	Cu %
1.5 g/t Au cut off	2.59	3.34	0.20
1.0 g/t Au cut off	4.11	2.56	0.20
Production data	2.14	3.29	0.26

The production data after Lahtinen et al. (2005)

No clear spatial trend can be seen in the distribution of the gold grades. The vertical distribution of the Au grades was investigated by calculating the average grades and resource tonnages of the 'A' ore body along 5-meter intervals. The results are presented in Figure 52. The bulk of the ore is located between the levels 240–170 m, but it should be noted that the available drilling data are sparse below the 170 m level. The average grade distribution varies within the 240-170 m level, with increasing

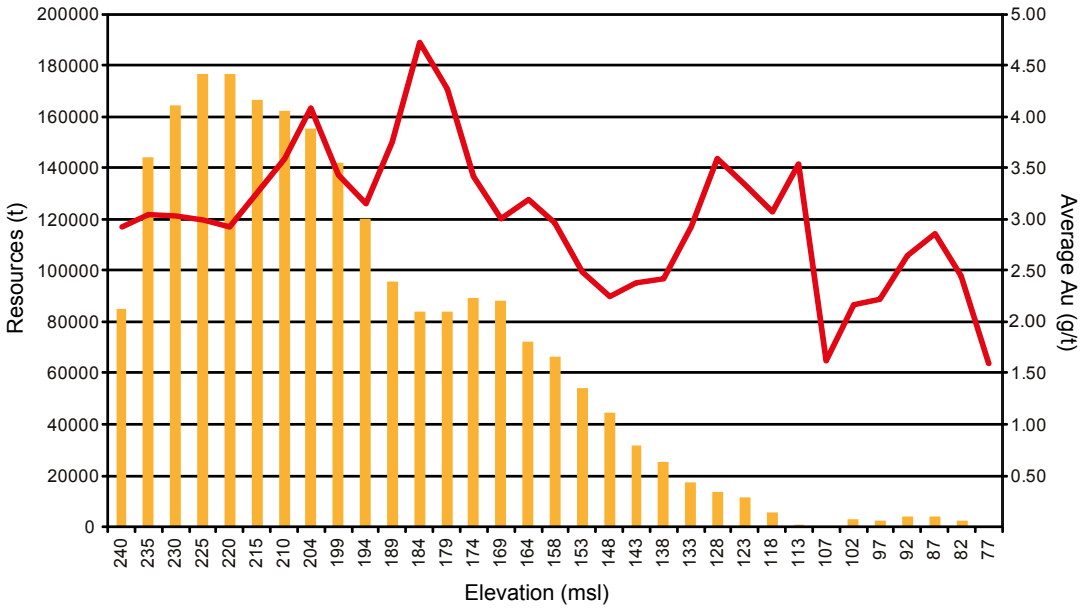

Fig. 52. Vertical distribution of Au-grade (line) and tonnage (bars) in the 'A' ore body (1.5 g/t Au cut off). Elevation in meters above sea level (the bedrock surface at Saattopora is between 230–240 m).

grades between 190-175 m and the highest grades around 185 m. The average grade starts to drop below 160 m, together with the resource tonnages. The erratic behavior of the grades at lower levels is probably influenced by the small number of cells in this region (at the 107 and 77 m levels there is only 1 cell in the voxet envelope).

The model suggests that the 'B' ore spatially follows the SE-striking shear zone 3 (Figs. 48 and 50). The northern 'A' ore does appear to be somewhat spread along the ENE-striking shear zone 1 at its western end, but for the majority of the ore body there appears to be no shear zone controlling of the ore body. The 'A' ore body is mainly located within the phyllite zone sandwiched between the mafic tuff unit in the hanging wall and the komatiite unit at the footwall. The drill core and observation data on the phyllite indicates that this unit, especially within the ore zone, is intensely albitized. The drill core data on the contact between phyllite and komatiite are sheared, as the komatiite is commonly logged as talc-chlorite or talc-chlorite-carbonate schist within a few meters of the contact zone.

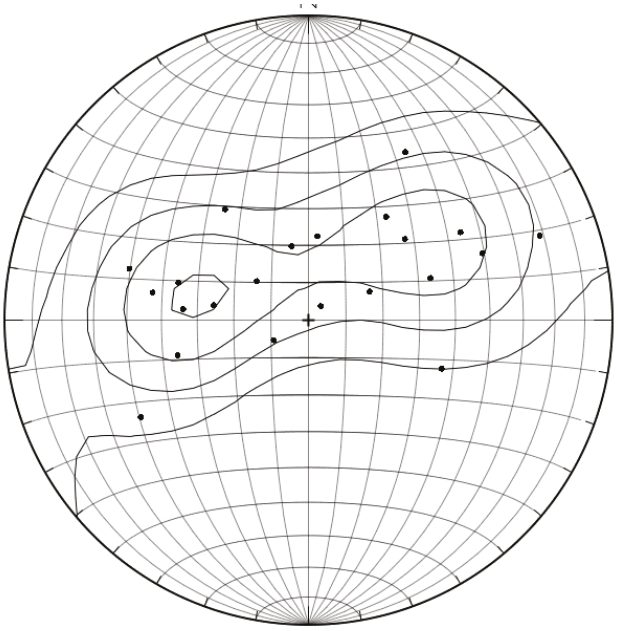

Fig. 53. Fold axis measurements from the outcrops around the Saattopora deposit. The axis appears to focus around orientations of 280/47 and 057/50 degrees. Equal area projection.

The modeled komatiite unit displays a clear folding pattern with a fold axis plunge of ca. 050/45 (Fig. 50D). Only a limited amount of structural outcrop data from the Saattopora area is available. However, outcrops with an F_3 orientation similar to the one shown in the model exists a few hundred meters north of the deposit. The limited fold axis data from nearby areas shows that the fold axis plots around two orientations, with average plunges at 280/47 and 057/50 (Fig. 53). The folding observed in the modeled komatiite unit is very close to the latter average.

DISCUSSION

In earlier geological maps (e.g. Lehtonen et al. 1998), the Sirkka thrust zone has been interpreted as a two-part thrust system, which in the Saattopora area was considered to be doubly dipping: the northern segment dipping south, and southern segment dipping north. It was considered that the Saattopora deposit was located at the southern segment of this structure and very probably the northward dipping stratigraphy at Saattora, also shown in the 3D lithological model, was one of the factors for this interpretation. The deep seismic FIRE4 profile reveals the Sirkka thrust zone as a set of south-dipping zones reaching depths of 8 to 10 km, with no indication of any north-dipping structures at the site of the profile (Patison et al. 2006, Niiranen et al. 2010). The modeled dips of shear zones at Saattopora are sub-vertical to northwards, and are most likely lower-order splays related to the Sirkka thrust. They were initially formed either during the thrusting event or the subsequent D_3 stage when the Sirkka structure was re-activated as a strike-slip shear zone (e.g. Saalmann & Niiranen 2010). We suggest that the north-dipping character of the stratigraphy at Saattopora is due to thrust folding generated during the northward-directed thrusting of the Sirkka thrust zone in the D_{1-2} stage(s), i.e. there is a broad, roughly E–W-trending sub-horizontal to horizontal F_{1-2} fold axis at the site, and the Saattopora is located at the northern fold limb of this structure. This structure was refolded during the D_3 stage, resulting in the F_3 crenulation folds detected in the outcrops and folding visible in the lithological model. This event can be correlated with the NNW-verging folding of Patison (2007) and D_4 of Saalmann and Niiranen (2010).

The geological evidence from the Saattopora and surrounding area indicates that the mineralization took place late with respect to the regional deformation and metamorphism. The completely brittle veins and breccias are macroscopically undeformed rocks and cut the last ductile deformation event (Fig. 49). The 'A' ore appears to be controlled by the albitized phyllite, i.e. it is in a location with strong rheological contrast between the host rocks. The 'B' ore appears to be controlled by a shear zone within an albitized phyllite.

The resource model generated is relatively consistent with the production data at the 1.5 g/t Au cut-off. Based on the available drilling data, there are several locations where an extension could be expected to depth. According to Korvuo (1995), the bottoms of the open pits are at 160 m and 210 m for 'A' and 'B' ores, respectively. The lowest parts of the underground stopes are at 90 m for the 'B' ore and 80 m for the 'A' ore. For the 'A' ore body, the 80 m level is about the lowest level that the lowermost ore blocks reach in our model (1.5 g/t Au cut off). For the 'B' ore, the lowest ore blocks only reach down to the level of 140 m. Based on the available drilling data, there are several locations where an extension could be expected to greater depths. However, the production drill holes, including the sludge drill holes, were not available for our work, and this is consequently somewhat uncertain.

CONCLUSIONS

The Saattopora Au(-Cu) deposit is an orogenic gold deposit with atypical metal association. The deposit consists of two separate ore bodies that are predominantly hosted by the >2.2 Ga Savukoski group phyllites and mica schist, and to a lesser degree komatiite and mafic tuff units. The mineralization style is completely brittle, consisting of N–S-striking sub-vertical veins, vein arrays, and hydrothermal breccias. The mineralization overprints the D_3 folding with a fold axis orientation of ca. 050/45. The mineralization is partly controlled by the lower-order shear zones of the Sirkka thrust zone, and partially by the intensely albitized lithologies that have made the host rocks brittle. The earliest alteration phase, the albitization, pre-dates the last ductile folding and was followed by early carbonation, which was possibly folded during the D_3 stage. The mineralized veins post-date both of the early alteration features, and no clear alteration halo has been detected in association with the veins.

CHAPTER VII.
THE LAUTTASELKÄ 3D MODEL

Tero Niiranen, Ilkka Lahti, Vesa Nykänen and Tuomo Karinen

INTRODUCTION

The Geological Survey of Finland (GTK) carried out gold exploration in the Lauttaselkä area during 2006–2010. The exploration included bedrock mapping, diamond drilling, geochemical sampling of the Quaternary geological deposits and bedrock outcrops, and geophysical surveys. The results of this work have been presented in Hulkki et al. (2011) and in Karinen et al. (2011). A geological 3D model was constructed based on the data collected during the exploration work in order to better understand the geological framework of the target area. This chapter briefly presents the geological background of the Lauttaselkä area and the constructed model.

GEOLOGY OF THE STUDY AREA

Lauttaselkä is located at the eastern contact of the Kittilä terrane. The geology of the study area can be divided into two main parts: in the eastern part the bedrock consists of a rift-related volcano-sedimentary sequence of 2.44–2.0 Ga Salla, Sodankylä, and Savukoski Group rocks deposited on the Archean basement, whereas the tholeiitic volcanic rocks and associated sedimentary rocks of the ca. 2.0 Ga Kittilä Group comprise the western part (Fig. 54). These two main units are bound by tectonic contact and Nuttio Suite serpentinites, which have been interpreted to represent fragments of ophiolite (Hanski 1997).

The 2.44 Ga felsic to intermediate volcanic rocks of the Salla Group comprise the lowermost unit in the eastern part. In regional stratigraphy, the Salla Group is overlain by mafic to andesitic volcanic rocks of the Kuusamo Group. These are, however, lacking from the study area. Instead, the Salla Group rocks within the study area are overlain by quartzites, mica schists, and carbonaceous sedimentary rocks of the >2.2 Ga Sodankylä Group. The uppermost stratigraphical unit in the eastern part of the study area consists of graphite-bearing phyllites and schist, with tholeiitic volcanic rocks of the Matarakoski Fm and komatiitic volcanic rocks of the Sattasvaara Fm comprising the >2.05 Ga Savukoski Group in the area.

The supracrustal sequence of the western part of the study area is divided into the Kautoselkä, Porkonen, and Vesmajärvi Formations, representing the Kittilä Group. The oldest Kautoselkä Fm consists of mafic amygdaloidal lavas, tuffs, and tuffites, which are relatively evolved Fe-rich tholeiitic basalts and andesites in their chemical composition (Lehtonen et al. 1998, Hanski & Huhma 2005). The uppermost Vesmajärvi Fm consists of submarine Mg-tholeiitic lavas, which have geochemical affinity with oceanic basalts (Hanski & Huhma 2005). Between these two units occur graphite- and sulfide-bearing tuffites, tuffs, cherts, and banded iron formations (BIFs) belonging to the Porkonen Formation. Sm/Nd data on the Vesmajärvi tholeiites yield an isochron age of 1.990 ± 35 Ma with $\varepsilon_{Nd} = +3.7 \pm 0.2$ (Hanski & Huhma 2005).

Based on the presence of Nuttio Suite serpentinites at the contact of the Kittilä Group and the surrounding rocks, as well as the geochemical evidence and tectonic contacts outlining the

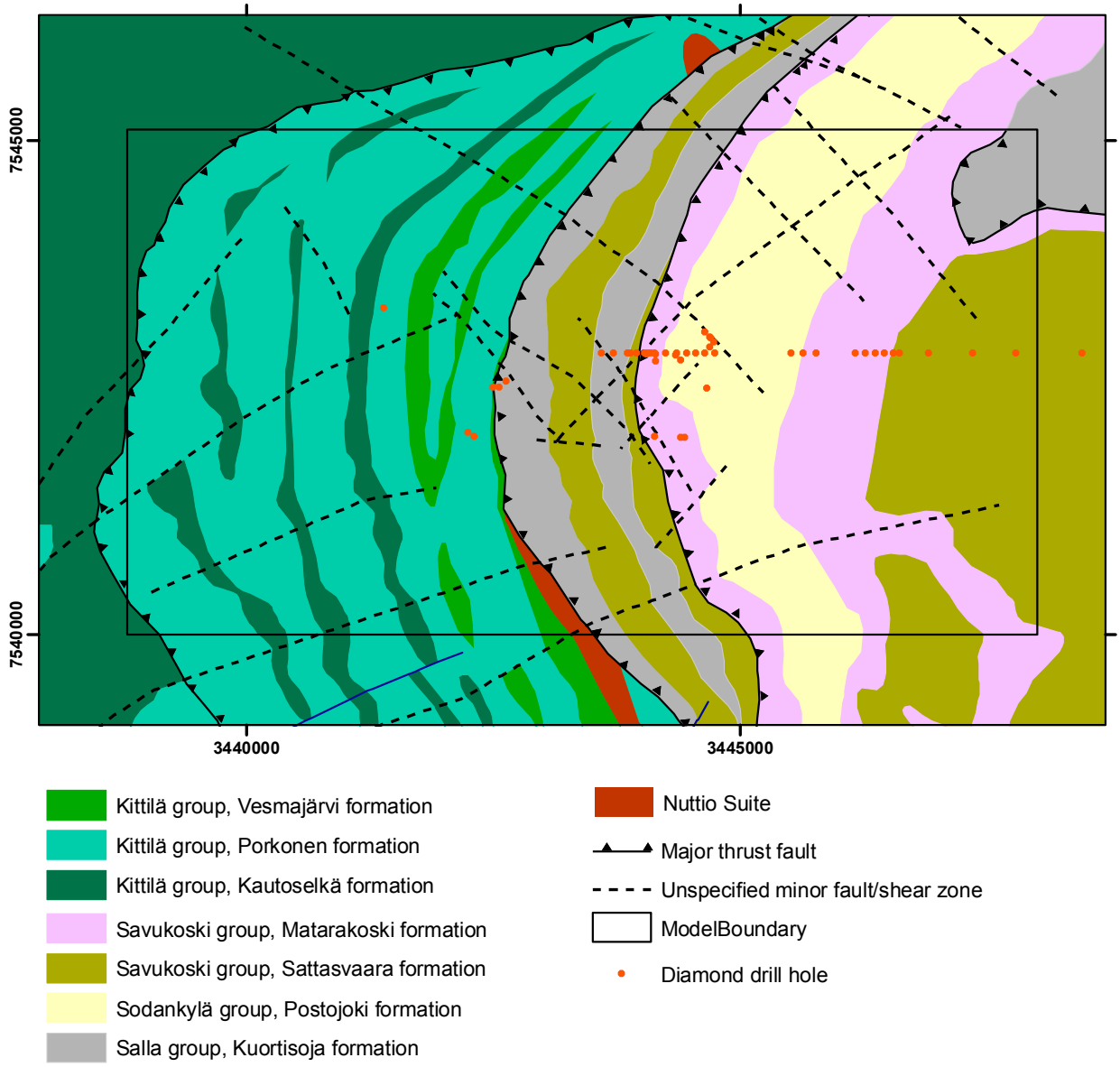

Fig. 54. Geological map of the study area with the location of drill holes and the model boundary. Modified after the Bedrock of Finland – DigiKP.

Kittilä Group, it has been interpreted to represent an allochthonous or para-autochthonous terrane (e.g. Hanski 1997, Lehtonen et al. 1998, Hanski & Huhma 2005, Lahtinen et al. 2005).

DATA AND METHODS

The modeling was based on bedrock observations, drilling data, ground geophysics, and geochemical data recorded in the study area during 2006–2010 (see Karinen et al. 2011, for further details). The locations of the drill holes used in modeling work are indicated in Figure 54. Airborne geophysics and gravity data of GTK were used in combination with the new data. The geochemical correlation of the different lithological units observed in the outcrops and drill cores with the regional lithological data and the known units is presented in Karinen et al. (2011). The existing bedrock map (GTK digital bedrock map) was updated during the process, and it was used as a basis for the modeling. The lithological units were modeled using Gocad^{tm} software and the Mira geoscience mining utilities plugin.

MODEL

The constructed 3D model of the Lauttaselkä area is presented in Figure 55. The model shows the topmost bedrock units of the study area. The top of the model is at the current surface, which is an average of 285 meters above sea level. The lowermost parts of the model reach depths of ca. 600 meters.

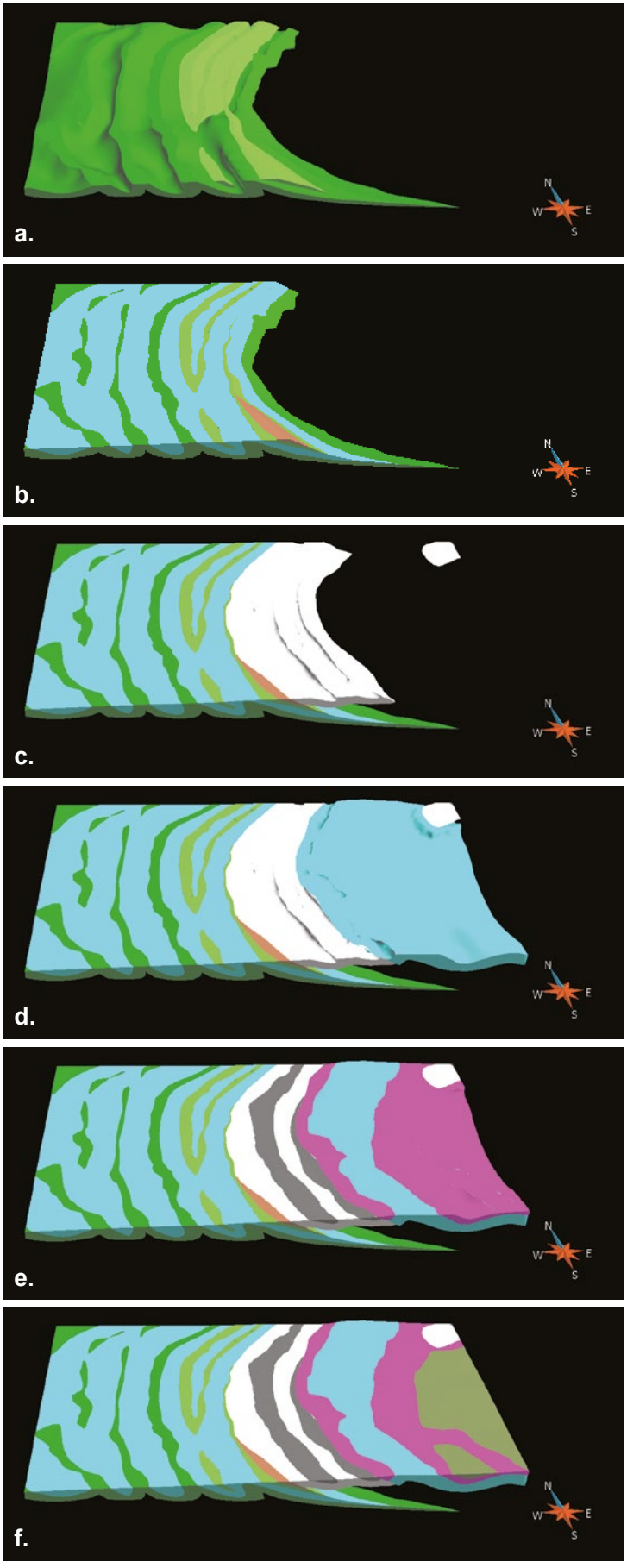

Fig. 55. The Lauttaselkä 3D model layer by layer. A. Kautoselkä Fm (dark green) and Vesmajärvi Fm (light green), B. Porkonen Fm (blue) and Nuttio Suite (orange), C. Kuortisoja Fm, D. Postojoki Fm, E. Matarakoski Fm (pink), Sotkaselkä Fm (gray), F. Sattasvaara Fm. Oblique view from the SSW. The top of the model is at the current surface (ca. 285 m), while the deepest modeled parts reach -600 m below sea level.

DISCUSSION

Based on the 3D model, the repeating pattern of the Kittilä Group formations in the western part of the area is explained by west-vergent thrust folding with N–S axial planes dipping 30° to 60° east (Fig. 55). The modeled folding also explains the observed 20° to 30° E dipping nature of the bedding in the area (Karinen et al. 2011). The Salla Group rocks have been thrusted on top of the Kittilä Group rocks along a thrust plane into which the Nuttio Suite serpentinite has been obducted (Fig 55c). A second E-dipping thrust plane occurs between the Salla Group and Sodankylä-Savukoski Group package (Fig 55d). Both of these thrusts have been observed in outcrops and drilling, and according to Karinen et al. (2011) they are also reflected in topography.

Karinen et al. (2011) raises a question of the vergence of the thrusting and folding, which is to 180° opposite in orientation in the Nuttio area some 20 km south of the Lauttaselkä area. They explain the change in vergence with reorienting of the structures during later stages of the regional deformation. While this is a possible scenario, especially in relation to the fold structures, it seems unlikely that refolding could result in a complete reversal of the thrust plane orientations, as they are presented in the current model. Clearly, more work needs to be carried out to resolve this problem.

ACKNOWLEDGEMENTS

The authors wish to thank regional directors Risto Pietilä and Kimmo Pietikäinen for their support of this work. Several personnel of the GTK Northern Finland Office were involved in the project, and we would like acknowledge the efforts of all of them. The authors wish to thank Dr Eeva-Liisa Laine for constructive criticism of the manuscript.

REFERENCES

Agterberg, F. P., Bonham-Carter, G. F. & Wright, D. F. 1990. Statistical pattern integration for mineral exploration. In: Gaal, G. & Merriam, D. (eds) Computer applications in resource estimation. Prediction and assessment for metals and petroleum. Oxford: Pergamon Press, 1–21.

Archibald, N., Gow, P. & Boschetti, F. 1999. Multiscale edge analysis of potential field data. Exploration Geophysics 30, 38–44.

Archibald, N., Holden, D., Mason, R., Power, B., Boschett, F., Horowitz, F. & Hornby, P. 2001. There's a worm in my soup: wavelet based analysis for interpretation of crustal scale potential field data and implications for identification of giant hydrothermal ore systems: 2001 – A hydrothermal odyssey, Townsville, Queensland, Queensland: EGRU James Cook University, 5–7.

Austin, J. R. & Blenkinsop, T. G. 2008. The Cloncurry Lineament: Geophysical and geological evidence for a deep crustal structure in the Eastern Succession of the Mount Isa Inlier. Precambrian Research 163, 50–68.

Bedrock of Finland – DigiKP. Digital map database [Electronic resource]. Espoo: Geological Survey of Finland [referred 31.12.2012]. Version 1.0.

Berthelsen, A. & Marker, M. 1986. 1.9–1.8 Ga old strike-slip megashears in the Baltic Shield, and their plate tectonic implications. Tectonophysics 128, 163–181.

Bierlein, F. P., Murphy, F. C., Weinberg, R. F. & Lees, T. 2006. Distribution of orogenic gold deposits in relation to fault zones and gravity gradients: targeting tools applied to the Eastern Goldfields, Yilgarn Craton,Western Australia. Mineralium Deposita 41, 107–126.

Bonham-Carter, G. F. 1994. Geographic Information Systems for Geoscientists – Modelling with GIS. Computer Methods in the Geosciences 13. Oxford: Pergamon. 398 p.

Bonham-Carter, G. F., Agterberg, F. P. & Wright, D. F. 1988. Integration of geological datasets for gold exploration in Nova Scotia. Photogrammetric Engineering and Remote Sensing 54, 77, 1585–1592.

Caumon, G., Antoine, C. & Tertois, A.-L. 2007. Building 3D geological surfaces from field data using implicit surfaces: Proceedings to 27th Gocad Meeting, Nancy, France.

Chernicoff, C. J., Richards, J. P. & Zappettini, E. O. 2002. Crustal lineament control on magmatism and mineralization in northwestern Argentina; geological, geophysical, and remote sensing evidence. Ore Geology Reviews 21 (3–4), 127–155.

Eilu, P. 1999. FINGOLD; a public database on gold deposits in Finland. Geological Survey of Finland, Report of Investigation 146. 224 p., 2 apps.

Eilu, P. 2007. FINGOLD; brief descriptions of all drilling-indicated gold occurrences in Finland; the 2007 data. Geological Survey of Finland, Report of Investigation 166. 35 p.

Eilu, P., Pankka, H., Keinanen, V. J., Kortelainen, V., Niiranen, T. & Pulkkinen, E. 2007. Characteristics of gold mineralisation in the greenstone belts of northern Finland. In: Ojala, V. J. (ed.) Gold in the Central Lapland

Greenstone Belt. Geological Survey of Finland, Special Paper 44, 57–106.

Elo, S. 1998. Gravity investigations of the Geological Survey of Finland 1995–1997. Bulletin d'Information – Bureau Gravimetrique International 83, 59–63.

Elo, S., Lanne, E., Ruotoistenmaki, T. & Sindre, A. 1989. Interpretation of gravity anomalies along the POLAR profile in the northern Baltic Shield. Tectonophysics 162 (1–2), 135–150.

Frietsch, R., Tuisku, P., Martinsson, O. & Perdahl, J. 1997. Early Proterozoic Cu-(Au) and Fe ore deposits associated with regional Na-Cl metasomatism in northern Fennoscandia. Ore Geology Reviews 12 (1), 1–34.

Gaal, G., Berthelsen, A., Gorbatschev, R., Kesola, R., Lehtonen, M. I., Marker, M. & Raase, P. 1989. Structure and composition of the Precambrian crust along the POLAR profile in the northern Baltic Shield. Tectonophysics 162 (1–2), 1–25.

Goldfarb, R. J., Groves, D. I. & Gardoll, S. 2001. Orogenic gold and geologic time; a global synthesis. Ore Geology Reviews 18 (1–2), 1–75.

Groves, D. I., Goldfarb, R. J., Gebre-Mariam, M., Hagemann, S. G., Robert, F. & Arne, D. C. 1998. Orogenic gold deposits; a proposed classification in the context of their crustal distribution and relationship to other gold deposit types. Ore Geology Reviews 13 (1–5), 7–27.

Hanski, E. S. 1997. The Nuttio serpentinite belt, central Lapland; an example of Paleoproterozoic ophiolitic mantle rocks in Finland. Ofioliti 22 (1, Special Issue), 35–46.

Hanski, E., Huhma, H. & Vaasjoki, M. 2001. Geochronology of northern Finland; a summary and discussion. In: Vaasjoki, M. (ed.) Radiometric age determinations from Finnish Lapland and their bearing on the timing of Precambrian volcano-sedimentary sequences. Geological Survey of Finland, Special Paper 33, 255–279.

Hanski, E. & Huhma, H. 2005. Central Lapland greenstone belt. Developments in Precambrian Geology 14, 139–193.

Hiltunen, A. 1982. The Precambrian geology and skarn iron ores of the Rautuvaara area, northern Finland. Geological Survey of Finland, Bulletin 318.

Hiltunen, A. & Tontti, M. 1976. The stratigraphy and tectonics of the Rautuvaara iron ore district, northern Finland. Bulletin of the Geological Society of Finland 48 (1–2), 95–109.

Holden, D. J., Archibald, N. J., Boschetti, F. & Jessell, M. W. 2000. Inferring geological structures using wavelet-based multiscale edge analysis and forward models. Exploration Geophysics (Melbourne) 31 (4), 617–621.

Hölttä, P., Väisänen, M., Väänanen, J. & Manninen, T. 2007. Paleoproterozoic metamorphism and deformation in central Lapland, Finland. In: Ojala, V. J. (ed.) Gold in the Central Lapland Greenstone Belt. Geological Survey of Finland, Special Paper 44, 7–56.

Hornby, P., Boschetti, F. & Horowitz, F. G. 1999. Analysis of potential field data in the wavelet domain. Geophysical Journal International 137 (1), 175–196.

Hulkki, H., Keinänen, V., Karinen, T., Karvinen, A., Sarala, P., Sarapää, O., Salmirinne, H., Sandgren, E. & Lahti, I. 2011. Pohjois-Suomen kultahankkeen 2551009 loppuraportti. Geological Survey of Finland archive report 50/2011. 8 p., 9 apps. (in Finnish)

Jaques, A. L., Jaireth, S. & Walshe, J. L. 2002. Mineral systems of Australia; an overview of resources, settings and processes. Australian Journal of Earth Sciences 49 (4), 623–660.

Kääriäinen, J. & Mäkinen, J. 1997. The 1979-1996 gravity survey and results of the gravity survey of Finland 1945-1996. Publications of the Finnish Geodetic Institute 125.

Karinen, T., Keinänen, V., Sarala, P., Hulkki, H., Sandgren, E. & Nykänen, V. 2011. Tutkimustyöselostus Kittilän kunnassa valtausalueilla Lauttaselkä1-3 (8411/1, 8466/1, 8570/1) suoritetuista malmitutkimuksista vuosina 2006-2010. Geological Survey of Finland, archive report M06/26/2011. 52 p. 8 apps. (in Finnish)

Korja, T., Hjelt, S. E. O., Kaikkonen, P., Koivukoski, K., Rasmussen, T. M. & Roberts, R. G. 1989. The geoelectric model of the POLAR profile, northern Finland. Tectonophysics 162 (1–2), 113–133.

Korja, T., Tuisku, P., Pernu, T. & Karhu, J. 1996. Field, petrophysical and carbon isotope studies on the Lapland granulite belt; implications for deep continental crust. Terra Nova 8 (1), 48–58.

Korkalo, T., Lappalainen, S., Vaajoensuu, K. & Heikkinen, R. 1988. Kittilän Saattoporan Kultaesiintymän Kannattavuustarkastelu. Unpublished Outokumpu Oyj Report 090/2741 04/TTK/KTR/88. 35 p. 60 apps. (in Finnish)

Korvuo, E. 1995. Saattoporan kaivoksen loppuraportti. Outokumpu Finnmines Oy. Unpublished Outokumpu Oy report. (in Finnish)

Kukkonen, I. T. & Lahtinen, R (eds) 2006. Finnish Reflection Experiment FIRE 2001–2005. Geological Survey of Finland, Special Paper 43. 247 p., 15 apps., 1 CD-ROM.

Kukkonen, I. T., Heikkinen, P., Heinonen, S. & Laitinen, J. 2011. Reflection seismics in exploration for mineral deposits; initial results from the HIRE project. In: Nenonen, K. & Nurmi, P. A. (ed.) Geoscience for society: 125th anniversary volume. Geological Survey of Finland, Special Paper 49, 49–58.

Lahtinen, J., Aarnisalo, J., Anttonen, R. & Rekola, T. 2005. Saattopora - Pahtavuoma Area, Western Kittilä Greenstone Belt, Northern Finland. Compilation of exploration and mineral resource data. Unpublished Outokumpu Mining Oy report. 48 p., 4 apps.

Lahtinen, R., Korja, A. & Nironen, M. 2005. Paleoproterozoic tectonic evolution. Developments in Precambrian Geology 14, 481–531.

Lehtonen, M., Airo, M.-L., Eilu, P., Hanski, E., Kortelainen, V., Lanne, E., Manninen, T., Rastas, P., Räsänen, J. & Virransalo, P. 1998. The stratigraphy, petrology and geochemistry of the Kittilä greenstone area, northern Finland. A report of the Lapland Volcanite Project. Geological Survey of Finland, Report of Investigation 140. 144 p. (in Finnish)

Mäkelä, M. & Tammenmaa, J. 1978. Lapin rikki-isotooppitutkimus vuosina 1974-1976. Geological Survey of Finland, Report of Investigation 24. 65 p.

Marker, M. 1988. Early Proterozoic thrusting of the Lapland granulite belt and its geotectonic evolution, northern Baltic Shield. Geologiska Föreningens i Stockholm Förhandlingar 110 (4), 405–410.

McCuaig, T. C. & Kerrich, R. 1998. P-T-t-deformation-fluid characteristics of lode gold deposits; evidence from alteration systematics. Ore Geology Reviews 12 (6), 381–454.

Mutanen, T. 1997. Geology and ore petrology of the Akanvaara and Koitelainen mafic layered intrusions and the Keivitsa-Satovaara layered complex, northern Finland. Geological Survey of Finland, Bulletin 395. 233 p., 5 apps.

Naldrett, A. J. 2011. Fundamentals of magmatic sulfide deposits. Reviews in Economic Geology 17, 1–50.

Niiranen, T., Poutiainen, M. & Mänttäri, I. 2007. Geology, geochemistry, fluid inclusion characteristics, and U-Pb age studies on iron oxide-Cu-Au deposits in the Kolari

region, northern Finland. Ore Geology Reviews 30 (2), 75–105.

Niiranen, T., Nykänen, V., Lahti, I. & Karinen, T. 2009. A Geological interpretation of the upper crust along the FIRE 4A and 4B seismic profiles. Geological Survey of Finland, archive report K31.4/2009/78. 22 p., 2 apps.

Niiranen, T., Hulkki, H., Nykänen, V. & Lahti, I. 2012. Hydrothermal alteration, fluid inclusion characteristics and tectonic setting of the Paleoproterozoic Saattopora orogenic Au(-Cu) deposit, northern Finland. International Geological Congress, Abstracts; Congres Geologique International, Resumes 34, p. 3934.

Nykänen, V. 2008. Spatial data analysis as a tool for mineral prospectivity mapping. Spatial data analysis as a tool for mineral prospectivity mapping. Espoo: Geological Survey of Finland. 92 p. (dissertation)

Nykänen, V. & Salmirinne, H. 2007. Prospectivity analysis of gold using regional geophysical and geochemical data from the Central Lapland greenstone belt, Finland. In: Ojala, V. J. (ed.) Gold in the Central Lapland Greenstone Belt. Geological Survey of Finland, Special Paper 44, 251–269.

Nykänen, V., Groves, D. I., Ojala, V. J. & Gardoll, S. J. 2008a. Combined conceptual/empirical prospectivity mapping for orogenic gold in the northern Fennoscandian Shield, Finland. Australian Journal of Earth Sciences 55 (1), 39–59.

Nykänen, V., Groves, D. I., Ojala, V. J., Eilu, P. & Gardoll, S. J. 2008b. Reconnaissance-scale conceptual fuzzy-logic prospectivity modelling for iron oxide copper-gold deposits in the northern Fennoscandian Shield, Finland. Australian Journal of Earth Sciences 55 (1), 25–38.

Obuchowski, N. A. 2003. Receiver operating characteristic curves and their use in radiology. Radiology, 229, (1), 3–8.

Patison, N. L. 2007. Structural controls on gold mineralisation in the Central Lapland greenstone belt. In: Ojala, V. J. (ed.) Gold in the Central Lapland Greenstone Belt. Geological Survey of Finland, Special Paper 44, 107–124.

Patison, N. L., Korja, A., Lahtinen, R. & Ojala, V. J. 2006. FIRE seismic reflection profiles 4, 4A and 4B; insights into the crustal structure of northern Finland from Ranua to Näätämö. In: Kukkonen, I. T. & Lahtinen, R (eds) Finnish Reflection Experiment FIRE 2001–2005. Geological Survey of Finland, Special Paper 43, 161–222.

Pitcairn, I. K. 2011. Background concentrations of gold in different rock types. Applied Earth Science 120 (1), 31–38.

Pitcairn, I. K., Teagle, D. A. H., Craw, D., Olivo, G. R., Kerrich, R. & Brewer, T. S. 2006. Sources of metals and fluids in orogenic gold deposits; insights from the Otago and Alpine Schists, New Zealand. Economic Geology and the Bulletin of the Society of Economic Geologists 101 (8), 1525–1546.

Raines, G. L. 1999. Evaluation of weights of evidence to predict epithermal-gold deposits in the Great Basin of the Western United States. Natural Resources Research (New York, N.Y.) 8 (4), 257–276.

Risto, R., Breede, K., MacFarlane, G.R., Roberts, S., Watts, G. & Hinzer, J. 2010. Technical report on the mineral resource estimates and preliminary assessment of the Hannukainen project, Finland for Northland Resources S.A. Watts, Griffis and McQuat, Toronto. 218 p.

Saalmann, K. & Niiranen, T. 2010. Hydrothermal alteration and structural control on gold deposition in the Hanhimaa shear zone and western part of the Sirkka Line. Geological Survey of Finland, archive report M19/2741/2010/58. 30 p., 2 apps.

Sawatzky, D. L., Raines, G. L., Bonham-Carter, G. F. & Looney, C. G. 2009. Spatial Data Modeller (SDM): ArcMAP 9.3 geoprocessing tools for spatial data modelling using weights of evidence, logistic regression, fuzzy logic and neural networks. Available at: http://arcscripts.esri.com/details.asp?dbid=15341.

Sibson, R. H., Robert, F. & Poulsen, K. H. 1988. High-angle reverse faults, fluid-pressure cycling, and mesothermal gold-quartz deposits. Geology (Boulder) 16 (6), 551–555.

Tuisku, P. & Huhma, H. 2006. Evolution of migmatitic granulite complexes; implications from Lapland granulite belt; Part II, Isotopic dating. Bulletin of the Geological Society of Finland 78 (2), 143–175.

Tuisku, P., Mikkola, P. & Huhma, H. 2006. Evolution of migmatitic granulite complexes; implications from Lapland granulite belt; Part 1, Metamorphic geology. Bulletin of the Geological Society of Finland 78 (1), 71–105.

Väänänen, J. 1998. Kolarin ja Kurtakon kartta-alueiden kallioperä. Summary: Pre-Quaternary Rocks of the Kolari and Kurtakko Map-Sheet areas. Geological Map of Finland 1:100 000, Explanation to the Maps of Pre-Quaternary Rocks, Sheets 2713 and 2731. Geological Survey of Finland. 87 p. + 3 app.

Väisänen, M. 2002. Structural features in the central Lapland greenstone belt, northern Finland. Geological Survey of Finland, archive report K 21.42/2002/3. 20 p., 16 apps.

Ward, P., Härkönen, I., Nurmi, P. A. & Pankka, H. S. 1989. Structural studies in the Lapland greenstone belt, northern Finland and their application to gold mineralization. In: Autio, S. (ed.) Geological Survey of Finland, Current Research 1988. Geological Survey of Finland, Special Paper 10, 71–77.

www.gtk.fi
info@gtk.fi

In this report, we present the results of the Central Lapland Greenstone Belt 3D modeling project carried out in 2007-2012. The report describes five deposit to regional scale 3D models, the use of the multiscale edge detection method in the prospectivity modeling of orogenic gold deposits, and the Fuzzy Logic Ni prospectivity modeling results with Receiver Operating Characteristics model validation in the Central Lapland area.

ISBN 978-952-217-302-7 (PDF)
ISSN 0781-4240